ISSN:2146-0957
eISSN:2146-5703

Volume:14 Number:1
January 2024

An International Journal of Optimization and Control: Theories & Applications

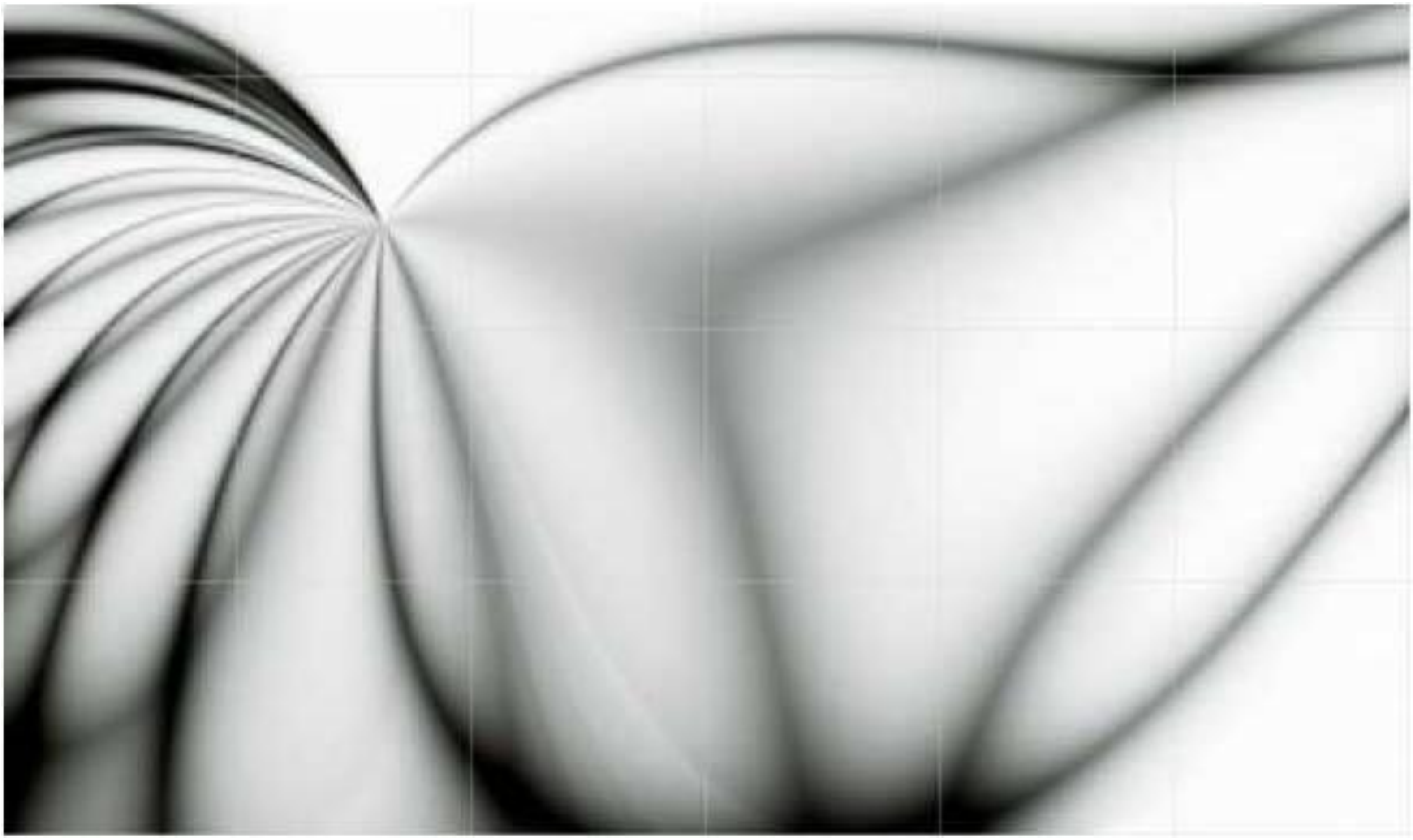

www.ijocta.org

An International Journal of Optimization and Control:
Theories & Applications

Volume: 14, Number: 1

January 2024

http://www.ijocta.org
editor@ijocta.org

Publisher & Owner *(Yayımcı & Sahibi)*:

Prof. Dr. Ramazan YAMAN
Atlas Vadi Campus, Anadolu St.
No. 40, Kagithane, Istanbul, Turkey
Atlas Vadi Kampüsü, Anadolu Cad. No. 40, Kağıthane, İstanbul, Türkiye

ISSN: 2146-0957

eISSN: 2146-5703

Press *(Basımevi)*:

İdeal Kültür, Topkapı Mahallesi, Kahalbaşı Sokak, No: 31/1, 34093, Fatih, İstanbul, Türkiye
Ideal Kultur, Topkapi District, Kahalbasi Street, No: 31/1, 34093, Fatih, Istanbul, Turkey

Date Printed *(Basım Tarihi)*:

January 2024
Ocak 2024

Responsible Director (Sorumlu Müdür):

Prof. Dr. Ramazan YAMAN

IJOCTA is an international, quarterly, and peer-reviewed journal indexed/abstracted by *(IJOCTA, yılda dört kez yayımlanan ve aşağıdaki indekslerce taranan/dizinlenen uluslararası hakemli bir dergidir)*:

- Emerging Sources Citation Index (ESCI)
- Scopus - Applied Mathematics
- Scopus - Control and Optimization
- Zentralblatt MATH
- ProQuest - Electronics & Communications Abstracts
- Proquest - Computer & Information Systems Abstracts
- Proquest - Mechanical & Transportation Eng. Abstracts
- EBSCOHost
- MathSciNet
- TR Dizin - Ulakbim (Science Database)
- Directory of Open Access Journals (DOAJ)

We Use Plagiarism Detection iThenticate Learn More »

An International Journal of Optimization and Control: Theories & Applications

Volume: 14 Number: 1
January 2024

CONTENTS

RESEARCH ARTICLES

An International Journal of Optimization and Control: Theories & Applications
ISSN:2146-0957 eISSN:2146-5703
Vol.14, No.1, pp.1-11 (2024)
http://doi.org/10.11121/ijocta.1428

RESEARCH ARTICLE

Controllability of nonlinear fractional integrodifferential systems involving multiple delays in control

Abdul Haq[a*], Nagarajan Sukavanam[b]

[a] *Department of Mathematics, School of Advanced Sciences, Vellore Institute of Technology, Vellore, Tamil Nadu, India*
[b] *Department of Mathematics, Indian Institute of Technology, Roorkee, Roorkee, Uttarakhand, India*
abdulhaqiitr@gmail.com, nsukavanam@gmail.com

ARTICLE INFO

Article History:
Received 12 July 2023
Accepted 18 October 2023
Available Online 7 January 2024

Keywords:
Fractional derivative
Delay system
Mild solution
Controllability

AMS Classification 2010:
70Q05; 93C10

ABSTRACT

This work studies the existence of solutions and approximate controllability of fractional integrodifferential systems with Riemann-Liouville derivatives and with multiple delays in control. We establish suitable assumptions to prove the existence of solutions. Controllability of the system is shown by assuming a range condition on control operators and Lipschitz condition on non-linear functions. We use the concepts of strongly continuous semigroup rather than resolvent operators. Finally, an example is give to illustrate the theory.

1. Introduction

There are many problems in which the current rate of change of a function can be obtained from the past values of that function. Time delay systems are mathematical models of these types of problems. A system may have variable or constants delays eithre in control action or in the state variable or in both. Therefore it is reasonable to study the existence or controllability property of delay dynamical systems. Some of biological and physical systems having time delays are population growth, prey predator problems, mixing of liquids, equations having feedback control, etc.

In several biological, engineering and physical problems, differential systems of fractional-order are found to be suitable models. Therefore, in last twenty years, they attracted more attention from researchers. In fact, for the illustration of memory and hereditary properties, fractional derivatives provide a better instrument. For this reason, they have given a lot of applications in the areas of control theory, aerodynamics, viscoelasticity, physics, electrodynamics of complex medium, heat conduction, electricity mechanics, etc. [1–12]. For the modeling of the anomalous phenomena in the theory of complex systems as well as in nature, systems of fractional-order became more appropriate and interesting [1, 13]. Therefore, to describe diffusion in media with fractal geometry, the fractional diffusion equation was introduced in physics by substituting the first-order derivative by a fractional derivative in classical diffusion equation, which becomes appropriate for many applications.

In some areas such as dynamics of nuclear reactor and thermoelasticity, it is required to reflect the memory effect of systems in their models. In the modeling of these problems, if differential equations are utilized, which involve functions at any given space and time, the effect of previous outcomes is omitted. For this reason, to incorporate the memory effect in these differential equations,

*Corresponding Author

a term of integration is introduced, which turns to integrodifferential equation. The integrodifferential equations have given a huge applications in mechanics, viscoelastic fluid dynamics, control theory, thermoelastic contact, heat conduction, financial mathematics, industrial mathematics, biological models, aerospace systems, chemical kinetics, etc. (see [15–21]).

The existence and controllability results for different types of linear and non-linear systems are proved in many articles [14, 20–34, 36–42, 44–51, 53]. Among them, approximate controllability of fractional systems with Riemann-Liouville derivatives was proved by Liu and Li [38] assuming Lipschitz continuity. In [36], Zhu et al. analyzed the approximate controllability of fractional semilinear systems using itegral contractor. Using fractional resolvent, Ji and Yang [21] obtained the solution to fractional integrodifferential systems with Riemann-Liouville derivatives without assuming the Lipschitz condition. Ibrahim et. al. [33] analyzed approximate controllability of functional equations with Riemann-Liouville derivative by applying iterative technique. Approximate controllability for higher order fractional integrodifferential equation was discussed by Raja et al. [52]. Making use of fractional resolvent, existence and controllability of higher order Riemann-liouville fractional equations were derived in [35]. However, the controllability of fractional integrodifferential equations with multiple delays in control is still an untreated topic. Our purpose is to obtain a set of new sufficient conditions for the existence and uniqueness of solutions and approximate controllability of the following fractional integrodifferential systems:

$$\begin{cases} D_t^\kappa z(t) = Az(t) + \sum_{j=0}^{m} B_j u(t-b_j) \\ +f\left(t, z(t), \int_0^t \xi(t,s,z(s))\,ds\right), \qquad t \in (0,\hbar], \\ I_t^{1-\kappa} z(t)\big|_{t=0} = y_0 \in V, \ u(t)=0, \quad t \in [-b_m, 0], \end{cases} \tag{1}$$

where $0 < \kappa \le 1 < p\kappa$ and D_t^κ is the κ-order Riemann-Liouville derivative. The control $u \in U = L_p([0,\hbar];V')$, the state $z \in Z = L_p([0,\hbar];V)$, where V and V' are complete normed spaces. b_j $j = 0,1,2,\dots,m$, are constant delays such that $0 = b_0 < b_1 < b_2 < \cdots < b_m < \hbar$. The linear operator $A : D(A) \subseteq V \to V$ generates a C_0-semigroup $T(t)$. $B_j : U \to Z$, $j = 0,1,2,\dots,m$, are linear maps. f and ξ are V-valued non-linear functions defined on $[0,\hbar]\times V\times V$ and $\Delta \times V$, respectively; where $\Delta = \{(t_1,t_2) : 0 \le t_2 \le t_1 \le \hbar\}$.

The article is structured as follows: After introduction, we have given the preliminaries in Section 2. In Section 3, the existence and uniqueness of solutions are proven. Controllability of the system is shown in Section 4. Finally, an example is given in Section 5.

2. Preliminaries

Definition 1. *The Riemann-Liouville fractional integral of order κ is given by*

$$I_t^\kappa \varphi(t) = \frac{1}{\Gamma(\kappa)} \int_0^t (t-s)^{\kappa-1}\varphi(s)\,ds, \quad \kappa > 0,$$

where Γ is the gamma function.

Definition 2. *The Riemann-Liouville fractional derivative of order κ is given by*

$$D_t^\kappa \varphi(t) = \frac{1}{\Gamma(m-\kappa)} \frac{d^m}{dt^m} \int_0^t (t-s)^{m-\kappa-1}\varphi(s)\,ds,$$

where $1 + [\kappa] = m$.

Definition 3. *The Mittag-Leffler function $E_{\kappa,\widehat{\kappa}}(\cdot)$ is given by*

$$E_{\kappa,\widehat{\kappa}}(\zeta) = \sum_{j=0}^{\infty} \frac{\zeta^j}{\Gamma(\kappa j + \widehat{\kappa})}.$$

For $\widehat{\kappa} = 1$, it is denoted by $E_\kappa(\cdot)$.
Consider the complete normed space

$$C_{1-\kappa}([0,\hbar];V) = \{\varphi : t^{1-\kappa}\varphi(t) \in C([0,\hbar];V)\}$$

with the norm

$$\|\varphi\|_{C_{1-\kappa}} = \sup_{t\in[0,\hbar]} \{t^{1-\kappa}\|\varphi(t)\|_V\},$$

where $C([0,\hbar];V)$ is the set of V-valued continuous functions defined on $[0,\hbar]$. For C_0-semigroup $T(t)$, we assume $\sup_{t\in[0,\hbar]} \|T(t)\| \le \lambda_T < \infty$.

Definition 4. *[38] A function $z \in C_{1-\kappa}([0,\hbar];V)$ is said to be a mild solution of (1) if*

$$\begin{aligned} z(t) =& t^{\kappa-1}T_\kappa(t)y_0 + \int_0^t (t-s)^{\kappa-1} \\ &\cdot T_\kappa(t-s)\Bigg(\sum_{j=0}^{m} B_j u(s-b_j) \\ &+ f\left(s, z(s), \int_0^s \xi(s,\varsigma,z(\varsigma))\,d\varsigma\right)\Bigg)ds, \end{aligned} \tag{2}$$

where

$$T_\kappa(t) = \kappa \int_0^\infty \vartheta \zeta_\kappa(\vartheta) T(t^\kappa \vartheta) d\vartheta,$$

$$\zeta_\kappa(\vartheta) = \frac{1}{\kappa}\vartheta^{-1-\frac{1}{\kappa}}\omega_\kappa\left(\vartheta^{-\frac{1}{\kappa}}\right),$$

$$\omega_\kappa(\vartheta) = \frac{1}{\pi}\sum_{j=1}^{\infty}\frac{(-1)^{j-1}\Gamma(j\kappa+1)}{\vartheta^{j\kappa+1}j!}\sin(j\pi\kappa),$$
$$0<\vartheta<\infty.$$

Definition 5. *The set given by*

$$\mathfrak{R}_\hbar(f) = \{z_u(\hbar)\in V : u\in U\}$$

is called the reachable set of (1), where $z_u(\cdot)$ is the mild solution of (1) corresponding to u.

Definition 6. *The system (1) is said to be approximately controllable on $[0,\hbar]$ if $\overline{\mathfrak{R}_\hbar(f)} = V$.*

Lemma 1. *[34] For every $t\in[0,\infty)$, $T_\kappa(t)$ is continuous linear map such that*

$$\|T_\kappa(t)y\| \le \frac{\lambda_T}{\Gamma(\kappa)}\|y\| \ \forall\ y\in V.$$

Lemma 2. *[38] If the semigroup $T(t)$ generated by A is differentiable, then*

(i) $T_\kappa(t)y\in D(A)\quad\forall\ t>0$ and $y\in V$;

(ii) $T_\kappa(t_1)T_\kappa(t_2) = T_\kappa(t_2)T_\kappa(t_1)\ \forall\ t_1,t_2>0$;

(iii) $\frac{dT^2_\kappa(t)y}{dt} = 2T_\kappa(t)\frac{dT_\kappa(t)y}{dt},\ t>0,\ y\in V$;

(iv) for any $y\in D(A)$, there is a $\varphi\in Z$ such that $\int_0^\hbar(\hbar-s)^{\kappa-1}T_\kappa(\hbar-s)\varphi(s)\,ds = y$.

3. Existence and Uniqueness of Mild Solution

To derive the existence result we assume the following:

(A_1) $T(t)$ is continuous with respect to operator norm for $t>0$.

(A_2) there is a $\lambda_f>0$ satisfying
$$\|f(t,y_1,y_1^*)-f(t,y_2,y_2^*)\| \le \lambda_f\left(\|y_1-y_2\|+\|y_1^*-y_2^*\|\right)$$
for all $y_i,y_i^*\in V,\ i=1,2,$

(A_3) there is a $\wp\in L_p([0,\hbar];\mathbb{R})$, and a $\lambda_f'>0$ such that
$$\|f(t,y,y^*)\| \le \wp(t)+\lambda_f' t^{1-\kappa}\left(\|y\|+\|y^*\|\right)$$
for a.e. $t\in[0,\hbar]$ and $y,y^*\in V$,

(A_4) there is a $\lambda_\xi>0$ verifying
$$\|\xi(t,s,y_1)-\xi(t,s,y_2)\| \le \lambda_\xi\|y_1-y_2\|$$
forall $y_1,y_2\in V$;

(A_5) there is a $\Theta\in L_p([0,\hbar];\mathbb{R})$ verifying
$$\|\xi(t,s,y)\|\le\Theta(s)$$
for all $(t,s)\in\Delta$ and $y\in V$.

Theorem 1. *Suppose assumptions (A_1)-(A_5) are true. Then, for each $u\in U$, the semilinear system (1) admits exactly one mild solution in $C_{1-\kappa}([0,\hbar];V)$.*

Proof. It is enough to prove that, the function $\mathcal{E}: C_{1-\kappa}([0,\hbar];V)\to C_{1-\kappa}([0,\hbar];V)$ defined by

$$\begin{aligned}(\mathcal{E}z)(t) &= t^{\kappa-1}T_\kappa(t)y_0 + \int_0^t (t-s)^{\kappa-1}\\ &\cdot T_\kappa(t-s)\Bigg(\sum_{j=0}^{m}B_j u(s-b_j)\\ &+ f\Big(s,z(s),\int_0^s\xi(s,\varsigma,z(\varsigma))\,d\varsigma\Big)\Bigg)\,ds,\end{aligned}$$

has exactly one fixed point in $C_{1-\kappa}([0,\hbar];V)$. Due to above assumptions, the function $\mathcal{E}$ is well defined.
Let $z,z^*\in C_{1-\kappa}([0,\hbar];V)$. Then,

$$\begin{aligned}&t^{1-\kappa}\|(\mathcal{E}z)(t)-(\mathcal{E}z^*)(t)\|\\
&\le t^{1-\kappa}\int_0^t\Bigg\|(t-s)^{\kappa-1}T_\kappa(t-s)\\
&\cdot\Bigg(f\Big(s,z(s),\int_0^s\xi(s,\varsigma,z(\varsigma))\,d\varsigma\Big)\\
&-f\Big(s,z^*(s),\int_0^s\xi(s,\varsigma,z^*(\varsigma))\,d\varsigma\Big)\Bigg)\Bigg\|\,ds\\
&\le\frac{\lambda_T\lambda_f}{\Gamma(\kappa)}t^{1-\kappa}\int_0^t(t-s)^{\kappa-1}\Bigg(\|z(s)-z^*(s)\|\\
&+\int_0^s\|\xi(s,\varsigma,z(\varsigma))-\xi(s,\varsigma,z^*(\varsigma))\|\,d\varsigma\Bigg)\,ds\\
&\le\frac{\lambda_T\lambda_f}{\Gamma(\kappa)}t^{1-\kappa}\int_0^t(t-s)^{\kappa-1}\\
&\cdot\Bigg(s^{\kappa-1}s^{1-\kappa}\|z(s)-z^*(s)\|\\
&+\lambda_\xi\int_0^s\varsigma^{\kappa-1}\varsigma^{1-\kappa}\|z(\varsigma)-z^*(\varsigma)\|\,d\varsigma\Bigg)\,ds\\
&\le\frac{\lambda_T\lambda_f}{\Gamma(\kappa)}t^{1-\kappa}\int_0^t(t-s)^{\kappa-1}\left(s^{\kappa-1}+\lambda_\xi\frac{s^\kappa}{\kappa}\right)\,ds\\
&\cdot\|z-z^*\|_{C_{1-\kappa}}\\
&=\frac{\lambda_T\lambda_f}{\Gamma(\kappa)}t^\kappa\left(\frac{(\Gamma(\kappa))^2}{\Gamma(2\kappa)}+\frac{\lambda_\xi\Gamma(\kappa)\Gamma(\kappa+1)t}{\kappa\Gamma(2\kappa+1)}\right)\\
&\cdot\|z-z^*\|_{C_{1-\kappa}}\\
&\le\frac{\Gamma(\kappa)\lambda_T\lambda_f}{\Gamma(2\kappa)}t^\kappa\left(1+\frac{\lambda_\xi\hbar}{2\kappa}\right)\|z-z^*\|_{C_{1-\kappa}}.\end{aligned}$$

Repeating the above process, we can get

$$\begin{aligned}&t^{1-\kappa}\|(\mathcal{E}^n z)(t)-(\mathcal{E}^n z^*)(t)\|\\
&\le\frac{\Gamma(\kappa)(\lambda_T\lambda_f)^n}{\Gamma((n+1)\kappa)}t^{n\kappa}\left(\prod_{i=1}^{n}\left(1+\frac{\lambda_\xi\hbar}{(i+1)\kappa}\right)\right)\\
&\cdot\|z-z^*\|_{C_{1-\kappa}}\end{aligned}$$

$$\leq \frac{\Gamma(\kappa)\left(\lambda_T\lambda_f\hbar^\kappa\left(1+\frac{\lambda_\xi\hbar}{2\kappa}\right)\right)^n}{\Gamma((n+1)\kappa)}\|z-z^*\|_{C_{1-\kappa}}.$$

Therefore,

$$\|\mathcal{E}^n z-\mathcal{E}^n z^*\|_{C_{1-\kappa}} \leq \frac{\Gamma(\kappa)\left(\lambda_T\lambda_f\hbar^\kappa\left(1+\frac{\lambda_\xi\hbar}{2\kappa}\right)\right)^n}{\Gamma((n+1)\kappa)}\|z-z^*\|_{C_{1-\kappa}}.$$

We know that the Mittag-Leffler series

$$E_{\kappa,\kappa}\left(\lambda_T\lambda_f\hbar^\kappa\left(1+\frac{\lambda_\xi\hbar}{2\kappa}\right)\right) = \sum_{i=0}^{\infty}\frac{\left(\lambda_T\lambda_f\hbar^\kappa\left(1+\frac{\lambda_\xi\hbar}{2\kappa}\right)\right)^i}{\Gamma((i+1)\kappa)}$$

is convergent. Therefore, for sufficiently large value of n,

$$\frac{\left(\lambda_T\lambda_f\hbar^\kappa\left(1+\frac{\lambda_\xi\hbar}{2\kappa}\right)\right)^n}{\Gamma((n+1)\kappa)} < \frac{1}{\Gamma(\kappa)}.$$

Thus, from Banach contraction principle $\mathcal{E}$ has exactly one fixed point in $C_{1-\kappa}([0,\hbar];V)$. ☐

4. Controllability analysis

Define the operator $\Psi_f : C_{1-\kappa}([0,\hbar];V) \to Z$ given by

$$(\Psi_f(\omega))(t) = f\left(t,\omega(t),\int_0^t \xi(t,s,\omega(s))\,ds\right),\quad \omega\in C_{1-\kappa}([0,\hbar];V)$$

and the bounded linear operator $\Phi : Z\to V$ given by

$$\Phi(\omega)=\int_0^\hbar(\hbar-s)^{\kappa-1}T_\kappa(\hbar-s)\omega(s)\,ds,\ \omega\in Z.$$

Remark 1. *From Definition 6, the system (1) is approximately controllable if and only if for each $\varepsilon>0$ and a $\widehat{y}\in V$, there exists a control $u_\varepsilon\in U$ such that the mild solution z_ε corresponding to u_ε satisfies*

$$\left\|\widetilde{y}-\Phi(\Psi_f(z_\varepsilon))-\Phi\left(\sum_{j=0}^m B_j u_\varepsilon(\cdot-b_j)\right)\right\|\leq\varepsilon,$$

where $\widetilde{y}=\widehat{y}-\hbar^{\kappa-1}T_\kappa(\hbar)y_0$.

To prove the controllability of original system, we assume the following:

(A_6) there is a $\widehat{\lambda}_f>0$ verifying
$$\|f(t,y_1,y_1^*)-f(t,y_2,y_2^*)\| \leq \widehat{\lambda}_f t^{1-\kappa}\left(\|y_1-y_2\|+\|y_1^*-y_2^*\|\right)$$
forall $y_i,y_i^*\in V,\ i=1,2$;

(A_7) there is a $\widehat{\lambda}_\xi>0$ verifying
$$\|\xi(t,s,y_1)-\xi(t,s,y_2)\|\leq\widehat{\lambda}_\xi s^{1-\kappa}\|y_1-y_2\|$$
forall $y_i\in V,\ i=1,2$;

(A_8) for given $\varepsilon>0$ and a $z\in Z$, we can get a $u\in U$ such that
$$\|\Phi(z)-\Phi(B_0u)\|_V\leq\varepsilon$$
and
$$\|B_0u\|_Z\leq\lambda_0\|z\|_Z,$$
where λ_0 is constant and it does not dependent on z;

(A_9) $0<\frac{\lambda_T\widehat{\lambda}_f\lambda_0\lambda_p\hbar\left(1+\widehat{\lambda}_\xi\hbar^{2-\kappa}\right)E_\kappa\left(\lambda_T\widehat{\lambda}_f\hbar\right)}{\Gamma(\kappa)-\lambda_T\widehat{\lambda}_f\widehat{\lambda}_\xi\hbar^{3-\kappa}\kappa^{-1}E_\kappa\left(\lambda_T\widehat{\lambda}_f\hbar\right)}<1$, where $\lambda_p=\left(\frac{p-1}{p\kappa-1}\right)^{1-\frac{1}{p}}$;

(A_{10}) $R(B_0)\supseteq R(B_1)\supseteq\cdots\supseteq R(B_m)$, where R stands for the range of operators.

Remark 2. *Note that (A_2) and (A_4) are weaker assumptions than (A_6) and (A_7), respectively. Thus, by Theorem 1, the semilinear system (1) admits a unique solution in $C_{1-\kappa}([0,\hbar];V)$ for fixed $u\in U$ if assumptions (A_1), (A_3) and (A_5)-(A_7) are true.*

We derive the following lemma:

Lemma 3. *Under assumptions (A_1), (A_3), (A_5)-(A_7) and (A_9) any mild solutions of (1) satisfy the following*

(i)
$$\|z\|_{C_{1-\kappa}}\leq k_1E_\kappa\left(\lambda_T\lambda_f'\hbar\right),\ u\in U,$$

(ii)
$$\|z_1-z_2\|_{C_{1-\kappa}}\leq k_2E_\kappa\left(\lambda_T\widehat{\lambda}_f\hbar\right)\left\|\sum_{j=0}^m B_ju_1(\cdot-b_j)-\sum_{j=0}^m B_ju_2(\cdot-b_j)\right\|_Z,\quad u_1,u_2\in U,$$

where

$$k_1=\frac{\lambda_T}{\Gamma(\kappa)}\left[\|y_0\|+\lambda_p\left(\left\|\sum_{j=0}^m B_ju(\cdot-b_j)\right\|_Z+\|\wp\|_{L_p}\right)\hbar^{1-\frac{1}{p}}+\lambda_f'\hbar^{3-\kappa-\frac{1}{p}}\kappa^{-1}\|\Theta\|_{L_p}\right]$$

and

$$k_2=\frac{\lambda_T\lambda_p\hbar^{1-\frac{1}{p}}}{\Gamma(\kappa)-\lambda_T\widehat{\lambda}_f\widehat{\lambda}_\xi\hbar^{3-\kappa}\kappa^{-1}E_\kappa\left(\lambda_T\widehat{\lambda}_f\hbar\right)}.$$

Proof. Let $z \in C_{1-\kappa}([0,\hbar];V)$ be a mild solution of (1) for $u \in U$, then

$$z(t) = t^{\kappa-1}T_\kappa(t)y_0 + \int_0^t (t-s)^{\kappa-1} \cdot T_\kappa(t-s)\left(\sum_{j=0}^m B_j u(s-b_j) + f\left(s, z(s), \int_0^s \xi(s,\varsigma,z(\varsigma))\,d\varsigma\right)\right) ds.$$

Therefore

$$\begin{aligned} t^{1-\kappa}\|z(t)\|_V &\le \|T_\kappa(t)y_0\| + t^{1-\kappa}\int_0^t \left\|(t-s)^{\kappa-1} \cdot T_\kappa(t-s)\left(\sum_{j=0}^m B_j u(s-b_j) + f\left(s, z(s), \int_0^s \xi(s,\varsigma,z(\varsigma))\,d\varsigma\right)\right)\right\| ds \\ &\le \frac{\lambda_T}{\Gamma(\kappa)}\left[\|y_0\| + t^{1-\kappa}\int_0^t (t-s)^{\kappa-1} \cdot \left\|\sum_{j=0}^m B_j u(s-b_j)\right\| ds + t^{1-\kappa}\int_0^t (t-s)^{\kappa-1} \left(\wp(s) + \lambda_f' s^{1-\kappa}\|z(s)\|_V + \lambda_f' s^{1-\kappa}\int_0^s \Theta(\varsigma)\,d\varsigma\right) ds\right] \\ &\le \frac{\lambda_T}{\Gamma(\kappa)}\left[\|y_0\| + \left(\frac{p-1}{p\kappa-1}\right)^{1-\frac{1}{p}} \cdot \left(\left\|\sum_{j=0}^m B_j u(\cdot-b_j)\right\|_Z + \|\wp\|_{L_p}\right)\hbar^{1-\frac{1}{p}} + \lambda_f'\hbar^{3-2\kappa-\frac{1}{p}}\int_0^t (t-s)^{\kappa-1}\,ds\|\Theta\|_{L_p} + \lambda_f'\hbar^{1-\kappa}\int_0^t (t-s)^{\kappa-1}s^{1-\kappa}\|z(s)\|_V\,ds\right] \\ &\le k_1 + \frac{\lambda_T\lambda_f'\hbar^{1-\kappa}}{\Gamma(\kappa)}\int_0^t (t-s)^{\kappa-1}s^{1-\kappa}\|z(s)\|_V\,ds. \end{aligned}$$

From Corollary 2 of [43], we obtain

$$t^{1-\kappa}\|z(t)\|_V \le k_1 E_\kappa(\lambda_T\lambda_f'\hbar).$$

Therefore,

$$\|z\|_{C_{1-\kappa}} \le k_1 E_\kappa(\lambda_T\lambda_f'\hbar).$$

Next, let $z_i \in C_{1-\kappa}([0,\hbar];V)$ be the mild solution of (1) for $u_i \in U, \quad i = 1,2$. Then

$$z_i(t) = t^{\kappa-1}T_\kappa(t)y_0 + \int_0^t (t-s)^{\kappa-1} \cdot T_\kappa(t-s)\left(\sum_{j=0}^m B_j u_i(s-b_j) + f\left(s, z_i(s), \int_0^s \xi(s,\varsigma,z_i(\varsigma))\,d\varsigma\right)\right) ds.$$

We have

$$\begin{aligned} t^{1-\kappa}\|z_1(t)-z_2(t)\|_V &\le \frac{\lambda_T}{\Gamma(\kappa)}t^{1-\kappa}\left[\int_0^t (t-s)^{\kappa-1}\left\|\sum_{j=0}^m B_j u_1(s-b_j) - \sum_{j=0}^m B_j u_2(s-b_j)\right\| ds + \int_0^t (t-s)^{\kappa-1} \cdot \left\|f\left(s, z_1(s), \int_0^s \xi(s,\varsigma,z_1(\varsigma))\,d\varsigma\right) - f\left(s, z_2(s), \int_0^s \xi(s,\varsigma,z_2(\varsigma))\,d\varsigma\right)\right\| ds\right] \\ &\le \frac{\lambda_T\lambda_p}{\Gamma(\kappa)}\hbar^{1-\frac{1}{p}}\left\|\sum_{j=0}^m B_j u_1(\cdot-b_j) - \sum_{j=0}^m B_j u_2(\cdot-b_j)\right\|_Z + \frac{\lambda_T\widehat{\lambda}_f}{\Gamma(\kappa)}\hbar^{1-\kappa} \cdot \int_0^t (t-s)^{\kappa-1}s^{1-\kappa}\left(\|z_1(s)-z_2(s)\| + \widehat{\lambda}_\xi\int_0^s \varsigma^{1-\kappa}\|z_1(\varsigma)-z_2(\varsigma)\|\,d\varsigma\right) ds \\ &\le \frac{\lambda_T\lambda_p}{\Gamma(\kappa)}\hbar^{1-\frac{1}{p}}\left\|\sum_{j=0}^m B_j u_1(\cdot-b_j) - \sum_{j=0}^m B_j u_2(\cdot-b_j)\right\|_Z + \frac{\lambda_T\widehat{\lambda}_f}{\Gamma(\kappa)}\hbar^{1-\kappa} \cdot \left(\int_0^t (t-s)^{\kappa-1}s^{1-\kappa}\|z_1(s)-z_2(s)\|\,ds + \widehat{\lambda}_\xi\int_0^t (t-s)^{\kappa-1}\hbar^{2-\kappa}\,ds\|z_1-z_2\|_{C_{1-\kappa}}\right) \\ &\le \frac{\lambda_T\lambda_p}{\Gamma(\kappa)}\hbar^{1-\frac{1}{p}}\left\|\sum_{j=0}^m B_j u_1(\cdot-b_j) - \sum_{j=0}^m B_j u_2(\cdot-b_j)\right\|_Z + \frac{\lambda_T\widehat{\lambda}_f\widehat{\lambda}_\xi}{\Gamma(\kappa)}\hbar^{3-\kappa}\kappa^{-1} \cdot \|z_1-z_2\|_{C_{1-\kappa}} + \frac{\lambda_T\widehat{\lambda}_f}{\Gamma(\kappa)}\hbar^{1-\kappa}\int_0^t (t-s)^{\kappa-1} \cdot s^{1-\kappa}\|z_1(s)-z_2(s)\|\,ds. \end{aligned}$$

From Corollary 2 of [43], we obtain

$$t^{1-\kappa}\|z_1(t)-z_2(t)\|_V \le \frac{\lambda_T}{\Gamma(\kappa)}\left[\lambda_p\hbar^{1-\frac{1}{p}}\left\|\sum_{j=0}^m B_j u_1(\cdot-b_j) - \sum_{j=0}^m B_j u_2(\cdot-b_j)\right\|_Z + \widehat{\lambda}_f\widehat{\lambda}_\xi\hbar^{3-\kappa}\kappa^{-1} \cdot \|z_1-z_2\|_{C_{1-\kappa}}\right]E_\kappa\big(\lambda_T\widehat{\lambda}_f\hbar\big).$$

Therefore,

$$\|z_1-z_2\|_{C_{1-\kappa}} \le \frac{\lambda_T}{\Gamma(\kappa)}\left[\lambda_p\hbar^{1-\frac{1}{p}}\left\|\sum_{j=0}^m B_j u_1(\cdot-b_j) - \sum_{j=0}^m B_j u_2(\cdot-b_j)\right\|_Z + \widehat{\lambda}_f\widehat{\lambda}_\xi\hbar^{3-\kappa}\kappa^{-1} \cdot \|z_1-z_2\|_{C_{1-\kappa}}\right]E_\kappa\big(\lambda_T\widehat{\lambda}_f\hbar\big).$$

This gives

$$\begin{aligned}\|z_1-z_2\|_{C_{1-\kappa}} &\le \frac{\lambda_T\lambda_p\hbar^{1-\frac{1}{p}}E_\kappa\big(\lambda_T\widehat{\lambda}_f\hbar\big)}{\Gamma(\kappa)-\lambda_T\widehat{\lambda}_f\widehat{\lambda}_\xi\hbar^{3-\kappa}\kappa^{-1}E_\kappa\big(\lambda_T\widehat{\lambda}_f\hbar\big)} \cdot\left\|\sum_{j=0}^m B_j u_1(\cdot-b_j) - \sum_{j=0}^m B_j u_2(\cdot-b_j)\right\|_Z \\ &= k_2 E_\kappa\big(\lambda_T\widehat{\lambda}_f\hbar\big) \cdot\left\|\sum_{j=0}^m B_j u_1(\cdot-b_j) - \sum_{j=0}^m B_j u_2(\cdot-b_j)\right\|_Z.\end{aligned}$$

□

Theorem 2. *Under assumptions (A_1), (A_3) and (A_5)-(A_{10}), the semilinear system (1) is approximately controllable if the semigroup $T(t)$ is differentiable.*

Proof. First we prove that for each $u^* \in U$, there is a $u \in U$ such that

$$B_0u^*(\cdot) = B_0u(\cdot) + B_1u(\cdot-b_1) + \cdots + B_mu(\cdot-b_m). \tag{3}$$

For this, set $\hbar = b_{m+1}$ and $r = \min\{b_j - b_{j-1} : j = 1,2,\ldots,m+1\}$. Since $0 = b_0 < b_1 < b_2 < \cdots < b_m < b_{m+1}$ therefore for each b_{j+1} there exist a positive integer n_j and a constant $\vartheta_j \in [0,r)$ such that $b_{j+1} = b_j + n_jr + \vartheta_j$, $j = 1,2,\ldots,m$. For $t \in [0,b_1]$, we have

$$B_0u^*(\cdot) - B_1u(\cdot-b_1) - \cdots - B_mu(\cdot-b_m) = B_0u^*(\cdot).$$

Take $u(t) = u^*(t)$ for $t \in [0,b_1]$. For $t \in (b_1, b_1+r]$, we have $(t-b_1) \in (0,r] \subset (0,b_1]$ and

$$B_0u^*(\cdot) - B_1u(\cdot-b_1) - \cdots - B_mu(\cdot-b_m) = B_0u^*(\cdot) - B_1u^*(\cdot-b_1) = B_0u_{11}(\cdot)(say),$$

where $u_{11}(\cdot)$ is known. Take $u(t) = u_{11}(t)$ for $t \in (b_1, b_1+r]$.

Now, if $t \in (b_1+r, b_1+2r]$, then $(t-b_1) \in (r,2r] \subset (0, b_1+r]$ and $u(\cdot-b_1)$ is known. Therefore, in this case

$$B_0u^*(\cdot) - B_1u(\cdot-b_1) - \cdots - B_mu(\cdot-b_m) = B_0u^*(\cdot) - B_1u(\cdot-b_1) = B_0u_{12}(\cdot)(say),$$

where $u_{12}(\cdot)$ is known. Take $u(t) = u_{12}(t)$ for $t \in (b_1+r, b_1+2r]$. Similarly, we can find $u_{13}(\cdot), u_{14}(\cdot), \ldots, u_{1n_1}(\cdot)$ for the intervals $(b_1+2r, b_1+3r], (b_1+3r, b_1+4r], \ldots, (b_1+(n_1-1)r, b_1+n_1r]$; respectively. If $\vartheta_1 > 0$, then we can also find $u_{1\overline{n_1+1}}(\cdot)$ for the next interval $(b_1+n_1r, b_1+n_1r+\vartheta_1]$. Thus $u(\cdot)$ is completely known for $t \in (b_1, b_1+n_1r+\vartheta_1] = (b_1,b_2]$. Denote $u(\cdot)$ by $u_1(\cdot)$ for $t \in (b_1, b_2]$.

Repeating the above process, one can obtain $u_2(\cdot), u_3(\cdot), \ldots, u_m(\cdot)$ for the intervals $(b_2,b_3], (b_3,b_4], \ldots, (b_m, b_{m+1}]$; respectively. Hence the control function $u(\cdot) \in U$, given by

$$u(t) = \begin{cases} u^*(t), & t \in [0,b_1]; \\ u_j(t), & t \in (b_j, b_{j+1}], \quad j = 1,2,\ldots,m \end{cases}$$

is completely known and it satisfies

$$B_0u^*(\cdot) - B_1u(\cdot-b_1) - \cdots - B_mu(\cdot-b_m) = B_0u(\cdot).$$

Next, we prove that $D(A) \subseteq \overline{\mathfrak{R}_\hbar(f)}$, that is, for any $\varepsilon > 0$ and $\widehat{y} \in D(A)$, we are able to find a control $u_\varepsilon \in U$ satisfying

$$\left\|\widetilde{y} - \Phi(\Psi_f(z_\varepsilon)) - \Phi\left(\sum_{j=0}^m B_ju_\varepsilon(\cdot-b_j)\right)\right\|_V \le \varepsilon,$$

where $\widetilde{y} = \widehat{y} - \hbar^{\kappa-1}T_\kappa(\hbar)y_0$ and $z_\varepsilon(t) = z_{u_\varepsilon}(t)$. By Lemma 2, there is a $\wp \in Z$ such that $\Phi(\wp) = \widetilde{y}$. Let $\varepsilon > 0$ be given and $v_1 \in U$. Then by assumption (A_8) and (3), there is a control $v_2 \in U$ such that

$$\left\|\widetilde{y} - \Phi(\Psi_f(z_1)) - \Phi\left(\sum_{j=0}^m B_jv_2(\cdot-b_j)\right)\right\|_V \le \frac{\varepsilon}{3^2},$$

where $z_1(t) = z_{v_1}(t)$. Denote $z_2(t) = z_{v_2}(t)$, in view of (A_8) and (3), there is a control $\omega_2 \in U$

such that

$$\left\|\Phi(\Psi_f(z_2)-\Psi_f(z_1)) - \Phi\left(\sum_{j=0}^{m} B_j\omega_2(\cdot-b_j)\right)\right\|_V \le \frac{\varepsilon}{3^3}$$

and

$$\begin{aligned}
&\left\|\sum_{j=0}^{m} B_j\omega_2(\cdot-b_j)\right\|_Z \\
&\le \lambda_0 \|\Psi_f(z_2)-\Psi_f(z_1)\|_Z \\
&= \lambda_0\left[\int_0^{\hbar}\left\|f\left(t, z_2(t), \int_0^t \xi(t,\varsigma,z_2(\varsigma))\,d\varsigma\right)\right.\right. \\
&\qquad \left.\left. - f\left(t, z_1(t), \int_0^t \xi(t,\varsigma,z_1(\varsigma))\,d\varsigma\right)\right\|_V^p dt\right]^{\frac{1}{p}} \\
&\le \lambda_0\widehat{\lambda}_f\left[\int_0^{\hbar}\left(t^{1-\kappa}\|z_2(t)-z_1(t)\|\right.\right. \\
&\qquad \left.\left. + \widehat{\lambda}_\xi t^{1-\kappa}\int_0^t \varsigma^{1-\kappa}\|z_2(\varsigma)-z_1(\varsigma)\|\,d\varsigma\right)^p dt\right]^{\frac{1}{p}} \\
&\le \lambda_0\widehat{\lambda}_f\left(\int_0^{\hbar}\left(1+\widehat{\lambda}_\xi\hbar^{2-\kappa}\right)^p dt\right)^{\frac{1}{p}}\|z_2-z_1\|_{C_{1-\kappa}} \\
&= \lambda_0\widehat{\lambda}_f\hbar^{\frac{1}{p}}\left(1+\widehat{\lambda}_\xi\hbar^{2-\kappa}\right)\|z_2-z_1\|_{C_{1-\kappa}} \\
&\le \lambda_0\widehat{\lambda}_f\hbar^{\frac{1}{p}}\left(1+\widehat{\lambda}_\xi\hbar^{2-\kappa}\right)k_2E_\kappa\left(\lambda_T\widehat{\lambda}_f\hbar\right) \\
&\qquad \cdot\left\|\sum_{j=0}^{m} B_ju_1(\cdot-b_j)-\sum_{j=0}^{m} B_ju_2(\cdot-b_j)\right\|_Z \\
&= \frac{\lambda_T\widehat{\lambda}_f\lambda_0\lambda_p\hbar\left(1+\widehat{\lambda}_\xi\hbar^{2-\kappa}\right)E_\kappa\left(\lambda_T\widehat{\lambda}_f\hbar\right)}{\Gamma(\kappa)-\lambda_T\widehat{\lambda}_f\widehat{\lambda}_\xi\hbar^{3-\kappa}\kappa^{-1}E_\kappa\left(\lambda_T\widehat{\lambda}_f\hbar\right)} \\
&\qquad \cdot\left\|\sum_{j=0}^{m} B_jv_1(\cdot-b_j)-\sum_{j=0}^{m} B_jv_2(\cdot-b_j)\right\|_Z.
\end{aligned}$$

Now, if we define

$$v_3(t)=v_2(t)-\omega_2(t), \quad v_3\in U,$$

then

$$\begin{aligned}
&\left\|\widetilde{y}-\Phi(\Psi_f(z_2))-\Phi\left(\sum_{j=0}^{m} B_jv_3(\cdot-b_j)\right)\right\|_V \\
&\le \left\|\widetilde{y}-\Phi(\Psi_f(z_1))-\Phi\left(\sum_{j=0}^{m} B_jv_2(\cdot-b_j)\right)\right\|_V \\
&\quad + \left\|\Phi(\Psi_f(z_2)-\Psi_f(z_1)) - \Phi\left(\sum_{j=0}^{m} B_j\omega_2(\cdot-b_j)\right)\right\|_V \\
&\le \left(\frac{1}{3^2}+\frac{1}{3^3}\right)\varepsilon.
\end{aligned}$$

By inductions, we get a sequence $\{v_n\}$ in U satisfying

$$\begin{aligned}
&\left\|\widetilde{y}-\Phi(\Psi_f(z_n))-\Phi\left(\sum_{j=0}^{m} B_jv_{n+1}(\cdot-b_j)\right)\right\|_V \\
&\le \left(\frac{1}{3^2}+\frac{1}{3^3}+\cdots+\frac{1}{3^{n+1}}\right)\varepsilon,
\end{aligned}$$

where $z_n(t)=z_{v_n}(t)$, and

$$\begin{aligned}
&\left\|\sum_{j=0}^{m} B_jv_{n+1}(\cdot-b_j)-\sum_{j=0}^{m} B_jv_n(\cdot-b_j)\right\|_Z \\
&\le \frac{\lambda_T\widehat{\lambda}_f\lambda_0\lambda_p\hbar\left(1+\widehat{\lambda}_\xi\hbar^{2-\kappa}\right)E_\kappa\left(\lambda_T\widehat{\lambda}_f\hbar\right)}{\Gamma(\kappa)-\lambda_T\widehat{\lambda}_f\widehat{\lambda}_\xi\hbar^{3-\kappa}\kappa^{-1}E_\kappa\left(\lambda_T\widehat{\lambda}_f\hbar\right)} \\
&\qquad \cdot\left\|\sum_{j=0}^{m} B_jv_n(\cdot-b_j)-\sum_{j=0}^{m} B_jv_{n-1}(\cdot-b_j)\right\|_Z,
\end{aligned}$$

which shows that the sequence

$$\left\{\sum_{j=0}^{m} B_jv_n(\cdot-b_j) : n=1,2,\ldots\right\}$$

is Cauchy in Z. Since Z is complete and Φ is bounded therefore, the sequence

$$\left\{\Phi\left(\sum_{j=0}^{m} B_jv_n(\cdot-b_j)\right) : n=1,2,\ldots\right\}$$

is Cauchy in V. Thus, we can get a $n_0\in\mathbb{N}$ such that

$$\left\|\Phi\left(\sum_{j=0}^{m} B_jv_{n_0+1}(\cdot-b_j)\right) - \Phi\left(\sum_{j=0}^{m} B_jv_{n_0}(\cdot-b_j)\right)\right\|_V \le \frac{\varepsilon}{3}.$$

Now,

$$\begin{aligned}&\left\|\widetilde{y}-\Phi(\Psi_f(z_{n_0}))-\Phi\left(\sum_{j=0}^{m}B_jv_{n_0}(\cdot-b_j)\right)\right\|_V\\
&\leq\left\|\widetilde{y}-\Phi(\Psi_f(z_{n_0}))\right.\\
&\qquad\left.-\Phi\left(\sum_{j=0}^{m}B_jv_{n_0+1}(\cdot-b_j)\right)\right\|_V\\
&\qquad+\left\|\Phi\left(\sum_{j=0}^{m}B_jv_{n_0+1}(\cdot-b_j)\right)\right.\\
&\qquad\quad\left.-\Phi\left(\sum_{j=0}^{m}B_jv_{n_0}(\cdot-b_j)\right)\right\|_V\\
&\qquad\leq\left(\frac{1}{3^2}+\frac{1}{3^3}+\cdots+\frac{1}{3^{n_0+1}}\right)\varepsilon+\frac{\varepsilon}{3}\\
&\qquad<\varepsilon.\end{aligned}$$

As $D(A)$ is dense in V therefore, $\overline{\mathfrak{R}_\hbar(f)}=V$. ☐

5. Example

For $x\in[0,\pi]$, consider the system with the given boundary condition

$$\begin{cases}D_t^{\frac{2}{3}}z(t,x)=\frac{\partial^2}{\partial x^2}z(t,x)+\sum_{j=0}^{m}u(t-b_j)\\
+f\big(t,z(t,x),\int_0^t\xi(t,s,z(s,x))\,ds\big),\quad 0<t\leq1,\\
I_t^{\frac{1}{3}}z(t,x)\big|_{t=0}=y_0(x),u(t)=0,\quad -b_m\leq t\leq0,\\
z(t,0)=z(t,\pi)=0,\qquad 0<t\leq1,\end{cases}\tag{4}$$

where $0=b_0<b_1<\cdots<b_m<1$.
Take $V=V'=L_2[0,\pi]$ and $A:D(A)\subset V\to V$ given by

$$Ay=y_{xx}$$

with the domain

$$\begin{aligned}D(A)=\{y\in V: y,\ y_x\quad &\text{are absolutely continuous}\\ &\text{and } y_x\in V,\ y(0)=0=y(\pi)\}.\end{aligned}$$

Then, A has the spectral representation

$$Ay=\sum_{n=1}^{\infty}(-n^2)\langle y,q_n\rangle q_n,\quad y\in D(A),$$

which generates a semigroup $T(t)$ given by

$$T(t)y=\sum_{n=1}^{\infty}\exp(-n^2t)\langle y,q_n\rangle q_n,\quad y\in V$$

with

$$\|T(t)\|\leq\exp(-1)<1;$$

where $q_n(x)=\sqrt{\frac{2}{\pi}}\sin nx$ are eigen functions of A associated with the eigenvalues $\lambda_n=-n^2$, $n\in\mathbb{N}$ and the set $\{q_n:n\in\mathbb{N}\}$ form an orthonormal basis for V.
If we take

$$z^*(t,x)=\int_0^t\xi(t,s,z(s,x))\,ds$$

and

$$\begin{aligned}&f\left(t,z(t,x),z^*(t,x)\right)\\
&=f\left(t,z(t,x),\int_0^t\xi(t,s,z(s,x))\,ds\right)\\
&=(1+t^2)+k_0t^{a_0}\bigg(z(t,x)+\int_0^tk_1\left(t^2+s^2\right)s^{a_1}\\
&\quad\cdot\cos(ts)\cos(1+z(s,x))\,ds\bigg),\end{aligned}$$

where

$$\xi(t,s,z(s,x))=k_1\left(t^2+s^2\right)s^{a_1}\cos(ts)\cos(1+z(s,x))$$

and $a_i\geq1-\kappa,\ i=0,1$. Then (A_2), (A_3) and (A_6) are satisfied with $\lambda_f=\lambda'_f=\widehat{\lambda}_f=|k_0|$. Also, the conditions (A_4) and (A_7) are satisfied with $\lambda_\xi=\widehat{\lambda}_\xi=4|k_1|$.
Now,

$$\begin{aligned}\|\xi(t,s,z(s,\cdot))\|&\leq|k_1|\left(1+s^2\right)s^{a_1}\\&=\Theta(s)\in L_p([0,1];\mathbb{R}^+).\end{aligned}$$

Hence (A_5) is satisfied. If we choose the constants k_0 and k_1 small enough so that (A_9) is satisfied, then from Theorem 2, the approximate controllability of (4) follows.

References

[1] Kilbas, A.A., Srivastava, H.M. & Trujillo J.J. (2006). *Theory and Applications of Fractional Differential Equations.* North-Holland Math. Stud., 204, Elsevier Science, Amsterdam.

[2] Heymans, N. & Podlubny, I. (2006). Physical interpretation of initial conditions for fractional differential equations with Riemann-Liouville fractional derivatives. *Rheologica Acta,* 45, 765-771.

[3] Galucio, A.C., Deu, J.F. & Ohayon, R. (2005). A fractional derivative viscoelastic model for hybrid active-passive damping treatments in time domain-application to sandwich beams. *Journal of Intelligent Material Systems and Structures,* 16(1), 33-45.

[4] Baleanu, D. & Golmankhaneh, A.K. (2010). On electromagnetic field in fractional space. *Nonlinear Analysis: Real World Applications,* 11(1), 288-292.

[5] Hilfer, R. (2000). *Applications of Fractional Calculus in Physics.* Singapore: World Scientfic Publ Co.

[6] Jia, J.H., Shen, X.Y. & Hua, H.X. (2007). Viscoelastic behavior analysis and application of the fractional derivative Maxwell model. *Journal of Vibration and Control,* 13(4), 385-401.

[7] Koeller, R.C. (1984). Applications of fractional calculus to the theory of viscoelasticity. *Journal of Applied Mechanics,* 51(2), 299-307.

[8] Li, J., Liu, F., Feng, L. & Turner I. (2017). A novel finite volume method for the Riesz space distributed-order diffusion equation. *Computers & Mathematics with Applications,* 74, 772-783.

[9] Liu, X.Y., Liu, Z.H. & Fu, X. (2014). Relaxation in nonconvex optimal control problems described by fractional differential equations. *Journal of Mathematical Analysis and Applications,* 409(1), 446-458.

[10] Liu, Z.H., Zeng, S.D. & Bai, Y.R. (2016). Maximum principles for multi-term space-time variable-order fractional diffusion equations and their applications.*Fractional Calculus and Applied Analysis,* 19(1), 188-211.

[11] Liu, Z.H. & Zeng, S.D. (2017). Differential variational inequalities in infinite Banach spaces. *Acta Mathematica Scientia,* 37B(1), 26-32.

[12] Samko, S.G., Kilbas, A.A. & Marichev, O.I. (1993). *Fractional Integral and Derivatives: Theory and Applications*, Gordon and Breach, New York.

[13] Podlubny, I. (1999). *Fractional Differential Equations,* Academic Press, San Diego, CA.

[14] Balachandran, K., Govindaraj, V. , Rivero, M. & Trujillo J.J. (2015). Controllability of fractional damped dynamical systems. *Applied Mathematics and Computation,* 257, 66-73.

[15] Liu, Z.H., Sun, J.H. & Szanto, I. (2013). Monotone iterative technique for Riemann-Liouville fractional integrodifferential equations with advanced arguments. *Results in Mathematics,* 63, 1277–1287.

[16] Hosseini, S.M. & Shahmorad, S. (2003). Numerical solution of a class of integrodifferential equations by the tau method with an error estimation.*Applied Mathematics and Computation,* 136(2-3), 559-570.

[17] Shakeri, F. & Dehghan, M. (2013). A high order finite volume element method for solving elliptic partial integrodifferential equations. *Applied Numerical Mathematics,* 65, 105-118.

[18] Dehghan, M. & Salehi, R. (2012). The numerical solution of the non-linear integrodifferential equations based on the meshless method. *Journal of Computational and Applied Mathematics,* 236(9), 2367-2377.

[19] Dehghan, M. (2006). Solution of a partial integrodifferential equation arising from viscoelasticity. *International Journal of Computer Mathematics,* 83(1), 123-129.

[20] Wang, L. (2009). Approximate controllability of integrodifferential equations with multiple delays. *Journal of Optimization Theory and Applications,* 143, 185-206.

[21] Ji, S. & Yang, D. (2019). Solution to Riemann-Liouville fractional integrodifferential equations via fractional resolvents. *Advances in Difference Equations,* 524, 1-17.

[22] Sheng, J. & Jiang, W. (2017). Existence and uniqueness of the solution of fractional damped dynamical systems. *Advances in Continuous and Discrete Models,* 16, 1-14.

[23] Davies, I. & Jackreece, P. (2005). Controllability and null controllability of linear systems. *Journal of Applied Sciences and Environmental Management,* 9, 31-36.

[24] Haq, A. & Sukavanam, N. (2020). Controllability of second-order nonlocal retarded semilinear systems with delay in control. *Applicable Analysis,* 99(16), 2741-2754.

[25] Klamka, J. (2009). Constrained controllability of semilinear systems with delays. *Nonlinear Dynamics,* 56, 169-177.

[26] Liu, S., Debbouche, A. & Wang, J. (2018). ILC method for solving approximate controllability of fractional differential equations with noninstantaneous impulses. *Journal of Computational and Applied Mathematics,* 339, 343-355.

[27] Kumar, S. & Sukavanam, N. (2012). Approximate controllability of fractional order semilinear systems with bounded delay. *Journal of Differential Equations,* 252, 6163-6174.

[28] Rykaczewski, K. (2012). Approximate controllability of differential inclutions in Hilbert spaces. *Nonlinear Analysis,* 75, 2701-2702.

[29] Wang, J.R. & Zhou, Y. (2011). A class of fractional evolution equations and optimal controls. *Nonlinear Analysis: Real World Application,* 12, 262-272.

[30] Yang, M. & Wang, Q. (2016). Approximate controllability of Riemann-Liouville fractional differential inclusions. *Applied Mathematics and Computation,* 274, 267-281.

[31] Mahmudov, N.I. & McKibben, M.A. (2015). On the Approximate controllability of fractional evolution equations with generalized Riemann-Liouville fractional derivative. *Jouranl of Function Spaces,* 2015, 1-9.

[32] Li, K., Peng, J. & Jia, J. (2012). Cauchy problems for fractional differential equations with Riemann-Liouville fractional derivatives. *Journal of Functional Analysis,* 263, 476-510.

[33] Ibrahim, BHE., Fan, Z. & Li, G. (2017). Approximate controllability for functional equations with Riemann-Liouville derivative by iterative and approximate method. *Journal of Function Spaces,* 2017, 1-7.

[34] Haq, A. (2022). Partial-approximate controllability of semi-linear systems involving two Riemann-Liouville fractional derivatives. *Chaos, Solitons & Fractals,* 157, 111923. https://doi.org/10.1016/j.chaos.2022.111923

[35] Haq, A. & Sukavanam, N. (2022). Existence and controllability of higher-order nonlinear fractional integrodifferential systems via fractional resolvent, *Mathematical Methods in the Applied Sciences,* 45(16), 9034-9048.

[36] Zhu, S., Fan, Z. & Li, G. (2018). Approximate controllability of Riemann-Liouville fractional evolution equations with integral contractor assumption. *Journal of Applied Analysis & Computation,* 8, 532-548.

[37] Chang, Y.K., Pereira, A. & Ponce, R. (2017). Approximate controllability for fractional differential equations of sobolev type via properties on resolvent operators. *Fractional Calculus and Applied Analysis,* 20(4), 963-987.

[38] Liu, Z. & Li, X. (2015). Approximate controllability of fractional evolution systems with Riemann–Liouville fractional derivatives. *SIAM Journal on Control Optimization,* 53(1), 1920-1933.

[39] He, B., Zhou, H. & Kou, C. (2016). The controllability of fractional damped dynamical systems with control delay. *Communications in Nonlinear Science and Numerical Simulation,* 32, 190-198.

[40] Debbouche, A. & Antonov, V. (2017). Approximate controllability of semilinear Hilfer fractional differential inclusions with impulsive control inclusion conditions in Banach spaces. *Chaos, Solitons & Fractals,* 102, 140-148.

[41] Li, X., Liu, Z., Li, J. & Tisdell, C. (2019). Existence and controllability for non-linear fractional control systems with damping in Hilbert spaces. *Acta Matematica Scientia,* 39B(1), 229-242.

[42] Aimene, D., Baleanu, D. & Seba, D. (2019). Controllability of semilinear impulsive Atangana-Baleanu fractional differential equations with delay.*Chaos, Solitons & Fractals,* 128, 51-57.

[43] Ye, H.P., Gao, J.M. & Ding, Y.S. (2007). A generalized Gronwall inequality and its application to a fractional differential equation. *Journal of Mathematical Analysis and Applications,* 328, 1075-1081.

[44] Haq, A. & Sukavanam, N. (2022). Mild solution and approximate controllability of second-order retarded systems with control delays and nonlocal conditions. *Bulletin of the Iranian Mathematical Society,* 48(2), 447-464.

[45] Haq, A. & Sukavanam, N. (2021). Mild solution and approximate controllability of retarded semilinear systems with control delays and nonlocal conditions. *Numerical Functional Analysis and Optimization,* 42(6), 721-737.

[46] Sharma, M. (2021). Solvability and optimal control of nonautonomous fractional dynamical systems of neutral-type with nonlocal conditions. *Iranian Journal of Science and Technology, Transaction A: Science,* 45, 2121-2133. https://doi.org/10.1007/s40995-021-01215-z

[47] Patel, R., Shukla, A. & Jadon, S.S. (2020). Existence and optimal control problem for semilinear fractional order $(1,2]$ control system. *Mathematical Methods in the Applied Sciences,* https://doi.org/10.1002/mma.6662.

[48] Shukla, A., Vijayakumar, V. & Nisar, K.S. (2021). A new exploration on the existence and approximate controllability for fractional semilinear impulsive control systems of order $r \in (1,2)$. *Chaos, Solitons & Fractals,* 1-20.

[49] Dineshkumar, C., Udhayakumar, R., Vijayakumar, V., Shukla, A. & Nisar, K.S. (2021). A note on approximate controllability for nonlocal fractional evolution stochastic integrodifferential inclusions of order $r \in (1,2)$ with delay. *Chaos, Solitons & Fractals,* 153, 111565.

[50] Shukla, A., Sukavanam, N. & Pandey, D.N. (2015). Complete controllability of semi-linear stochastic system with delay. *Rendiconti del Circolo Matematico di Palermo,* 64, 209-220.

[51] Sahijwani, L. & Sukavanam, N. (2023). Approximate controllability for Riemann-Liouville fractional differential equations. *International Journal of Optimization & Control: Theories & Applications,* 13, 59-67.

[52] Raja, M.M., Vijayakumar, V., Shukla, A., Nisar, K.S. & Baskonus, H.M. (2022). On the approximate controllability results for fractional integrodifferential systems of order $1 < r < 2$ with sectorial operators. *Journal of Computational and Applied Mathematics,* 415, 114492. https://doi.org/10.1016/j.cam.2022.114492

[53] Shukla, A., Sukavanam, N. & Pandey, D.N. (2015). Approximate controllability of semilinear fractional control systems of order $\alpha \in (1,2]$. *SIAM Proceedings of the Conference on Control and its Applications.* https://doi.org/10.1137/1.9781611974072.2

Abdul Haq *is working as an Assistant Professor in the Department of Mathematics, School of Advanced Sciences, Vellore Institute of Technology, Vellore, India. He has obtained his M.Sc. & Ph.D. from Indian Institute of Technology Roorkee, India, in the year 2020. His area of research is mathematical control theory.*

`https://orcid.org/0000-0003-1912-978X`

Nagarajan Sukavanam *is a Professor and former Head of the Department at Department of Mathematics, Indian Institute of Technology Roorkee, Roorkee, India. He has obtained his Ph.D. from Indian Institute of Science, Bangalore, India in the year 1985. He has supervised more than 25 scholars to obtain their doctorate degrees and has adjudicated several doctoral thesis from different universities. He has published more than 150 research articles in international journals of high repute.*

`https://orcid.org/0000-0001-9627-8653`

An International Journal of Optimization and Control: Theories & Applications
ISSN:2146-0957 eISSN:2146-5703
Vol.14, No.1, pp.12-19 (2024)
http://doi.org/10.11121/ijocta.1409

RESEARCH ARTICLE

On analyzing two dimensional fractional order brain tumor model based on orthonormal Bernoulli polynomials and Newton's method

Iman Masti,[a] Khosro Sayevand,[a*] Hossein Jafari[b]

[a] *Faculty of Mathematics and Statistics, Malayer University, Malayer Iran*
[b] *Department of Mathematical Sciences, University of South Africa, UNISA0003, South Africa*
iman.masty@gmail.com, ksayehvand@malayeru.ac.ir, jafariusern@gmail.com

ARTICLE INFO

Article History:
Received 31 May 2023
Accepted 19 August 2023
Available Online 8 November 2023

Keywords:
Brain tumor
Operational matrix
Orthonormal Bernoulli polynomials
Fractional Caputo derivative

AMS Classification 2010:
74J35; 76B25; 35Q53; 35R11

ABSTRACT

Recently, modeling problems in various field of sciences and engineering with the help of fractional calculus has been welcomed by researchers. One of these interesting models is a brain tumor model. In this framework, a two dimensional expansion of the diffusion equation and glioma growth is considered. The analytical solution of this model is not an easy task, so in this study, a numerical approach based on the operational matrix of conventional orthonormal Bernoulli polynomials (OBPs) has been used to estimate the solution of this model. As an important advantage of the proposed method is to obtain the fractional derivative in matrix form, which makes calculations easier. Also, by using this technique, the problem under the study is converted into a system of nonlinear algebraic equations. This system is solved via Newton's method and the error analysis is presented. At the end to show the accuracy of the work, we have examined two examples and compared the numerical results with other works.

1. Introduction

Modeling problems and natural phenomena in various sciences such as chemistry, physics, biology and even economics with the help of mathematics [1], and especially with using fractional calculus [2–8], has been welcomed by scientists. This has led to the emergence of various fractional equations, such as partial differential equations of fractional orders. Also, to improve the results and increase the accuracy of the presented models, different definitions of fractional derivatives were presented. For more details see [9–12]. Solving these problems exactly in many situations are impossible and it is necessary that some acceptable schemes are implemented to provide their approximate solution.

Glioblastoma tumor is an aggressive type of cancer that can develop in the brain, but the brain type is more common. The structure of this tumor is made up of cells called astrocytes that support the nerve cells of the brain. This cancer can occur at any age, but it is more common in the elderly. Therefore, the treatment of this tumor requires more detailed studies and better understanding of the tumor. One of these types of studies is the mathematical modeling of this brain tumor. For this reason, a model based on the two main components of cancer cell proliferation and dissemination for tumor growth and based on the Burgess equation was presented in [13] and [14]. For more details regarding the recent history of fractional calculus and brain models the reader is advised to consult the research works presented in [15] and [16].

The main two dimensional model provided for this issue is as follows [13]:

$$\frac{\partial B(e,r)}{\partial r} = D\nabla^2 B(e,r) + \rho B(e,r), \qquad (1)$$

*Corresponding Author

where D, $\partial_r B(e,r)$, $\nabla^2 B(e,r)$ and $B(e,r)$ denote the diffusion coefficient expressed as cm^2 per day, change of tumor cell density, diffusion of tumor cells and cell density at time t, respectively. Also ρ is rate of growth of cells. It should be noted that according to the two dimensional model presented in Eq. (1), the rate of change in tumor cell density is equal to the total rate of tumor cell proliferation and tumor cell growth.

In [13], Eq. (1) is given by

$$\partial_r B(e,r) = D\frac{1}{e^2}\partial_e\big(e^2\partial_e B(e,r)\big)+\rho B(e,r). \quad (2)$$

By adding a parameter based on killing to the Eq. (2), the following equation will be obtain [14]:

$$\partial_r B(e,r) = D\tfrac{1}{e^2}\partial_e\big(e^2\partial_e B(e,r)\big)+\rho B(e,r) - k_r B(e,r). \quad (3)$$

Eq. (3) can be written as follows:

$$\begin{aligned}\partial_r B(e,r) = D\Big(&\partial_{ee}B(e,r)\\ &+\frac{2}{e}\partial_e B(e,r)\Big)+(\rho-k_r)B(e,r).\end{aligned} \quad (4)$$

Suppose that $t = 2Dr, x = e$ and $\Phi(x,t) = uB(e,r)$. Therefore, we have

$$\frac{\partial r}{\partial t} = \frac{1}{2D}, \quad (5)$$

$$\partial_t\Phi(x,t) = x\partial_t B(x,r) = \frac{x}{2D}\partial_r B(x,r), \quad (6)$$

$$\partial_x\Phi(x,t) = x\partial_x B(x,r) + B(x,r), \quad (7)$$

$$\partial_{xx}\Phi(x,t) = x\partial_{xx}B(x,r) + 2\partial_x B(x,r). \quad (8)$$

From Eqs. (6-8), one will set

$$\begin{aligned}\partial_r B(x,r) &= \frac{2D}{x}\partial_t\Phi(x,t),\\ \partial_x B(x,r) &= \frac{1}{x}\big(\partial_x\Phi(x,t) - B(x,r)\big),\\ \partial_{xx}B(x,r) &= \frac{1}{x}\big(\partial_{xx}\Phi(x,t) - 2\partial_x B(x,r)\big).\end{aligned}$$

Thus, Eq. (4) becomes to

$$\partial_t\Phi(x,t) = \frac{1}{2}\partial_{xx}\Phi(x,t) + \frac{\rho-k_t}{2D}\Phi(x,t). \quad (9)$$

Let $S(x,t) = \frac{\rho-k_t}{2D}\Phi(x,t)$ and suppose that $\Phi(x,t_0)$ is initial growth profile. Then, the following model is achieved:

$$\begin{aligned}&\partial_t\Phi(x,t) = \frac{1}{2}\partial_{xx}\Phi(x,t) + S(x,t), \quad (10)\\ &\Phi(x,t_0) = \xi(x), \quad x,t\in(a,b).\end{aligned}$$

The fractional model of Eq. (10) can be expressed as follows:

$$\begin{aligned}&\partial_t^\varsigma\Phi(x,t) = \frac{1}{2}\partial_{xx}\Phi(x,t) + S(x,t), \quad (11)\\ &\Phi(x,t_0) = \xi(x),\end{aligned}$$

where ∂_t^ς denotes the fractional Caputo derivative of order $0 < \varsigma \le 1$ which be defined in the follow-up.

Remark 1. *In Eq. (11), $S(x,t)$ can be linear or nonlinear. Here, the Newton's method is used to estimate the roots of the given equation.*

2. Preliminaries and notations

Definition 1. *The fractional Caputo derivative of order ς is defined by*

$$\begin{aligned}D_t^\varsigma\Phi(x,t) &= \frac{1}{\Gamma(n-\varsigma)}\int_0^t \frac{\Phi^{(n)}(x,s)}{(t-s)^{\varsigma-1+n}}ds,\\ n-1 &< \varsigma < n, \quad n\in\mathbb{N}. \quad (12)\end{aligned}$$

For more details about fractional derivatives, readers can refer to [11].

Definition 2. *[17]* The OBP of order M is defined as follows:

$$\mathcal{B}_M(t) = \sqrt{2M+1}\sum_{j=0}^{M}(-1)^j\binom{M}{j}\binom{2M-j}{M-j}t^{M-j}, \quad (13)$$

where $M = 0, 1, 2, \cdots$.

Therefore

$$\int_0^1 \mathcal{B}_r(u)\mathcal{B}_s(u)du = \begin{cases}1, & r=s,\\ 0, & otherwise.\end{cases} \quad (14)$$

Note: The function $\Phi(t) \in L^2(0,1)$ can be expanded in terms of OBPs as follows:

$$\Phi(t) = \sum_{i=0}^{M} q_i\mathcal{B}_i(t) = \mathcal{Q}^T B(t), \quad (15)$$

where $\mathcal{Q} = [q_0, q_1, \ldots, q_M]^T$ and $B(t) = [\mathcal{B}_0(t), \mathcal{B}_1(t), \ldots, \mathcal{B}_M(t)]^T$, with

$$q_r = \int_0^1 \Phi(u)\mathcal{B}_r(u)du. \quad (16)$$

Definition 3. *[17]* Two dimensional OBP of order M, N is defined in the following form

$$\mathcal{B}_{M,N}(x,t) = \mathcal{B}_M(x)\mathcal{B}_N(t),\ M, N = 0, 1, 2, \cdots . \tag{17}$$

Therefore

$$\int_0^1 \int_0^1 \mathcal{B}_{m,n}(x,t)\mathcal{B}_{p,q}(x,t)dxdt = \begin{cases} 1, & m = p, n = q, \\ 0, & otherwise. \end{cases} \tag{18}$$

Consequently, a two variables function $\Phi(x,t) \in L^2\big((0,1) \times (0,1)\big)$ can be approximated in terms of OBPs as follows:

$$\Phi(x,t) \simeq \sum_{r=0}^{M}\sum_{s=0}^{M} q_{r,s}\mathcal{B}_r(x)\mathcal{B}_s(t) = \mathcal{B}^T(x)\mathcal{Q}\mathcal{B}(t), \tag{19}$$

where $\mathcal{Q} = [q_{ij}]_{(m+1)\times(m+1)},\ i,j = 0,1,\cdots,m$ and

$$q_{ij} = \int_0^1 \int_0^1 \mathcal{B}_i(u)Q(u,v)\mathcal{B}_j(v)dvdu. \tag{20}$$

Assume now that
$B(u) = [\mathcal{B}_0(u), \mathcal{B}_1(u), \cdots, \mathcal{B}_m(u)]^T$.
Now, as a direct consequence of Eq. (13), we get

$$B(s) = AT_M(s), \tag{21}$$

where

$$T_M(s) = [1, s, \cdots, s^M]^T, \tag{22}$$

and $A_{(m+1)\times(m+1)}$ is signified by

$$\begin{pmatrix} (-1)^0\binom{0}{0}\binom{0}{0} & 0 & \dots & 0 \\ (-1)^1\sqrt{3}\binom{1}{1}\binom{1}{0} & (-1)^0\sqrt{3}\binom{1}{0}\binom{2}{1} & \dots & 0 \\ \vdots & \vdots & \vdots & \vdots \\ (-1)^m\sqrt{2m+1}\binom{m}{m}\binom{m}{0} & (-1)^{m-1}\sqrt{2m+1}\binom{m}{m-1}\binom{m+1}{1} & \dots & (-1)^0\sqrt{2m+1}\binom{m}{0}\binom{2m}{m} \end{pmatrix}, \tag{23}$$

Since $det(A) \neq 0$, therefore

$$T_M(s) = A^{-1}B(s). \tag{24}$$

Taking the derivative of vector $\mathcal{B}(t)$, we will have

$$\frac{d}{dt}\mathcal{B}(t) = D\mathcal{B}(t), \tag{25}$$

where

$$\mathcal{R}^{-1}D\mathcal{R} = \begin{pmatrix} 0 & 0 & 0 & \cdots & 0 & 0 \\ 1 & 0 & 0 & \cdots & 0 & 0 \\ 0 & 2 & 0 & \cdots & 0 & 0 \\ \vdots & \vdots & \vdots & \ddots & \vdots & \vdots \\ 0 & 0 & 0 & \cdots & M & 0 \end{pmatrix},$$

and $\mathcal{R} = [r_{ij}], i,j = 0,1,\ldots,M$, and

$$r_{i,j} = \begin{cases} \binom{i}{j}B_{i-j}, & i \geq j, \\ 0, & i < j. \end{cases}$$

Also, for $s \geq 2$, we have

$$\frac{d^s}{dt^s}\mathcal{B}(t) = D^s\mathcal{B}(t). \tag{26}$$

Therefore

$$D_t^{\tau}\beta(t) \simeq D^s\beta(t), \tag{27}$$

where

$$\Lambda^{\zeta} = \begin{pmatrix} 0 & 0 & \cdots & 0 \\ \Omega_{1,0,k} & \Omega_{1,1,k} & \cdots & \Omega_{1,M,k} \\ \Omega_{2,0,k} & \Omega_{2,1,k} & \cdots & \Omega_{2,M,k} \\ \vdots & \vdots & \ddots & \vdots \\ \Omega_{M,0,k} & \Omega_{M,1,k} & \cdots & \Omega_{M,M,k} \end{pmatrix},$$

and

$$\Omega_{i,j,k} = \sum_{k=1}^{i} w_{i,k}\sigma_{k,j}\frac{\Gamma(k+1)}{\Gamma(k-\zeta+1)},$$
$$\omega_{i,k} = \begin{pmatrix} i \\ k \end{pmatrix}\beta_{i-k}, \tag{28}$$

Let $\mathcal{B}(t)$ be the orthonormal Bernoulli vector defined in Eq. (15) and suppose that $\varsigma > 0$. Thus, by using Eqs. (13) and the Caputo's fractional differentiation, $D^{\varsigma}B_m(t)$ is equal to

$$\begin{aligned} &\sqrt{2m+1}\sum_{i=0}^{m}(-1)^i\binom{i}{m}\binom{2m-i}{m-i}D^{\varsigma}(t^{m-i}) \\ &= \sqrt{2m+1}\sum_{i=\lceil\varsigma\rceil}^{m}(-1)^i\binom{i}{m}\binom{2m-i}{m-i}\frac{\Gamma(m-i+1)}{\Gamma(m-i-\varsigma+1)}t^{m-i-\varsigma}, \end{aligned} \tag{29}$$

where $p = 0, 1, \cdots, m$.

Approximating t^j with $j = m - i - \varsigma$ by means of the orthonormal Bernoulli, leads to:

$$t^j \simeq \sum_{r=0}^{M} q_{r,j}B_r(t). \tag{30}$$

Hence, $q_{r,j} = \int_0^1 t^jB_r(t)dt$ and is equal to

$$\sqrt{2r+1}\sum_{k=0}^{r}(-1)^k\binom{r}{k}\binom{2r-k}{r-k}\frac{1}{j+r-k+1}.$$

Therefore $D^{\varsigma}B_m(t)$ can be approximated as

$$\sum_{i=\lceil\varsigma\rceil}^{m}\sqrt{2m+1}(-1)^i\binom{m}{i}\binom{2m-i}{m-i}\frac{\Gamma(m-i+1)}{\Gamma(m-i-\varsigma+1)}\sum_{r=0}^{N}q_{r,j}B_r(t)$$
$$=\sum_{r=0}^{N}\left(\sqrt{2m+1}\sum_{i=\lceil\varsigma\rceil}^{m}(-1)^i\binom{m}{i}\binom{2m-i}{m-i}\frac{\Gamma(m-i+1)}{\Gamma(m-i-\varsigma+1)}q_{r,j}\right)$$
$$\times B_r(t)$$
$$=\sum_{r=0}^{N}\left(\sum_{i=\lceil\varsigma\rceil}^{m}\omega_{m,i,j,r}\right)B_r(t), \tag{31}$$

where $\omega_{m,i,j,r}$ is given by

$$\sqrt{2m+1}(-1)^i\binom{m}{i}\binom{2m-i}{m-i}\frac{\Gamma(m-i+1)}{\Gamma(m-i-\varsigma+1)}q_{r,j}. \tag{32}$$

Let us rewrite Eq. (31) in the vector form

$$D^{\varsigma}\mathcal{B}_p(t)\simeq\Big[\sum_{i=\lceil\varsigma\rceil}^{m}\omega_{p,i,j,0},\sum_{i=\lceil\varsigma\rceil}^{m}\omega_{p,i,j,1},\ldots,\sum_{i=\lceil\varsigma\rceil}^{m}\omega_{p,i,j,m}\Big]\phi(v), \tag{33}$$

where $p=0,1,\cdots,m$. In other words

$$D^{\varsigma}\mathcal{B}(v)\simeq D^{(\varsigma)}\mathcal{B}(v), \tag{34}$$

where $D^{(\varsigma)}$ is as follows

$$\begin{pmatrix}
\sum_{i=\lceil\varsigma\rceil}^{m}w_{0,i,j,0} & \sum_{i=\lceil\varsigma\rceil}^{m}w_{0,i,j,1} & \cdots & \sum_{i=\lceil\varsigma\rceil}^{m}w_{0,i,j,m}\\
\vdots & \vdots & \cdots & \vdots\\
\sum_{i=\lceil\varsigma\rceil}^{m}w_{i,i,j,0} & \sum_{i=\lceil\varsigma\rceil}^{m}w_{i,i,j,1} & \cdots & \sum_{i=\lceil\varsigma\rceil}^{m}w_{i,i,j,m}\\
\vdots & \vdots & \cdots & \vdots\\
\sum_{i=\lceil\varsigma\rceil}^{m}w_{m,i,j,0} & \sum_{i=\lceil\varsigma\rceil}^{m}w_{m,i,j,1} & \cdots & \sum_{i=\lceil\varsigma\rceil}^{m}w_{m,i,j,m}
\end{pmatrix}. \tag{35}$$

Lemma 1. *Let $\varsigma>0$, then $D_v^{\varsigma}\mathcal{B}(u,v)$ is approximated as $\widehat{D}_v^{(\varsigma)}\mathcal{B}(u,v)$ where $\widehat{D}_t^{(\varsigma)}=I\otimes D^{(\varsigma)}$, and $I_{(m+1)\times(m+1)}$ is the identity matrix. Here $\otimes$ is Kronecker product.*

Proof. Using Eq. (34) we take

$$\begin{aligned}
\frac{\partial^{\varsigma}\mathcal{B}(u,v)}{\partial v^{\varsigma}} &= \frac{\partial^{\varsigma}(\mathcal{B}(u)\otimes\mathcal{B}(v))}{\partial v^{\varsigma}}\\
&= (I\mathcal{B}(u))\otimes(D^{(\varsigma)}\mathcal{B}(v))\\
&= (I\otimes D^{(\varsigma)})(\mathcal{B}(u)\otimes\mathcal{B}(v))\\
&:= \widehat{D}_v^{(\varsigma)}\mathcal{B}(u,v).
\end{aligned} \tag{36}$$

□

3. Error analysis

Theorem 1. *Suppose that $\phi_m(t)=\mathcal{Q}^T\mathcal{B}(t)$ where $\mathcal{Q}=[q_0,q_1,\cdots,q_m]^T$, is an approximation of a continuous function $\phi(t)$ on $[0,1]$ by the OBPs. Then, the coefficients q_n for $n=0,1,\cdots,m$ are bounded as follows:*

$$|\,q_n\,|\leq\Theta_n, \tag{37}$$

where

$$\Theta_n=\rho\sqrt{2n+1}\sum_{l=0}^{n}\binom{n}{l}\binom{2n-l}{n-l}, \tag{38}$$

here $\rho\in\mathbb{R}^+$ and $|\,\phi(t)\,|\leqslant\rho$.

Proof. Using the OBP, $\phi(t)$ can be approximated in the following form

$$\phi(t)=\phi_m(t)=\sum_{n=0}^{m}q_nB_r(t),$$

where q_n can be determined by

$$\begin{aligned}
q_n &= \int_0^1\phi(t)B_n(t)dt\\
&= \int_0^1\phi(t)\sqrt{2n+1}\sum_{l=0}^{n}(-1)^l\binom{n}{l}\binom{2n-l}{n-l}t^{n-l}dt\\
&= \sqrt{2n+1}\sum_{l=0}^{n}(-1)^l\binom{n}{l}\binom{2n-l}{n-l}\int_0^1\phi(t)t^{n-l}dt.
\end{aligned} \tag{39}$$

Since $\phi(t)$ is continuous on $[0,1]$, then based on the maximum-minimum Theorem one will set

$$\exists\;\rho>0,\;\forall t\in[0,1],\;|\,\phi(t)\,|<\rho.$$

Thus, we will have

$$|\,q_n\,|\leq\rho\sqrt{2n+1}\sum_{l=0}^{n}(-1)^l\binom{n}{l}\binom{2n-l}{n-l}. \tag{40}$$

□

Theorem 2. *Suppose that $\phi_m(t)=\mathcal{Q}^T\mathbb{B}(t)$ is an approximation of a continuous function $\phi(t)$ on $[0,1]$ by the OBPs. Then, the error bound is as follows:*

$$\|\,\phi(t)-\phi_m(t)\,\|_2\leq\left(\sum_{i=m+1}^{\infty}\Theta_i^2\right)^{\frac{1}{2}}, \tag{41}$$

which Θ is presented in Eq. (38).

Proof. Suppose that $\phi(t)=\sum_{i=0}^{\infty}z_iB_i(t)$ and $\phi_m(t)=\sum_{i=0}^{m}z_iB_i(t)$. Therefore

$$\phi(t) - \phi_m(t) = \sum_{i=m+1}^{\infty} q_i B_i(t). \tag{42}$$

Since $\int_0^1 B_i(t)B_j(t)dt = \delta_{ij}$, then

$$\begin{aligned} \| \phi(t) - \phi_m(t) \|_2^2 &= \int_0^1 |\phi(t) - \phi_m(t)|^2 dt \\ &= \int_0^1 |\sum_{i=m+1}^{\infty} q_i B_i(t)|^2 dt \\ &= \sum_{i=m+1}^{\infty} q_i^2 \leq \sum_{i=m+1}^{\infty} \Theta_i^2. \end{aligned} \tag{43}$$

□

Theorem 3. *[17]* Suppose $\phi_m(u,v) = \mathcal{Q}^T \mathbb{B}(u,v)$ is the best approximation for $\phi(u,v)$ by the two dimensional OBP. Then, we have

$$\| \phi(u,v) - \phi_m(u,v) \|_2 = \mathbb{O}(\frac{1}{(m+1)!2^{2m+1}}), \tag{44}$$

which means that if $m \longrightarrow \infty$, then $\phi_m(u,v) \longrightarrow \phi(u,v)$. Here, $\mathbb{O}$ is a big-$\mathbb{O}$ notation.

Corollary 1. *[17]* By an argument similar to Theorem (3), we have the convergence

$$\| \phi(u,v) - \phi_m(u,v) \|_2 \leq \frac{\rho}{(m+1)!2^{2m+1}}, \tag{45}$$

where ρ is defined as above.

Now, according to the stated theorem, we give the numerical results section.

4. Method in action and numerical overviews

In this section, we propose a numerical scheme based on collocation method and operational matrices to approximate the solution of (11). At first, we can approximate the solution of (11) via OBPs as follows:

$$Q(x,t) \simeq \sum_{r=0}^{M}\sum_{s=0}^{M} q_{r,s}\mathcal{B}_r(x)\mathcal{B}_s(t) = \mathcal{B}^T(x)\mathcal{Q}\mathcal{B}(t). \tag{46}$$

Then, by using ∂_t^ς on both sides of (46), we have

$$\partial_t^\varsigma Q(x,t) \simeq \mathcal{B}^T(x)\mathcal{Q}\Delta^\varsigma\mathcal{B}(t). \tag{47}$$

In other words, we get

$$\partial_{xx} Q(x,t) \simeq \left(D^2\mathcal{B}(x)\right)^T \mathcal{Q}\mathcal{B}(t). \tag{48}$$

Now, by substituting (47) and (48) into (11), we will have

$$\mathcal{B}^T(x)\mathcal{Q}\Delta^\varsigma\mathcal{B}(t) = \frac{1}{2}\left(D^2\mathcal{B}(x)\right)^T \mathcal{Q}\mathcal{B}(t) + S(x,t). \tag{49}$$

From (46), the initial condition can be expressed as follows:

$$\mathcal{B}^T(x)\mathcal{Q}\mathcal{B}(0) \simeq \xi(x). \tag{50}$$

If we collocate (49) and (50) at the points $x_i = \frac{i}{M}, i = 0, 1, \ldots, M$, and $t_j = \frac{j}{M}$, $j = 1, 2, \ldots, M$, we have the following system of equations

$$\begin{cases} \mathcal{B}^T(x_i)\mathcal{Q}\Delta^\varsigma\mathcal{B}(t_j) = \frac{1}{2}\left(D^2\mathcal{B}(x_i)\right)^T \mathcal{Q}\mathcal{B}(t_j) + S(x_i,t_j), \\ \mathcal{B}^T(x_i)\mathcal{Q}\mathcal{B}(0) \simeq \xi(x_i). \end{cases} \tag{51}$$

By solving this system with the help of Matlab software and Newton's method, the values of $\mathcal{Q}$ can be obtained and then by inserting in Eq. (46), the approximate solution of this model is achieved.

In the following, to show the effectiveness of the proposed technique, numerical results for two examples are reported. Matlab software was used to obtain these results.

Example 1. *Consider the following equation [18]:*

$$\partial_t^\varsigma Q(x,t) = \partial_{xx}Q(x,t) + Q(x,t) + \Gamma(2+\varsigma)e^x t, \tag{52}$$

where

$$\begin{cases} Q(x,0) = 0, \ \textit{for } 0 \leq x \leq 1, \\ Q(0,t) = t^{1+\varsigma}, \\ Q(1,t) = et^{1+\varsigma}, \ \textit{for } t > 0, \\ 0 < \varsigma \leq 1, \end{cases} \tag{53}$$

and the exact solution is

$$Q(x,t) = e^x t^{1+\varsigma}. \tag{54}$$

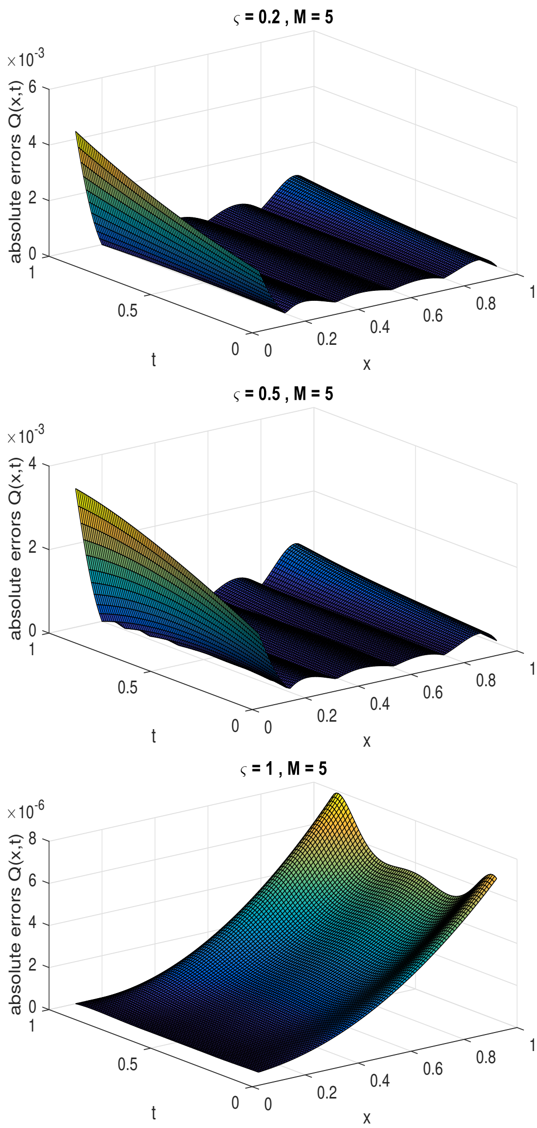

Figure 1. The absolute errors for $\varsigma = 0.2, 0.5, 1$ and $M = 5$ in Example 1.

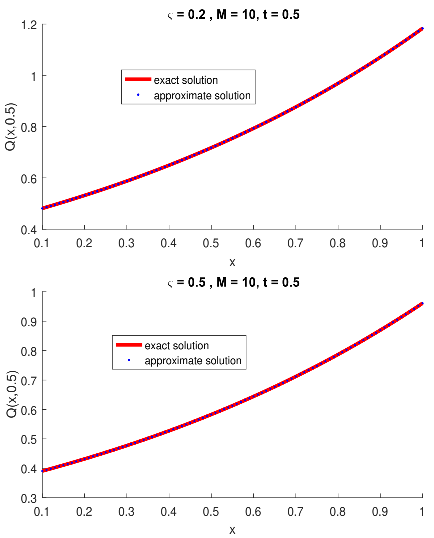

Figure 2. Comparison of analytical answer and approximate answer in Example 1 for different values of ς.

Table 1. Comparing L_∞-errors of Example 1 where $t = 0.5$ and $\varsigma = 0.5$ for different values of h.

h	[18]	Proposed method
0.25	1.2×10^{-3}	3.4×10^{-5}
0.125	3.9×10^{-4}	1.3×10^{-5}
0.0625	1.1×10^{-4}	7.5×10^{-6}

Fig. 1, shows the absolute errors for different values of ς and $M = 5$. A comparison of analytical answers and approximate answers for $\varsigma = 0.2, 0.5$, $M = 10$ and $t = 0.5$ is presented in Fig. 2. Also, in Table 1, a comparison is made between the B-spline wavelet operational method and our proposed method. The findings from this example demonstrate that the results are promising.

Example 2. *Consider the following equation [13]:*

$$\partial_t^\varsigma Q(x,t) = \frac{1}{2}\partial_{xx}Q(x,t) + \frac{1}{2}Q(x,t).$$

For this equation in the fractional state, no exact solution has been reported, but for $\varsigma = 1$, the initial conditions have been considered so that its exact solution is e^{x+t}. The obtained results of the maximum absolute error for $x = 1$ and for different values of t and ς are reported in Table 2. Comparison of the maximum absolute error by different values of ς is presented in Fig. 3 and is sorted in Table 2, where $M = 10$.

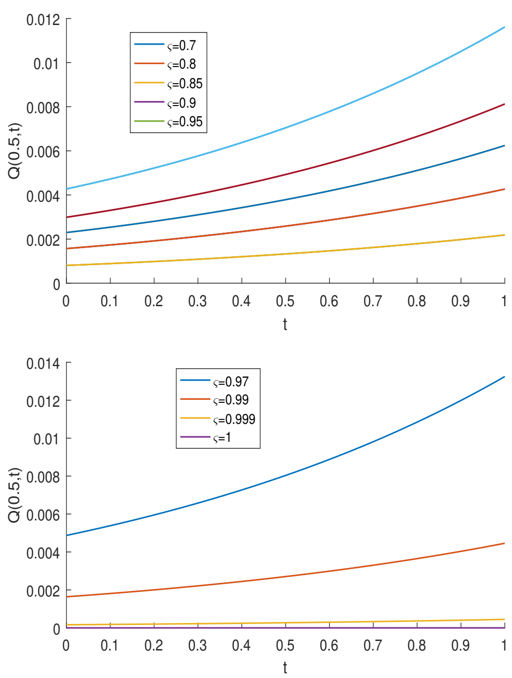

Figure 3. The absolute error of Example 2 for different values of ς where $M = 10$.

Table 2. Comparison of the maximum absolute error of Example 2 with setting $x = 1$ and for different values of t and ς.

ς	$t = 0.1$	$t = 0.3$	$t = 0.5$	$t = 0.7$	$t = 0.9$
$\varsigma = 0.7$	2.73768×10^{-1}	6.29163×10^{-1}	8.83953×10^{-1}	0.11094×10^{-1}	0.13240×10^{-1}
$\varsigma = 0.8$	1.40599×10^{-1}	3.63106×10^{-1}	5.27557×10^{-1}	6.75506×10^{-1}	8.18971×10^{-1}
$\varsigma = 0.85$	8.79442×10^{-2}	2.48710×10^{-1}	3.70498×10^{-1}	4.80560×10^{-1}	5.86404×10^{-1}
$\varsigma = 0.9$	4.52923×10^{-2}	1.48283×10^{-1}	2.26811×10^{-1}	2.98218×10^{-1}	3.67948×10^{-1}
$\varsigma = 0.95$	1.24112×10^{-2}	6.11041×10^{-2}	9.89665×10^{-2}	1.33438×10^{-1}	1.66726×10^{-1}
$\varsigma = 0.97$	3.65980×10^{-3}	3.20476×10^{-2}	5.41044×10^{-2}	7.41701×10^{-2}	9.36426×10^{-2}
$\varsigma = 0.99$	6.58061×10^{-4}	8.44130×10^{-3}	1.54557×10^{-2}	2.17713×10^{-2}	2.78533×10^{-2}
$\varsigma = 0.999$	1.89218×10^{-4}	6.98058×10^{-4}	1.36302×10^{-3}	1.91338×10^{-3}	2.32859×10^{-3}
$\varsigma = 0.9999$	2.08184×10^{-5}	6.61829×10^{-5}	1.20376×10^{-4}	1.20065×10^{-4}	9.60039×10^{-6}
$\varsigma = 1$	1.70126×10^{-8}	1.53014×10^{-6}	1.58226×10^{-5}	7.91219×10^{-5}	2.73071×10^{-4}

5. Concluding remarks

Glioblastoma tumor is an aggressive type of cancer that can develop in the brain but the brain type is more common. The structure of this tumor is made up of cells called astrocytes that support the nerve cells of the brain. This cancer can occur at any age, but it is more common in the elderly. Therefore, the treatment of this tumor requires more detailed studies and better understanding of the tumor. One of these types of studies is the mathematical modeling of this brain tumor. For this reason, a model based on the two main components of cancer cell proliferation and dissemination for tumor growth and based on the Burgess equation was presented (for more details see [13] and the references therein). In this study, using Caputo's derivative, a mathematical instrument was investigated to analysis this tumor case. The analytical solution of this model is not an easy task, so in this study, a numerical approach based on the operational matrix of conventional OBPs has been thoroughly used to estimate the solution of the proposed model. One of the advantages of this idea is to obtain the derivative of the fraction in matrix form, which makes calculations easier. Also, by using this technique, the problem under the study is converted to a system of nonlinear algebraic equations which was solved via Newton's method. In Table 1 and Table 2 we compare our method with Bernoulli polynomials operational method in Ref. [13] and B-spline wavelet operational method in Ref. [18]. Examination of these results show that the proposed method provides a more accurate answer than similar methods. In other words, the obtained results are interesting, promising and can be extended for other scientific models.

Acknowledgements

The authors would like to thank the editor and anonymous referees for helpful comments and suggestions.

References

[1] Murray, J. D. (1993). Mathematical Biology. 2nd ed. New York: Springer-Verlag.

[2] Ahmed, I., Akgül, A., Jarad, F., Kumam, P. & Nonlaopon, K. (2023). A Caputo-Fabrizio fractional-order cholera model and its sensitivity analysis, *Mathematical Modelling and Numerical Simulation with Applications*, 3(2), 170-187.

[3] Demirtas, M., & Ahmad, F. (2023). Fractional fuzzy PI controller using particle swarm optimization to improve power factor by boost converter, *An International Journal of Optimization and Control: Theories & Applications*, 13(2), 205–213.

[4] Evirgen, F., Ucar, E., Ucar, S. & Özdemir, N. (2023). Modelling influenza a disease dynamics under Caputo-Fabrizio fractional derivative with distinct contact rates, *Mathematical Modelling and Numerical Simulation with Applications*, 3(1), 58-73.

[5] Evirgen, F. (2023). Transmission of Nipah virus dynamics under Caputo fractional derivative, *Journal of Computational and Applied Mathematics*, 418, 114654, https://doi.org/10.1016/j.cam.2022.114654.

[6] Odionyenma, U. B. , Ikenna, N. & Bolaji, B. (2023). Analysis of a model to control the co-dynamics of Chlamydia and Gonorrhea using Caputo fractional derivative, *Mathematical Modelling and Numerical Simulation with Applications*, 3(2), 111-140.

[7] Tajadodi, H., Jafari, H., & Ncube, M. N. (2022). Genocchi polynomials as a tool for solving a class of fractional optimal control problems, *An International Journal of Optimization and Control: Theories & Applications*, 12(2), 160–168.

[8] Uzun, P. Y., Uzun, K., & Koca, I. (2023). The effect of fractional order mathematical modelling for examination of academic achievement in schools with stochastic behaviors, *An International Journal of Optimization and Control: Theories & Applications*, 13(2), 244–258.

[9] Baleanu, D., Guvenc, Z. B., & Machado, J. T. (2010). New Trends in Nanotechnology and Fractional Calculus Applications, Springer Science and Business Media, New York.

[10] Ghanbari, B., & Atangana, A. (2022). A new application of fractional Atangana-Baleanu derivatives: Designing ABC-fractional masks in image processing, *Physica A*, 542, 123516.

[11] Podlubny, I. (1999). Fractional Differential Equations, San Diego: Academic Press.

[12] Tuan, N. H., Ganji, R. M., & Jafari, H. (2020). A numerical study of fractional rheological models and fractional Newell-Whitehead-Segel equation with

non-local and non-singular kernel, *Chinese Journal of Physics*, 68, 308-320.

[13] Ganji, R. M., Jafari, H., Moshokoa, S. P, & Nkomo, N. S. (2021). A mathematical model and numerical solution for brain tumor derived using fractional operator, *Results in Physics*, 28, 104671.

[14] Gonzalez-Gaxiola, O., & Bernal-Jaquez, R. (2017). Applying Adomian decomposition method to solve Burgess equation with a non-linear source, *International Journal of Applied and Computational Mathematics*, 3(1), 213-224.

[15] Magin, R. L. (2021). Fractional Calculus in Bioengineering, Begell House Digital Library.

[16] Magin, R. L. (2010). Fractional calculus models of complex dynamics in biological tissues, *Computers and Mathematics with Applications*, 59(5), 1586-593.

[17] Pourdarvish. A., Sayevand. K., Masti. I., & Kumar, S. (2022). Orthonormal Bernoulli polynomials for solving a class of two dimensional stochastic Volterra-Fredholm integral equations, *International Journal of Applied and Computational Mathematics*, 8(31), https://doi.org/10.1007/s40819-022-01246-zr3.

[18] Kargar, Z., & Saeedi, H. (2017). B-spline wavelet operational method for numerical solution of time-space fractional partial differential equations, *International Journal of Wavelets, Multiresolution and Information Processing*, 15(4), 1750034.

Iman Masti *is a Ph.D. student at the Department of Mathematical Sciences, Malayer University. His research interests include bio-mathematics, fractional differential equations, and approximation methods.*
https://orcid.org/0009-0007-4454-5095

Khosro Sayevand *is a full professor in applied mathematics at the Department of Mathematical Sciences, Malayer University. His research interests include fractional calculus, modeling, perturbation theory, and linear programming.*
https://orcid.org/0000-0002-5397-1623

Hossein Jafari *is a full professor in applied mathematics. His research interests include bio-mathematics, fractional differential equations, Lie symmetry, and approximation methods.*
https://orcid.org/0000-0001-6807-6675

An International Journal of Optimization and Control: Theories & Applications
ISSN: 2146-0957 eISSN: 2146-5703
Vol.14, No.1, pp.20-31 (2024)
https://doi.org/10.11121/ijocta.1444

RESEARCH ARTICLE

Scheduling of distributed additive manufacturing machines considering carbon emissions

Ibrahim Kucukkoc

Department of Industrial Engineering, Balikesir University, 10145 Balikesir, Turkey
ikucukkoc@balikesir.edu.tr

ARTICLE INFO

Article history:
Received: 8 August 2023
Accepted: 2 November 2023
Available Online: 3 November 2023

Keywords:
Additive manufacturing
Production scheduling
Sustainability
Carbon emissions
Multi-site factory plants

AMS Classification 2010:
90B35, 90B50

ABSTRACT

Additive manufacturing is a rapidly growing technology shaping the future of manufacturing. In an increasingly competitive economy, additive manufacturing can help businesses to remain agile, innovative, and sustainable. This paper introduces the multi-site additive manufacturing (AM) machine scheduling problem considering carbon emissions caused by production and transportation. A mixed-integer linear programming model is developed aiming to optimise two separate objectives addressing economic and environmental sustainability in a multiple unrelated AM machine environment. The former is the total cost caused by production, transportation, set-up and tardiness penalty and the latter is the total amount of carbon emissions caused by production and transportation. The model is coded in Python and solved by Gurobi Optimizer. A numerical example is provided to represent the basic characteristics of the problem and show the necessity of the proposed framework. A comprehensive computational study is conducted under 600s and 1800s time limits for two main scenarios and the results have been elaborated. This article introduces the concept of considering both economic and environmental sustainability caused by production and transportation, proposing the first mathematical model and measuring its performance through a comprehensive experimental study.

1. Introduction

Additive manufacturing (AM) has a wide range of application areas from automotive to aeronautics and healthcare. Several AM techniques have been developed based on the idea that the parts are 3D modelled and fabricated layer-by-layer based on the cross sections of the computer-aided design model. Thus, it is also referred to as 3D printing. Compared to the traditional subtractive manufacturing methods, AM technologies utilise production by additively releasing materials [1].

AM has a significant role in today's competitive economy for several reasons. Firstly, it enables the production of complex geometries which otherwise difficult or even impossible via traditional methods. That also helps integrate multiple parts into a single component, reducing assembly processes and increasing product strength and durability [2]. The geometry flexibility that AM provides allows a higher degree of customization without incurring additional costs. This has been particularly useful in sectors like medical devices, where patient-specific products can be produced. Secondly, companies can print products on-demand rather than mass-producing and storing them in inventory, which saves storage space and costs, and reduces the risk of products becoming obsolete. Another cost advantage is gained by eliminating expensive moulds, tools and machine setups.

Thirdly, rapid prototyping is possible with additive manufacturing which significantly reduces the time to market. Moreover, the nature of the production that AM utilises results in significantly less waste compared to subtractive methods, which carve out parts from larger blocks of material. Also, the carbon footprint associated with the transport of goods can be reduced thanks to locally printed parts. Hence, all these advantages are related to the environment as well as the economic benefits and flexibility.

The recent pandemic has also highlighted the importance of the resilience of supply chains and the vulnerability of global supply chains. With additive manufacturing, companies can manufacture parts in-house or domestically, decreasing dependence on international suppliers, and increasing resilience [3, 4].

Efficient planning and scheduling of AM machines can lead to significant improvements in productivity, cost-efficiency, quality, and customer satisfaction. This is achieved through more effective resource use, reduced waste, improved delivery times, and enhanced flexibility and responsiveness to change. This paper addresses the AM machine scheduling problem where unrelated AM machines are dispersively located at different factory plants. The AM technology considered in this paper is selective laser melting (SLM) which uses a high-power laser beam to fuse fine metallic powders to create a high-density part with complex geometries. As a unique contribution to the field, a multi-objective mathematical model is developed to minimise total cost as well as total amount of carbon emissions (TCE), both caused by production and transportation.

The rest of the manuscript is organised as follows. Section 2 reviews the literature on the AM machine scheduling problem. Section 3 describes the main characteristics of the problem and presents the mathematical model developed. The results of the experimental study are provided in Section 4 and the paper is concluded in Section 5.

2. Related work

AM is an emerging field that attracts both academics and practitioners. The literature on the AM technology addressed in this paper, i.e. SLM, is rather extensive. Recently, a thorough examination and analysis of the key parameters affecting the SLM manufacturing process of difficult-to-cut alloys has been conducted based on an extensive review of the existing literature by Pimenov et al. [5]. Li et al. [6] proposed a new design method to concurrently achieve lightweight and self-sustaining design for SLM processes. However, the number of studies on the efficient planning and scheduling of these SLM machines is still limited.

As pioneering works on planning and scheduling of AM machines, Kucukkoc et al. [7] aimed to maximise the utilisation of AM machines, and Li et al. [2] focused on the minimisation of average cost by proposing a mathematical model as well as two constructive heuristics. Several researchers have followed these works, as will be summarised hereafter.

Chergui et al. [8] simultaneously addressed the scheduling and nesting problems in AM and proposed a heuristic algorithm to satisfy due dates. Kucukkoc et al. [9] proposed a genetic algorithm (GA) approach to minimise maximum lateness in a multiple heterogenous AM machine environment. Kucukkoc [1] aimed to minimise makespan in single, parallel identical and parallel unrelated AM machine scheduling problems through a MILP model developed. Li et al. [10] combined the order acceptance problem with the scheduling problem of SLM machines and proposed a dynamic and strategy-based decision-making approach. Kapadia et al. [11] have also studied the order acceptance and scheduling problem under such a condition that orders can be accepted fully or partially and proposed a GA to maximise profit. Zhang et al. [12] integrated the irregular packing constraints into the AM machine scheduling problem and proposed an improved evolutionary algorithm. Kucukkoc [13] showed the necessity of considering nesting and scheduling problems together to get applicable as well as better scheduling solutions.

Altekin and Bukchin [14] showed the necessity of considering cost and makespan objectives simultaneously and proposed a multi-objective optimisation approach to investigate the trade-off in between. Kucukkoc et al. [15] aimed to minimise the total tardiness in a parallel unrelated AM machine environment and proposed a GA-based approach. Alicastro et al. [16] aimed to minimise makespan via a reinforcement learning iterated local search algorithm in a multiple identical/non-identical AM machine environment. Another study addressing the makespan as well as total tardiness is conducted by Rohaninejad et al. [17], who developed a hybrid non-dominated sorting GA-based metaheuristic in addition to a bi-objective model. Arık [18] combined the AM machine scheduling problem with the planning of post-processing assembly operations and proposed a MILP model as well as a local search heuristic.

Hu et al. [19] solved the AM machine scheduling problem using MILP and an adaptive large neighbourhood search algorithm considering two-dimensional nesting and unequal part release times. Wu et al. [20] addressed the cloud-based 3D printing problem and proposed a heuristic algorithm for the scheduling of orders received through the cloud-based platform. Oh et al. [21] presented a taxonomy and comprehensive review of the nesting and scheduling problem in AM.

Different from the common approach caused by the nature of the AM machine scheduling problem, Kim and Kim [22] addressed the problem by considering the maximum processing time of parts when calculating the processing time of a batch. They proposed three meta-heuristics to minimise makespan considering sequence-dependent set-up times.

Che et al. [23] introduced the part orientation problem into the AM machine scheduling and proposed a MILP model as well as a simulated annealing algorithm for solving it. Oh and Cho [24] addressed the AM machine scheduling problem within a flow-shop environment considering both the build and post processes simultaneously. A mixed-integer programme was also proposed to minimise makespan for different scheduling policies. Ying et al. [25] proposed an adjusted iterated greedy search algorithm to solve the single AM machine scheduling problem. Zipfel et al. [26] proposed an iterated local search algorithm for customer order scheduling in additive manufacturing focusing on the total weighted tardiness of orders. Kucukkoc [27] considered the batch delivery of parts belonging to several customers when solving the multiple AM machine scheduling problem. Ying and Lin [28] attempted to minimise makespan in parallel AM machine scheduling problem with a two-stage assembly process. Lee and Kim [29] focused on the 3D rotation of parts and aimed to minimise makespan in parallel AM machine scheduling problem with 2D nesting constraints.

Dwivedi et al. [30] introduced the simultaneous production and transportation problem where the route of a mobile AM-installed vehicle is optimised considering the delivery due dates of customer orders. Exact and heuristic solution approaches were developed and their effectiveness has been tested through computational tests. Zehetner and Gansterer [31] addressed the multi-site AM machine scheduling problem to minimise the total cost accumulated by production, inventory, setup and transportation.

Although production scheduling and transportation problems have been integrated into other domains of scheduling literature [32-34], it has not been handled properly in the AM machine scheduling field. As seen from the survey given above, there is only one study which addresses the multi-site AM machine scheduling problem, by Zehetner and Gansterer [31]. However, Zehetner and Gansterer [31] only focused on the cost including transportation. In our work, we address the multi-site AM machine scheduling problem and employ a new objective function related to the sum of carbon emissions caused by production and transportation. Therefore, this study contributes to the literature by introducing the multi-site AM machine scheduling problem considering carbon emissions and proposing a MILP model for solving it. AM machines are unrelated (having different processing speed-, cost- and emission-related parameters) and orders received from geographically dispersed customers have certain tardiness penalty costs.

3. Problem definition

Part orders ($i \in I$) received from customers ($u \in U$) are assigned to machines ($m \in M$) located at geographically dispersed factory plants ($p \in P$) and allocated to batches ($j \in J$) to be produced sequentially. They are shipped to customers after production, in such a concept of on-demand production. The schematic representation of the addressed problem is given in Figure 1. Note that the numbers of plants, customers, part orders and machines provided in the figure are just for illustration purposes and they may vary in the practical applications.

Each part has a volume (v_i), area (a_i), height (h_i), due date (dd_i) and tardiness penalty cost (dc_i). Each machine's build platform has a maximum supported area (A_m) and height (H_m). Machines require different times to set-up (set_m), release per unit volume of material (vt_m) and powder-layering (rt_m). As the machines have different specifications, they cause different amounts of CO_2 equivalent emissions during production.

Batches are constituted of different combinations of parts seeking the main objective of the problem. As already done in the literature, the total volume and the maximum height of the parts are used to calculate the processing time of a batch in this paper as well. Hence, grouping parts with similar heights together may reduce the processing time. That yields reduced production costs and production emissions. However, as introduced in this paper, if there is more than one plant at which the machines are utilised, this approach might ignore additional costs and carbon emissions caused by transportation. That is because the solution that minimises the processing time-related measures (i.e. makespan or cost) does not necessarily minimise the delivery-related metrics such as transportation cost and transportation emissions. Therefore, a more sophisticated holistic approach is required to deal with all these considerations effectively. For this aim, a mixed-integer mathematical model is developed with two different objectives considering economic aspects and environmental sustainability.

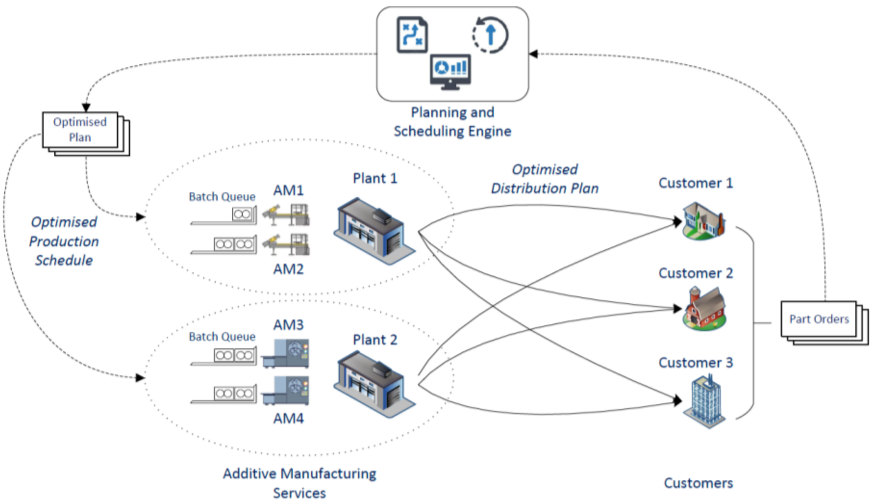

Figure 1. The schematic representation of the addressed problem

It was justified by Kucukkoc [1] that scheduling parallel AM machines to minimise makespan is strongly NP-hard, having additional complexities over classical batch scheduling problems. This is because the processing time of a batch is calculated via a function [1, 2]. Moreover, this paper focuses on total cost (instead of makespan) integrating the transportation problem in terms of both total cost and emission aspects, which increases the complexity of the problem even more.

The following subsection presents the model developed, followed by a numerical example.

3.1. Mathematical model

The mathematical model is developed over the work by Li et al. [2] and Kucukkoc [1]. It has two objectives, such that f_1 aims to minimise the total cost and f_2 aims to minimise the total amount of carbon emissions, i.e. TCE. The notation, parameters and decision variables are given below, followed by the model.

Notation:

i	: part index, where $i \in I$
j	: batch index, where $j \in J$
m	: machine index, where $m \in M$
u	: customer index, where $u \in U$
p	: factory plant index, where $p \in P$

Parameters:

dis_{pu}	: distance between factory plant p and customer u
P_p^M	: the set of machines available at factory plant p
U_u^I	: the set of parts belonging to customer u
h_i	: the height of part i
a_i	: the area of part i
v_i	: the volume of part i
dd_i	: the due date of part i
dc_i	: unit tardiness penalty cost for part i
A_m	: the area of machine m's build platform
H_m	: the maximum height of a part that can be built on machine m
vt_m	: the time required to form per unit volume of material on machine m
rt_m	: the unit recoating (powder-layering) time on machine m, *(the layer height unit is assumed to be the same with that used for the part height)*
set_m	: the time needed to set-up machine m
τ_m	: unit time cost for machine m
ψ	: a large enough positive number
$unit^{TC}$	: unit transportation cost
hc	: unit time cost for human work
ε^{Tr}	: unit carbon emissions amount released to transport per volume of part per km
ε_m^{Pr}	: unit carbon emissions amount released by machine m per unit time

Decision variables:

X_{ijm}	: 1, if part i is allocated to batch j on machine m; 0, otherwise
Y_{jm}	: 1, if batch j on machine m is utilised; 0, otherwise
PC_{jm}	: production cost for batch j on machine m
SC_{jm}	: set-up cost for batch j on machine m
He_{jm}	: the maximum height of the parts allocated to batch j on machine m
vol_{jm}	: the total volume of the parts assigned to batch j on machine m
TC_u	: total transportation cost for customer u
TV_{pu}	: total volume transported from factory plant p to customer u
ct_i	: completion time of part i
tt_i	: tardiness of part i
s_{jm}	: starting time of batch j on machine m
p_{jm}	: processing time of batch j on machine m
c_{jm}	: completion time of batch j on machine m
TE_{pu}	: carbon emissions caused by transportation from factory plant p to customer u
PE_m	: carbon emissons caused by production on machine m

Objective functions:

$$Min\ f_1 = \sum_{j\in J}\sum_{m\in M}\left(PC_{jm} + SC_{jm}\right) + \sum_{u\in U} TC_u + \sum_{i\in I} dc_i tt_i \tag{1}$$

$$Min\ f_2 = \sum_{p\in P}\sum_{u\in U} TE_{pu} + \sum_{m\in M} PE_m \tag{2}$$

Subject to:

$$\sum_{j\in J}\sum_{m\in M} X_{ijm} = 1 \quad \forall i \in I \tag{3}$$

$$\sum_{i\in I} X_{ijm} \le \psi Y_{jm} \quad \forall j \in J, m \in M \tag{4}$$

$$Y_{jm} \le \sum_{i\in I} X_{ijm} \quad \forall j \in J, m \in M \tag{5}$$

$$\sum_{i\in I} a_i X_{ijm} \le A_m \quad \forall j \in J, m \in M \tag{6}$$

$$PC_{jm} \ge vt_m \tau_m vol_{jm} + rt_m \tau_m He_{jm} \quad \forall j \in J, m \in M \tag{7}$$

$$SC_{jm} \ge set_m Y_{jm} hc \quad \forall j \in J, m \in M \tag{8}$$

$$He_{jm} \ge h_i X_{ijm} \quad \forall i \in I, j \in J, m \in M \tag{9}$$

$$TC_u \ge unit^{TC} \sum_{p\in P} dis_{pu} TV_{pu} \quad \forall u \in U \tag{10}$$

$$TV_{pu} \geq \sum_{i \in U_u^I} \sum_{j \in J} \sum_{m \in P_p^M} v_i X_{ijm} \quad \forall p \in P, u \in U \tag{11}$$

$$tt_i \geq ct_i - dd_i \quad \forall i \in I \tag{12}$$

$$ct_i \geq c_{jm} + \psi(X_{ijm} - 1) \quad \forall i \in I, j \in J, m \in M \tag{13}$$

$$ct_i \leq c_{jm} + \psi(1 - X_{ijm}) \quad \forall i \in I, j \in J, m \in M \tag{14}$$

$$c_{jm} \geq s_{jm} + p_{jm} \quad \forall j \in J, m \in M \tag{15}$$

$$s_{jm} \geq c_{j-1,m} + set_m Y_{jm} \quad \forall j \in J \text{ and } j > 1, m \in M \tag{16}$$

$$s_{jm} \geq set_m Y_{jm} \quad \forall j \in J \text{ and } j = 1, m \in M \tag{17}$$

$$s_{jm} \leq \varphi Y_{jm} \quad \forall j \in J, m \in M \tag{18}$$

$$p_{jm} \geq vt_m vol_{jm} + rt_m He_{jm} \quad \forall j \in J, m \in M \tag{19}$$

$$vol_{jm} \geq \sum_{i \in I} v_i X_{ijm} \quad \forall j \in J, m \in M \tag{20}$$

$$vol_{jm} \leq \psi \sum_{i \in I} X_{ijm} \quad \forall j \in J, m \in M \tag{21}$$

$$TE_{pu} \geq \varepsilon^{Tr} dis_{pu} TV_{pu} \quad \forall p \in P, u \in U \tag{22}$$

$$PE_m \geq \varepsilon_m^{Pr} \sum_{j \in J} p_{jm} \quad \forall m \in M \tag{23}$$

$$X_{ijm} \in \{0,1\} \quad \forall i \in I, j \in J, m \in M \text{ and } Y_{jm} \in \{0,1\} \quad j \in J, m \in M \tag{24}$$

$$PC_{jm}, SC_{jm}, He_{jm}, s_{jm}, p_{jm}, c_{jm}, vol_{jm} \geq 0 \quad \forall j \in J, m \in M \tag{25}$$

$$TV_{pu}, TE_{pu} \geq 0 \quad \forall p \in P, u \in U \tag{26}$$

$$TC_u \geq 0 \quad \forall u \in U \tag{27}$$

$$PE_m \geq 0 \quad \forall m \in M \tag{28}$$

$$tt_i, ct_i \geq 0 \quad \forall i \in I \tag{29}$$

The objective given in Eq. (1) aims to minimise the total cost accumulated from production, set-up, transportation and tardiness. The aim of the other objective given in Eq. (2) is to minimise the TCE calculated considering (i) the transportation of parts from plants to customers and (ii) their production on the machines. Note that the time consumed when setting up the machine is not included in this calculation. Eq. (3) ensures that every part is assigned to exactly one batch and machine. Eq. (4) prevents assigning a part to a batch if the batch is not utilised. Eq. (5) relates the two decision variables (Y_{jm} and X_{ijm}) to each other. Eq. (6) satisfies the area capacity of the building platform based on the specifications of the AM machines. Eq. (7) calculates the production cost of each batch using the total volume and the maximum height of the parts allocated to that batch. Eq. (8) is to calculate the set-up cost of each batch utilised. Eq. (9) gets the maximum height of the parts in the batch. Eq. (10) calculates the transportation cost for each customer based on the total volume of the parts shipped to that customer, which is calculated by Eq. (11). Tardiness of each part is calculated by Eq. (12), using its completion time (ct_i) calculated through Eq. (13) and Eq. (14). Note that these two constraints are specially formed to avoid non-linearity as the completion time of the part is gathered from the completion time of the batch that the part is allocated into. The completion time of a batch is obtained from Eq. (15). The start time of a batch is calculated by Eq. (16) and Eq. (17) taking the set-up time of the batch and completion time of the previous batch on the same machine (if any) into account. Eq. (18) sets the start time of the batch to zero if the batch is not utilised. Eq. (19) calculates the processing time of each batch based on its total volume (from Eq. (20)) and maximum height (by Eq. (9)). Similar to Eq. (18), Eq. (21) sets vol_{jm} to zero if there is no part in the batch. Carbon emissions are obtained through Eq. (22) and Eq. (23). In Eq. (22), the total volume shipped from each plant to each customer is multiplied by the unit transportation amount and distance to get the carbon emissions caused by transportation. In Eq. (23), carbon emissions by production in each batch is summed to get the TCE caused by production. Domain constraints are provided in Eqs. (24)-(29).

3.2. Numerical example

Here we consider a numerical example consisting of two factory plants, each of which has two AM machines (i.e. M1 and M2 at plant 1 and M3 and M4 at plant 2) to fabricate a total of 16 parts received from four customers. The complete data, including the specifications of parts and machines (generated based on the test data available by [1, 2]) and the distances between factory plants and customers, are provided in Appendices.

The problem is solved under two scenarios: (i) total cost is minimised using f_1 and (ii) TCE is minimised using f_2. When the model is run to optimise f_1, the optimal solution is obtained within 53.4s. The detailed production schedule and distribution plan based on the optimal solution are reported in Table 1 and Table 2, respectively. As seen from Table 1, five batches are utilised in total (four at plant 1 and one at plant 2).

Table 1. The production schedule based on the optimal solution considering the first objective function (f_1)

Plant	Mach.	Batch	Assigned Parts	PC_{jm}	SC_{jm}	vol_{jm}	He_{jm}	s_{jm}	p_{jm}	c_{jm}
1	M1	1	1,12,16	2525.38	40	1050.73	6.90	2.00	42.0897	44.0897
		2	11,14	8447.83	40	3990.77	12.59	46.0897	140.7970	186.8870
		3	9	3107.30	40	1142.25	11.81	188.887	51.7884	240.6750
	M2	1	8,10,15	14552.10	40	6869.78	21.79	2.00	242.535	244.5350
2	M3	1	2,3,4,5,6,7,13	11982.70	20	4025.19	36.50	1.00	149.783	150.7830

Table 2. The distribution plan based on the optimal solution considering the first objective function (f_1)

From Plant	To Customer	Shipped Parts	TV_{pu}	TE_{pu}
1	1	1	826.08	3097.80
	3	8,9,10,11,12	8453.26	47549.60
	4	14,15,16	3774.19	28306.40
2	1	2,3,4	1727.59	3239.23
	2	5,6,7	1982.60	1858.69
	4	13	315.00	1476.56

While there are three batches planned to be executed on M1, no batch is planned for M4. That is based on the optimal solution obtained by the model to minimise the total cost. The model determines the best combination of parts to be grouped and allocates them to the best machine and plant considering all the capacity constraints as well as the costs caused by production, set-up, transportation, and tardiness. For example, the batch that part 9 is allocated is scheduled on M1 after batch 2 (instead of after batch 1 on M2 at the same plant) as it can start to set-up at 186.887 (rather than 244.535).

When the problem is solved with an ultimate goal to minimise f_2 (scenario 2), the optimal solution is achieved within 7.15s (much shorter than that for scenario 1). The production schedules for machines and the distribution plan to customers are respectively provided in Table 3 and Table 4. A total of five batches have been utilised again but with a different combination of batches and tasks as clearly seen in the tables. This time both machines on both plants are employed to minimise the TCE majorly caused by transportation. As expected, parts belonging to Customer 3 are allocated to the machines at Plant 1 to minimise transportation emissions. For the same reason, other parts are scheduled for production at machines located at Plant 2. However, transportation is not the single factor causing carbon emissions. The model has the ability to minimise production emissions as well. For this aim, parts by different customers may be grouped into the same batch. For example, as seen in Table 3, parts 2, 5, 6, 7 and 15 belonging to three different customers are grouped to be produced in the same batch considering the capacity limits of the machines and height similarity of the parts.

The objective function values and their components are reported in Table 5, comparatively, for both scenarios. For the first scenario which aims to minimise the total cost (f_1), f_1 is obtained as 43895.9 and the TCE for this solution is calculated as $f_2 = 89327.7$. When the objective is altered to minimise the TCE, f_2 is obtained as 77216.4 and the total cost for this solution is acquired as $f_1 = 46463.5$. This clearly shows how the two objective functions act. In scenario 2, while the production emissions increase (from 3799.4 to 3851.9), the model reduces the transportation emissions with a significant amount (from 85528.3 to 73364.5) to minimise the TCE, i.e. 77216.4.

Table 3. The production schedule based on the optimal solution considering the second objective function (f_2)

Plant	Mach.	Batch	Assigned Parts	PC_{jm}	SC_{jm}	vol_{jm}	He_{jm}	s_{jm}	p_{jm}	c_{jm}
1	1	1	8,10	11061.40	40	4984.78	21.79	2.00	184.3560	186.3560
		2	11	5139.77	40	2204.41	12.59	188.356	85.6629	274.0190
	2	1	9,12	3332.90	40	1264.07	11.81	2.00	55.5483	57.5483
2	3	1	1,3,4,13,14,16	10354.90	20	3805.26	17.13	1.00	129.4370	130.6050
	4	1	2,5,6,7,15	13945.70	20	4820.20	36.50	1.00	174.3210	175.3210

Table 4. The distribution plan based on the optimal solution considering the second objective function (f_2)

From Plant	To Customer	Shipped Parts	TV_{pu}	TE_{pu}
1	3	8,9,10,11,12	8453.26	47549.60
2	1	1,2,3,4	2553.67	4788.13
	2	5,6,7	1982.60	1858.69
	4	13,14,15,16	4089.19	19168.10

Table 5. The comparison of the objective terms for the two optimal solutions

Objective	*Min f_1*	*Min f_2*
Total Cost (*GBP*)	43895.9	46463.5
$\sum_{j\in J}\sum_{m\in M}(PC_{jm}+SC_{jm})$	*40795.3*	*43994.6*
$\sum_{u\in U} TC_u$	*2280.7*	*1956.4*
$\sum_{i\in I} dc_i tt_i$	*819.9*	*512.5*
Total Emission (*gr CO_2 eq.*)	89327.7	77216.4
$\sum_{p\in P}\sum_{u\in U} TE_{pu}$	*85528.3*	*73364.5*
$\sum_{m\in M} PE_m$	*3799.4*	*3851.9*

3.3. Alternative scenarios

Additional scenarios have been constituted here to observe the behaviour of the model under different conditions with no time limit. Brief information on each scenario is as follows:

A-1: The objective is to minimise f_1 where the upper limit for f_2 is restricted to 80 kg.

A-2: The objective is to minimise f_2 where the upper limit for f_1 is restricted to 45000 GBP.

A-3: Lexicographically minimise both objectives, where the primary objective is to minimise f_1 and the secondary objective is to minimise f_2

A-4: Lexicographically minimise both objectives, where the primary objective is to minimise f_2 and the secondary objective is to minimise f_1

The problem has been solved under four different scenarios detailed above and the results have been summarised in Figure 2.

Table 6. Design of the test problems

Problem #	nbPlants	nbCustomers	nbParts	nbMachines	Machines at Plants
P1	2	2	10	2	[M1], [M2]
P2			10	2	[M2], [M1]
P3			14	2	[M1], [M2]
P4			14	2	[M2], [M1]
P5	2	3	12	2	[M1], [M2]
P6			12	2	[M2], [M1]
P7			16	3	[M1, M1], [M2]
P8			16	3	[M1], [M2, M2]
P9	2	4	18	2	[M1], [M2]
P10			18	2	[M2], [M1]
P11			20	3	[M1, M1], [M2]
P12			20	3	[M1], [M2, M2]
P13	2	5	20	3	[M1, M1], [M2]
P14			20	3	[M1], [M2, M2]
P15			22	4	[M1, M1], [M2, M2]
P16			22	4	[M1, M2], [M1, M2]
P17	3	3	14	3	[M1], [M1], [M2]
P18			14	3	[M2], [M2], [M1]
P19			16	4	[M1], [M2, M2], [M1]
P20			16	4	[M1, M2], [M1], [M2]
P21			20	4	[M2], [M1, M2], [M1]
P22	3	4	16	4	[M2], [M1, M1], [M2]
P23			20	4	[M1], [M2, M2], [M1]
P24			20	4	[M1, M2], [M1], [M2]
P25			28	4	[M2], [M1, M2], [M1]
P26			28	4	[M1], [M1], [M2, M2]
P27	3	5	30	4	[M2], [M1, M1], [M2]
P28			36	4	[M1], [M2, M2], [M1]
P29			36	4	[M1, M2], [M1], [M2]
P30			44	4	[M2], [M1, M2], [M1]
P31			44	4	[M1], [M1], [M2, M2]
P32	3	6	40	5	[M2, M2], [M1], [M1, M2]
P33			44	5	[M1, M1], [M2, M2], [M1]
P34			44	5	[M1, M2], [M1, M2], [M2]
P35			46	5	[M2], [M1, M1], [M2, M2]
P36			46	5	[M2], [M1, M2], [M1, M2]

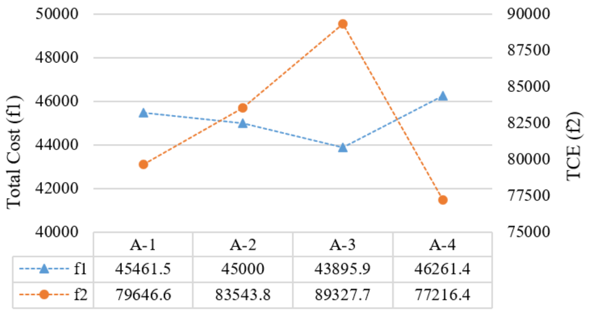

Figure 2. The comparison of the objective values belonging to the optimal solutions obtained under different scenarios

As seen in Figure 2, the minimum value for the total cost has been observed for A-3 where $f_1 = 43895.9$ and $f_2 = 89327.7$. The minimum value for the TCE has been observed for A-4 where $f_1 = 46261.4$ and $f_2 = 77216.4$. These results are in line with the expectations since f_1 is minimised primarily in A-3 while f_2 is minimised primarily in A-4.

In A-2, the TCE could be reduced to 83543.8 when the total cost was constrained with an upper limit of 45000. With regard to A-1, a solution has been obtained with $f_1 = 45461.5$ and $f_2 = 79646.6$ due to the conflicting objectives ensuring that the TCE was limited to a maximum value of 80 kg. As seen in these results, total cost increases in order to reduce the TCE to satisfy the constraint.

To sum up, this numerical example clearly shows the relationship between the conflicting objectives and the effectiveness of the proposed mathematical model.

4. Experimental study

A comprehensive computational study has been conducted to observe the performance of the mathematical model proposed. For this aim, a total of 36 test problems [35] have been generated and solved under different scenarios using a PC equipped with Intel(R) Core(TM) i7-1165G7 2.80GHz with 20 GB Ram. Descriptive information on the test problems is given in Table 6. The second, third, fourth and fifth columns in the table denote the number of plants, the number of customers, the number of parts and the total number of machines utilised at plants, respectively. The machine park at each plant is provided in the last column indicating their types. If we consider P8, the test problem has two plants with a total of three machines, to produce a total of 16 parts received from three customers. There is only one machine of type M1 at plant 1 and there are two machines of type M2 at plant 2.

The model has been coded in Python 3.11.4 and executed by Gurobi Optimizer 10.0.2. Each problem has been solved under two different scenarios, i.e. (i) total cost is minimised ($Min(f_1)$) and (ii) TCE is minimised ($Min(f_2)$). Two different time limits have been applied, i.e. 600s and 1800s, to better observe the model's performance and compare the results obtained under different conditions.

The values of the unit transportation cost ($unit^{TC}$), unit carbon emission amount caused by transportation (ε^{Tr}) and hourly human cost (hc) have been kept the same with the numerical example (as already provided in the Appendices).

Table 7 reports the results obtained by Gurobi Optimizer under the 600s time limit. First, each problem has been solved to minimise the total cost ($Min(f_1)$). The objective value of the solution is reported (second column) together with the optimality status of the model (third column) and the time consumed by the solver (fourth column). If the optimal solution is not achieved, the optimality gap of the best solution is given instead. The fifth column gives the TCE for the solution obtained when minimising total cost.

The sixth column corresponds to the objective value of the best solution when minimising TCE ($Min(f_2)$). The optimality status (and/or gap) and the consumed time are given in the seventh and eighth columns, respectively. The total cost (f_1) of the solution obtained when minimising TCE (f_2) is also provided in the last column.

As seen from Table 7, an optimal solution has been found for 13 out of 36 test problems when minimising f_1, i.e. P1-P8, P17-P18 and P20-P22. As for the remaining problems, the optimal solution was not verified within the time limit given (600s). Due to the complexity of the model, the time required to get the optimal solution increases with the increase in the number of parts, machines, plants and customers. For example, P1 and P2 have been solved optimally with around 1s running time while P22 required over 300s to get the optimal solution and verify it. Even, P9-P16 were unable to be solved within 600s time limit optimality, for which the optimality gap ranged between 1.18% and 4.27%. The optimality gap also tends to increase with the increased problem complexity and reaches as high as 14.94% for P35.

With regard to minimising TCE ($Min(f_2)$), Gurobi was able to retrieve the optimal solutions in 25 out of 36 test problems (as seen in Table 7). This time, the performance of the solver was higher in comparison to the above scenario. The reason lying behind could be the complexity of the total cost calculation, in comparison to the calculation of TCE. The optimality gap of the solutions was not high, with a maximum of 0.67 for P35.

Table 7. Results obtained under 600s time limit

Problem	$Min(f_1)$ / 600s				$Min(f_2)$ / 600s			
	f_1	Opt/Gap%	Time (s)	f_2	f_2	Opt/Gap%	Time (s)	f_1
P1	20289.39	Opt	0.92	21035.8	12389.50	Opt	0.06	22551.3
P2	20220.76	Opt	1.12	18462.2	12655.63	Opt	0.31	20576.7
P3	47200.17	Opt	12.24	37967.8	25914.56	Opt	2.02	51962.7
P4	47447.75	Opt	18.15	47252.1	42811.26	Opt	2.03	49050.2
P5	47902.08	Opt	4.81	104059.0	95392.25	Opt	0.17	51516.2
P6	47251.24	Opt	5.30	79652.1	70837.72	Opt	0.26	48358.7
P7	52509.16	Opt	293.34	118567.0	104784.77	Opt	0.73	7.50537e+07
P8	53425.41	Opt	439.24	115085.0	104784.77	Opt	2.06	56960.7
P9	56349.66	1.47	600	124532.0	108666.76	Opt	2.07	6.0064e+07
P10	55497.35	2.12	600	87588.1	84126.98	Opt	5.91	57011.8
P11	56195.39	2.09	600	130371.0	110672.94	Opt	3.71	67642
P12	57271.33	3.42	600	124984.0	110672.94	Opt	44.72	67464.5
P13	56265.97	1.18	600	133937.0	116906.02	Opt	5.20	63070.6
P14	57359.01	3.31	600	129050.0	116906.02	Opt	27.32	67043.8
P15	59224.73	3.86	600	144023.0	126371.48	Opt	133.49	64851.1
P16	58472.57	4.27	600	135850.0	101615.67	Opt	8.95	6.00628e+07
P17	48145.79	Opt	38.52	86458.4	80678.96	Opt	1.97	51049.9
P18	48172.25	Opt	26.77	81036.6	70257.92	Opt	0.20	50832.7
P19	52520.97	0.51	600	117055.0	104784.77	Opt	1.95	60258.7
P20	51807.17	Opt	218.52	90064.2	80194.22	Opt	3.37	1.0505e+08
P21	51777.71	Opt	178.09	88959.4	79928.09	Opt	0.55	56401.5
P22	51769.16	Opt	328.50	87811.8	80790.83	Opt	51.51	7.00524e+07
P23	56113.41	2.73	600	126655.0	110672.94	Opt	20.51	66408.5
P24	55469.07	3.32	600	100769.0	86129.99	Opt	18.01	8.75553e+07
P25	67381.39	8.98	600	75797.2	67843.31	Opt	288.12	1.40072e+08
P26	67340.38	8.30	600	87420.8	80114.86	0.3	600	72800.3
P27	73685.83	10.39	600	120263.0	103579.80	0.48	600	76800.2
P28	83390.44	10.78	600	139193.0	122773.54	0.11	600	93856
P29	83572.60	10.67	600	153428.0	135783.21	0.37	600	93922.8
P30	99175.03	14.03	600	158087.0	139492.17	0.14	600	124806
P31	99189.24	13.42	600	166476.0	152290.35	0.55	600	115397
P32	92832.03	12.51	600	166237.0	146158.08	0.59	600	2.62585e+08
P33	97749.64	12.51	600	180140.0	142728.23	0.21	600	1.45105e+08
P34	98855.99	13.99	600	174022.0	142605.50	0.16	600	135230
P35	104208.04	14.94	600	266096.0	162757.17	0.67	600	109776
P36	103919.76	14.55	600	169917.0	149400.53	0.16	600	129297

Table 8 reports the results obtained when the time limit was set to 1800s. As seen from the table, the number of optimal solutions has increased to 17 in comparison to 13 obtained under the 600s time limit when minimising f_1. For the remaining instances, the optimality of the solutions was not verified. However, it was observed that the optimality gap has reduced slightly, except for P10 (for which it was reduced from 2.2% to 0.55%).

As also observed for the 600s time limit, Gurobi was able to obtain and verify 25 optimal solutions in total under the 1800s time limit. However, the average of the optimality gap has been reduced from 0.34% to 0.325% for the remaining 11 test problems. For P30, increasing the time limit from 600s to 1800s has not contributed to the capability of the model as the same solutions with the same gap have been attained under both conditions. For some cases (such as P32), the increased time limit helped prune the lower bound further and reduced the gap (e.g. from 0.59% to 0.53%).

5. Conclusions and future work

This paper addressed the scheduling of parallel unrelated AM machines located at geographically dispersed factory plants. Due to the increasing environmental concerns and the requirements for the sustainable use of resources, the TCE (released during production and transportation of parts -from plants to customers) has been minimised through a separate objective function.

Table 8. Results obtained under 1800s time limit

Problem	$Min(f_1)$ / 1800s				$Min(f_2)$ / 1800s			
	f_1	Opt/Gap%	Time (s)	f_2	f_2	Opt/Gap%	Time (s)	f_1
P1	20289.39	Opt	0.88	21035.8	12389.50	Opt	0.06	22551.3
P2	20220.76	Opt	1.22	18462.2	12655.63	Opt	0.29	20576.7
P3	47200.17	Opt	11.18	37967.8	25914.56	Opt	1.88	51962.7
P4	47447.75	Opt	14.60	47252.1	42811.26	Opt	2.07	49050.2
P5	47902.08	Opt	3.87	104059.0	95392.25	Opt	0.17	51516.2
P6	47251.24	Opt	4.66	79652.1	70837.72	Opt	0.25	48358.7
P7	52509.16	Opt	283.43	118567.0	104784.77	Opt	0.65	7.50537e+07
P8	53425.41	Opt	439.22	115085.0	104784.77	Opt	2.07	56960.7
P9	56349.66	Opt	1037.79	124532.0	108666.76	Opt	2.11	6.0064e+07
P10	55497.35	0.55	1800	87588.1	84126.98	Opt	5.89	57011.8
P11	56195.39	Opt	1614.39	130371.0	110672.94	Opt	3.68	67642
P12	57188.60	2.60	1800	124116.0	110672.94	Opt	41.02	67464.5
P13	56265.97	Opt	808.61	133937.0	116906.02	Opt	4.72	63070.6
P14	57359.01	2.63	1800	129050.0	116906.02	Opt	25.88	67043.8
P15	59224.73	2.66	1800	144023.0	126371.48	Opt	118.60	64851.1
P16	58472.57	3.17	1800	135850.0	101615.67	Opt	8.14	6.00628e+07
P17	48145.79	Opt	38.84	86458.4	80678.96	Opt	1.85	51049.9
P18	48172.25	Opt	26.79	81036.6	70257.92	Opt	0.19	50832.7
P19	52520.97	Opt	701.57	117055.0	104784.77	Opt	1.80	60258.7
P20	51807.17	Opt	219.98	90064.2	80194.22	Opt	3.12	1.0505e+08
P21	51777.71	Opt	178.13	88959.4	79928.09	Opt	0.54	56401.5
P22	51769.16	Opt	329.59	87811.8	80790.83	Opt	47.23	7.00524e+07
P23	56113.41	1.47	1800	126655.0	110672.94	Opt	19.25	66408.5
P24	55424.50	1.74	1800	99097.5	86129.99	Opt	16.14	8.75553e+07
P25	67213.99	8.44	1800	82364.3	67843.31	Opt	267.75	1.40072e+08
P26	67340.38	6.93	1800	87420.8	80114.86	0.19	1800	72800.3
P27	73679.17	10.39	1800	120393.0	103579.80	0.41	1800	76800.2
P28	83346.94	10.17	1800	139193.0	122773.54	0.10	1800	93856
P29	83539.95	10.26	1800	151289.0	135783.21	0.35	1800	93922.8
P30	99175.03	13.45	1800	158087.0	139492.17	0.14	1800	124806
P31	98982.84	13.13	1800	171216.0	152267.39	0.53	1800	117297
P32	92825.93	12.30	1800	166235.0	146158.08	0.53	1800	2.62585e+08
P33	97748.12	11.69	1800	180517.0	142717.12	0.20	1800	1.77619e+08
P34	98855.99	13.34	1800	174022.0	142594.35	0.15	1800	7.01354e+07
P35	104130.56	14.41	1800	176594.0	162755.40	0.65	1800	109346
P36	103307.96	13.74	1800	167487.0	149387.44	0.14	1800	132740

A MILP model is proposed for the first time in literature, and a numerical example is presented to show the applicability and practicality of both the method and the addressed problem. Some practical scenarios have been constituted to show the applicability of the model and further elaborate results. A comprehensive computational study has also been conducted to test the performance of the model and it was observed that the number of instances solved optimally has increased when the time limit was increased from 600s to 1800s, as expected. The results of the computational tests indicate that the model is capable of producing practical results within a short amount of computation time. The methods proposed in this work can easily be adapted to solve real-world problems and increase the use of shareable resources environmentally friendly while minimising total cost. While the problem size may increase in real-life applications due to the enormous number of orders, parts and machines; the proposed models can still produce efficient solutions under certain time limits. They can also be integrated into existing decision support systems together with complex heuristic techniques to get quality solutions timely manner.

Future studies may consider implementing a heuristic and/or metaheuristic algorithm to quickly solve large-size problems especially. One can also develop lower bounds for the problem studied here for comparison purposes. It is also possible to further extend the MILP model proposed in this work with new industry-oriented constraints and/or energy considerations.

Acknowledgement

The authors acknowledge the financial support received from *Balikesir University Scientific Research Projects* department under grant number *BAP-2022-086*.

Appendices

Table A1. Data on parts used for the numerical example

u	i	h_i	a_i	v_i	dd_i	dc_i
1	1	6.9	209.06	826.08	120	1
	2	26.04	550.11	952.6	120	1
	3	15.97	23.63	71.91	120	1
	4	17.04	99.53	703.08	120	1
2	5	27.94	56.85	272.92	155	2.5
	6	36.5	742.97	1583.98	155	2.5
	7	17.38	50.02	125.7	155	2.5
3	8	18.46	300.66	3144.39	180	2
	9	11.81	435.66	1142.25	180	2
	10	21.79	131.88	1840.39	180	2
	11	12.59	349.83	2204.41	180	2
	12	2.67	84.97	121.82	180	2
4	13	17.13	48.27	315	320	3
	14	12.53	269.66	1786.36	160	3
	15	18.09	175.77	1885	160	3
	16	4.27	122.62	102.83	160	3

Table A2. Data on machines used for the numerical example

m	A_m	H_m	VT_m	RT_m	SET_m	τ_m	ε_m^{Pr}
1	625	32.5	0.030864	1.4	2	60	6
2	625	32.5	0.030864	1.4	2	60	6
3	1600	40	0.030864	0.7	1	80	6.25
4	1600	40	0.030864	0.7	1	80	6.25

Table A3. Parameter values for the numerical example

Parameter	Value
hc	20 GBP/hr
$unit^{TC}$	0.001 $GBP/(km * cm^3)$
ε^{Tr}	0.0375 $gr/(km * cm^3)$

Table A4. Distances between plants and customers (in *km*) used for the numerical example

Plant/Customer	1	2	3	4
1	100	75	150	200
2	50	25	225	125

References

[1] Kucukkoc, I., *MILP models to minimise makespan in additive manufacturing machine scheduling problems.* Computers & Operations Research, 2019. 105: p. 58-67.

[2] Li, Q., I. Kucukkoc, and D.Z. Zhang, *Production planning in additive manufacturing and 3D printing.* Computers & Operations Research, 2017. 83: p. 157-172.

[3] Bouchenine, A. and M.A.M. Abdel-Aal, *Towards supply chain resilience with additive manufacturing: A bibliometric survey.* Supply Chain Analytics, 2023. 2: p. 100014.

[4] Naghshineh, B. and H. Carvalho, *The implications of additive manufacturing technology adoption for supply chain resilience: A systematic search and review.* International Journal of Production Economics, 2022. 247: p. 108387.

[5] Pimenov, D.Y., et al., *Influence of selective laser melting process parameters on the surface integrity of difficult-to-cut alloys: comprehensive review and future prospects.* International Journal of Advanced Manufacturing Technology, 2023. 127(3-4): p. 1071-1102.

[6] Li, Z., et al., *Incorporating draw constraint in the lightweight and self-supporting optimisation process for selective laser melting.* The International Journal of Advanced Manufacturing Technology, 2018. 98(1): p. 405-412.

[7] Kucukkoc, I., Q. Li, and D.Z. Zhang. *Increasing the utilisation of additive manufacturing and 3D printing machines considering order delivery times*. in *19th International Working Seminar on Production Economics, February 22-26*. 2016. Innsbruck, Austria.

[8] Chergui, A., K. Hadj-Hamou, and F. Vignat, *Production scheduling and nesting in additive manufacturing.* Computers & Industrial Engineering, 2018. 126: p. 292-301.

[9] Kucukkoc, I., et al. *Scheduling of Multiple Additive Manufacturing and 3D Printing Machines to Minimise Maximum Lateness*. in *20th International Working Seminar on Production Economics, February 19-23*. 2018. Innsbruck, Austria.

[10] Li, Q., et al., *A dynamic order acceptance and scheduling approach for additive manufacturing on-demand production.* International Journal of Advanced Manufacturing Technology, 2019. 105(9): p. 3711-3729.

[11] Kapadia, M.S., et al., *A genetic algorithm for order acceptance and scheduling in additive manufacturing.* International Journal of Production Research, 2021: p. 1-18.

[12] Zhang, J., X. Yao, and Y. Li, *Improved evolutionary algorithm for parallel batch processing machine scheduling in additive manufacturing.* International Journal of Production Research, 2020. 58(8): p. 2263-2282.

[13] Kucukkoc, I. *Metal Additive Manufacturing: Nesting vs. Scheduling*. in *Optimization and Data Science: Trends and Applications*. 2021. Cham: Springer International Publishing.

[14] Altekin, F.T. and Y. Bukchin, *A multi-objective optimization approach for exploring the cost and makespan trade-off in additive manufacturing.* European Journal of Operational Research, 2021.

[15] Kucukkoc, I., Z. Li, and Q. Li, *2D Nesting and Scheduling in Metal Additive Manufacturing*, in *Communications in Computer and Information Science*. 2021. p. 97-112.

[16] Alicastro, M., et al., *A reinforcement learning iterated local search for makespan minimization in*

additive manufacturing machine scheduling problems. Computers and Operations Research, 2021. 131.
[17] Rohaninejad, M., et al., *A hybrid learning-based meta-heuristic algorithm for scheduling of an additive manufacturing system consisting of parallel SLM machines.* International Journal of Production Research, 2021: p. 1-21.
[18] Arık, O.A., *Additive manufacturing scheduling problem considering assembly operations of parts.* Operational Research, 2021.
[19] Hu, K., Y. Che, and Z. Zhang, *Scheduling unrelated additive manufacturing machines with practical constraints.* Computers & Operations Research, 2022. 144: p. 105847.
[20] Wu, Q., et al., *Online order scheduling of multi 3D printing tasks based on the additive manufacturing cloud platform.* Journal of Manufacturing Systems, 2022. 63: p. 23-34.
[21] Oh, Y., et al., *Nesting and scheduling problems for additive manufacturing: A taxonomy and review.* Additive Manufacturing, 2020. 36: p. 101492.
[22] Kim, Y.J. and B.S. Kim, *Part-grouping and build-scheduling with sequence-dependent setup time to minimize the makespan for non-identical parallel additive manufacturing machines.* The International Journal of Advanced Manufacturing Technology, 2022. 119(3): p. 2247-2258.
[23] Che, Y., et al., *Machine scheduling with orientation selection and two-dimensional packing for additive manufacturing.* Computers and Operations Research, 2021. 130.
[24] Oh, Y. and Y. Cho, *Scheduling of build and post processes for decomposed parts in additive manufacturing.* Additive Manufacturing, 2022. 59.
[25] Ying, K.C., et al., *Adjusted Iterated Greedy for the optimization of additive manufacturing scheduling problems.* Expert Systems with Applications, 2022. 198.
[26] Zipfel, B., J. Neufeld, and U. Buscher, *An iterated local search for customer order scheduling in additive manufacturing.* International Journal of Production Research, 2023: p. 1-21.
[27] Kucukkoc, I., *Batch Delivery Considerations in Additive Manufacturing Machine Scheduling Problem* in *Operations Research and Data Science in Public Services*, L.P. Matteo Cosmi, Alice Raffaele, Marcella Samà, Editor. 2023, Springer Cham: Switzerland.
[28] Ying, K.C. and S.W. Lin, *Minimizing makespan in two-stage assembly additive manufacturing: A reinforcement learning iterated greedy algorithm.* Applied Soft Computing, 2023. 138.
[29] Lee, S.J. and B.S. Kim, *Two-stage meta-heuristic for part-packing and build-scheduling problem in parallel additive manufacturing.* Applied Soft Computing, 2023. 136.
[30] Dwivedi, G., et al., *Simultaneous Production and Transportation Problem: A Case of Additive Manufacturing.* Transportation Science, 2023. 57(3): p. 741-755.
[31] Zehetner, D. and M. Gansterer, *The collaborative batching problem in multi-site additive manufacturing.* International Journal of Production Economics, 2022. 248: p. 108432.
[32] Cakici, E., S.J. Mason, and M.E. Kurz, *Multi-objective analysis of an integrated supply chain scheduling problem.* International Journal of Production Research, 2012. 50(10): p. 2624-2638.
[33] Low, C., C.M. Chang, and B.Y. Gao, *Integration of production scheduling and delivery in two echelon supply chain.* International Journal of Systems Science: Operations and Logistics, 2017. 4(2): p. 122-134.
[34] Aminzadegan, S., M. Tamannaei, and M. Fazeli, *An integrated production and transportation scheduling problem with order acceptance and resource allocation decisions.* Applied Soft Computing, 2021. 112.
[35] Kucukkoc, I. *Dataset used for the test problems*. 2023; Available from: http://ikucukkoc.baun.edu.tr/projects/Dataset_carbon.rar.

Ibrahim Kucukkoc *is an Associate Professor in the Industrial Engineering department at Balikesir University (Turkey) where he has been a faculty member since December 2009. He completed his PhD at the University of Exeter (UK) in 2015 (funded by a 4-year scholarship from the Turkish Council of Higher Education). His research interests lie in the area of modelling and optimisation of modern manufacturing systems (assembly line balancing in particular), production planning of additive manufacturing machines and application of modern algorithms on sophisticated combinatorial optimisation problems.*
https://orcid.org/0000-0001-6042-6896

An International Journal of Optimization and Control: Theories & Applications
ISSN: 2146-0957 eISSN: 2146-5703
Vol.14, No.1, pp.32-40 (2024)
https://doi.org/10.11121/ijocta.1435

RESEARCH ARTICLE

Bin packing problem with restricted item fragmentation: Assignment of jobs in multi-product assembly environment with overtime

Mustafa Ustuncelik, Cagri Koc*, Huseyin Tunc

Department of Business Administration, Social Sciences University of Ankara, Ankara, Turkiye
mustafa.ustuncelik@gmail.com, cagri.koc@asbu.edu.tr, huseyin.tunc@asbu.edu.tr

ARTICLE INFO

Article history:
Received: 20 July 2023
Accepted: 10 October 2023
Available Online: 3 November 2023

Keywords:
Bin packing problem
Item fragmentation
Multi product assembly jobs
Mixed integer programming

AMS Classification 2010:
90B35, 90C11

ABSTRACT

This paper studies the assignment problem of multi product assembly jobs to days. The problem aims to minimize the amount of overtime while avoiding assembly delays for jobs that can be fragmented into smaller sub-tasks. When sequence-dependent setup times are negligible, the problem considered transforms into the bin packing problem with restricted item fragmentation where jobs represent items and days stand for bins. We present a mixed integer programming model of the problem by extending earlier formulations in the literature. Computational experiments show that the mathematical model obtained optimal solutions for majority of instances tested within reasonable computation times.

1. Introduction

This study is inspired from a practical production scheduling problem encountered in a construction machinery manufacturing company. The company deals with intricate product assemblies including multiple sub-assembly groups and multi-level product trees. The intricate nature of these product structures, characterized by a multitude of sub-assembly groups and their corresponding multi-level trees, presents a significant challenge in effectively planning and managing material resources. Furthermore, the characteristics of the work centers vary depending on whether job setup times are dependent on the job sequence.

In operational research literature, scheduling and assignment problems are extensively studied [1-3]. When the objective is to determine only the production day for each job, without considering sequence dependent setup times, the problem aligns with the bin packing problem (BPP). Using this insight, we tackled the complex real-world problem using a BPP-based solution approach.

The BPP is one of the most extensively studied combinatorial optimization problems in the literature. The BPP, which is known to be NP-hard, involves packing a set of items into the minimum number of bins of fixed size where each item has a known size and each bin has a known capacity. The BPP has many practical applications, such as packing items in a warehouse or shipping containers, assigning tasks on a set of machines and allocating resources in cloud computing. Furthermore, the BPP has theoretical implications, as it is related to other problems such as the knapsack problem, the cutting stock problem, and the vehicle routing problem [4].

The BPP has been subject to a detailed scrutiny for several decades, resulting in various solution approaches to solve the problem under different objectives and constraints. A variety of heuristics have been developed to find good-quality solutions in a reasonable amount of time. These methods include heuristics such as first-fit, next-fit, best-fit and worst-fit, and metaheuristics such as genetic algorithms, simulated annealing and tabu search. Despite extensive research on the issue, there are still many remaining challenges due to its practical importance, making it a currently active topic in optimization.

The BPP and its variants have been extensively studied in the literature. Table 1 provides a summary of various BPP studies. The table categorizes these studies according to their objectives, constraints, and solution methods employed. This overview offers a

*Corresponding author

Table 1. Summary of the literature on the BPP.

Study	Objective							Constraints					Solution Method
	B	F	C	N	L	M	O	C	F	B	K	I	
Eilon and Christofides [5]	+										+		Zero-one programming mode, heuristic
Jansen [6]	+							+					Asymptotic approximation
Loh et al. [7]					+					+			Weight annealing
Khanafer et al. [8]	+							+					Dual-feasible functions Data-dependent dual-feasible functions
Crainic et al. [9]	+		+								+		Heuristic, lower bounds
Elhedhli et al. [10]	+							+					Branch-and-price algorithm
Fleszar and Charalambous [11]	+										+		Heuristic
Khanafer et al. [21]				+						+			Column-generation methods, Heuristic, tabu search
Casazza and Ceselli [14]		+								+			Exact algorithms, heuristics
Dokeroglu and Cosar [17]			+							+			Genetic algorithm
LeCun et al. [15]		+								+			Approximation algorithms
Arbib and Marinelli [20]						+				+			MIP
Byholm and Porres [16]		+								+			Approximation and metaheuristic algorithms
Casazza [18]			+						+		+		Branch-and-price algorithm
Bertazzi et al. [12]	+								+				Worst-case analysis
Ekici [13]	+							+	+				Heuristic
Ekici [19]			+					+	+		+		Heuristic, lower bounds
This study							**+**			**+**	**+**	**+**	MIP

Objectives: B: number of bins, F: number of fragmentations, C: cost, N: number of conflicts, L: load of bin, M: makespan, O: over capacity usage.
Constraints: C: conflict items, F: fragmentable items, B: number of bins, K: variable bin capacity, I: item-bin conflict.

comprehensive, yet not exhaustive, view of the diversity in approaches and strategies utilized within the BPP.

One of the primary objectives of the BPP is to minimize the number of bins used. Minimizing the number of bins leads to better space utilization, further cost savings, improved operational efficiency and enhanced sustainability. Apart from this, the studies also consider minimizing the total cost of packing items, the makespan and over capacity usage as well.

The constraints have a significant impact on the combinatorial nature of the problem. In BPPs, items that should not be placed in the same bin are referred to as conflicted items. This constraint is particularly critical in real-life scenarios such as chemical material transportation or storage. Several papers focused on conflicted items [6, 8]. These studies developed several mathematical models and metaheuristics to provide solutions while ensuring that conflicted items are assigned to different bins [10, 13, 19]. In BPPs, bins may have a fixed or variable capacity each may have different costs associated with its usage. In this regard, several studies used heterogenous bins [5, 9, 11, 18, 19].

Loh et al. [7] studied the one-dimensional BPP and proposed a weight annealing heuristic. Khanafer et al. [8] developed lower bounds for the BPP with conflicts. Crainic et al. [9] considered the variable cost and size BPP and developed lower bounds and heuristics. Elhedhli et al. [10] proposed a branch-and-price algorithm for the BPP with conflicts. Fleszar and Charalambous [11] developed bin-oriented heuristics for one-dimensional BPP by packing one bin at a time. Khanafer et al. [21] studied the min-conflict packing problem as well as the bi-objective version of the problem. Dokeroglu and Cosar [17] proposed a set of robust and scalable hybrid parallel algorithms to solve the BPP. Arbib and Marinelli [20] addressed the one-dimensional BPP to minimize completion time and lateness.

The BPP with item fragmentation (BPPIF) involves efficiently packing items into a limited number of bins where items can be fragmented into multiple bins. The BPP objective is to minimize the total number of bins used. Unlike the classic BPP, where items are treated as indivisible units, this variation enables better fitting within the bins as it allows items to be divided into smaller fragments. Given a collection of items, each with a specific size and a known fragmentation capacity, and a set of bins with fixed capacities, the BPPIF entails determining the optimal packing configuration that minimizes the number of bins required while adhering to the item fragmentation constraints.

When all items are fragmentable with no additional consideration, the BPPIF transforms into a linear optimization problem [13]. However, this usually does not reflect the reality and there often exists special considerations or constraints regarding fragmentation. In real-life scenarios, item fragmentation may lead to additional costs for subsequent operations. In the literature, several studies focused on the BPPIF aiming to reduce the overall assignment cost [18, 19]. There are also studies that aim to minimize the number of fragmentations [12-16]. This objective is particularly important for the cases where item fragmentation incurs a cost [14]. Those studies often consider a given number of identical bins.

Bertazzi et al. [12] investigated a few special splitting policies and developed the worst-case performance bounds. Ekici [13] introduced mathematical models and a column generation-based heuristic for the BPPIF. Casazza and Ceselli [14] studied the BPPIF and developed mathematical formulation and algorithms and greedy heuristics. LeCun et al. [15] investigated the complexity of the problem considered and proposed a constant factor approximation algorithm. Byholm and Porres [16] suggested performance improving operators for the heuristic algorithms introduced earlier in the literature. Casazza [18] considered BPPIF with heterogenous bins and developed a branch-and-price algorithm. Furthermore, due to the characteristics of the items to be packed, some items may not be fragmentable during the packing process. In this respect, Ekici [13] and [19] investigated the BPPIF with conflicted items. Here, one cannot pack fragments of conflicted items into the same bin. The former assumes the identical bins, whereas the latter considers variable sized bins.

This study investigates the BPPIF with additional side constraints so as to analyze the production scheduling problem with sequence independent setup times considered in a multi-product assembly environment. Here, items correspond to jobs and bins represent days in the production scheduling setting. Our contribution is two-fold. First, we consider the additional side constraints, namely item-bin conflict and restricted item fragmentation. The former refers that items (jobs) cannot be packed into any given bin (day). The latter, on the other hand, represents an item can be fragmented at most once, and the fragmented parts must be packed into the bins representing two subsequent days. Second, we extended the mathematical formulation in the literature to consider the aforementioned side constraints and evaluated its performance in a real-life inspired extensive numerical study.

The rest of the paper is organized as follows. In Section 2, we define the problem. We introduce the mathematical model used to solve the BPPIF in Section 3. We present the results of the computational study in Section 4. Concluding remarks are provided in Section 5.

2. Problem defitinion

The problem is inspired from the production scheduling problem in a company that manufactures and assembles industrial machines. The main body of the machine, consisting of steel plates, is manufactured internally by the company, whereas the remaining materials are procured from multiple external suppliers. The machine parts manufactured by the company undergo a series of process including cutting and forming, machining, welding, painting, and assembly. Specifically, the items that require welding have a sub-assembly product tree structure that can reach up to level seven.

In the context of products comprised of multiple subcomponents, it is critical to ensure that all manufacturing processes for the subcomponents are completed prior to initiating the assembly process. Failure to do so, may result in disruptions in production. Given that each product has a distinct product structure and follows a unique routing sequence, it is challenging, yet crucial, to develop a planning strategy that guarantees the timely completion of all necessary operations for each product.

The complexity of this planning problem arises from the diverse product structures and routing sequences. Each product necessitates a distinct set of operations and follows a unique sequence of steps. Creating the optimal plan to ensure all required operations are completed for each product is a major challenge.

Figure 1 illustrates a multi-level product BOM and routings for sub-assembly items. Figure 1(b) presents the work centers responsible for processing all the parts required for Sub Assembly 3 body production, according to the product tree structure depicted in Figure 1(a). All parts must be processed at different work centers with different priorities. According to the product tree structure, Item 2 and Item 3 must be processed first at the same work center in order to produce Item 6 in sub-assembly group 3. Any delay in processing Item 2 and Item 3 directly affects the completion time of sub-assembly group 3.

In the manufacturing company where this study is inspired, MRP program is used to determine the requirement dates of materials. The MRP program determines the latest requirement days of all materials by performing backward date calculations by considering the demand date of the product on a daily basis. Because all materials have pre-determined routings set in the MRP program, all jobs for each work centers are also determined on a daily basis when materials latest requirement dates are calculated.

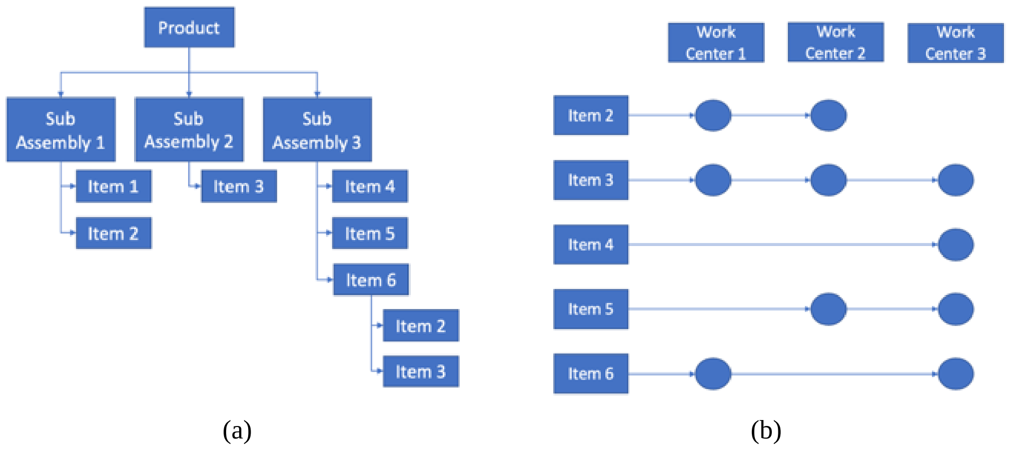

Figure 1. (a): Multi-level product BOM, (b): routings for sub-assembly items.

The MRP program does not consider the finite capacities of work centers and specific manufacturing conditions of jobs when determining the latest requirement dates. Backward calculation approach often results in unrealistic scenarios in production planning. For instance, a work center that operates only one shift per day may be loaded jobs with a total duration of two shifts.

Although knowing the deadlines of jobs is a necessity for an effective plan, it is not sufficient. In a work center, similar to the examples given earlier, there are two main challenges that can arise: exceeding the capacity of the work center and the unavailability of materials at the required time due to the involved nature of the sub-assembly products. These issues are typically addressed by resorting to overtime work.

To put it simply, when the workload surpasses the capacity of the work center or when the materials needed for production are not available, the solution often involves employing overtime work. Inevitably, this leads to additional hours of work beyond the regular schedule to compensate for the increased workload or to catch up on delayed tasks caused by material unavailability. By using overtime work strategically, these challenges can be effectively addressed and the smooth operation of the work center can be maintained.

In the company, when an overtime decision is made for a working day shift, three hours of overtime should be done as standard even if the total workload requirement is less than three hours. As such, this leads to additional costs for the company. In particular, the cost of overtime is fixed, i.e., when an overtime decision is made a fixed cost is incurred. This simply implies that it is cost-efficient to plan three hours of workload (full overtime capacity) if overtime is necessary.

In order to achieve a more balanced and cost-effective planning, it is necessary to consider the deadlines of tasks and plan them based on the capacity of the work center on a daily basis. By considering the capacity constraints, it is possible to allocate resources more efficiently, avoid excessive workloads, and ensure that materials are available when needed. This type of planning facilitates minimizing overtime work and reduces additional costs for the company.

We focus on a single work center and aim to determine the daily job assignments in there. The jobs do not have any sequence dependent setup costs, so the order in which the jobs are processed within a day does not have an impact on the total cost. Furthermore, it is allowed to leave at most one job unfinished during the day, which can be resumed in the following day. As such, this problem determines job-day assignments where the processing order of jobs within each day is not of interest. Since items can be considered as jobs, bins can be considered as days, and some jobs may not need to start and end at the same day, the resulting problem can be modelled as the BPPIF. The jobs that have to be completed within a day are referred to as non-fragmentable items. The remaining jobs are considered as fragmentable items whose processing operations must be completed at most one day after its starting day. As opposed to the common assumption adopted in the BPPIF literature, in our problem, each fragmentable job can be divided into at most two parts and fragmented parts can be packed into specific pair of bins, i.e., those referring to the subsequent days.

The objective of the problem is to minimize the total overtime while allocating jobs to variable-size bins (i.e., days at which only normal work hours are used and days at which the sum of normal work hours and overtime are used) with limited capacities. As the due dates of jobs are known, the number of days (bins) for planning is fixed. Each non-fragmentable job must be finished within one day, whereas each fragmentable job must be completed within either one day or two consecutive days. On any given day, only one job can be fragmented to the following day and the setup times between jobs are not sequence dependent. Also, we assume that processing time of a job cannot be longer then a working day capacity.

Figure 2 illustrates a feasible solution of the problem. The figure shows that since the total processing times of the jobs assigned to the first day exceed the capacity of that day, including overtime, the amount of work time that exceeds the capacity is transferred to the second day. As such, the amount of work transferred from the first day is also considered while determining the capacity need for the second day. If the remaining capacity of normal shift hours is insufficient to meet the daily scheduled requirement, overtime is considered as an additional capacity. As the setup times are not sequence-dependent, the fragmented item and hence the capacity transferred to the next day will be determined following the due dates. Put in other words, the solution does not impose a sequence within a given day.

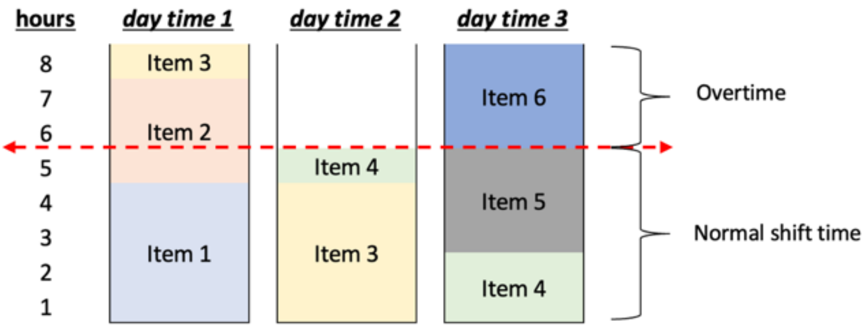

Figure 2. Illustration of a feasible solution.

3. Notation and mathematical model

We model the problem as MIP that balances the capacity utilization of the bins and minimizes the number of overtime hours required to complete all the jobs. We formulated the MIP with three binary decision variables indicating whether a job is assigned to a particular bin, whether a job is fragmented and whether an overtime decision is made or not. Furthermore, a continuous decision variable represents the fragmented part of a job that will be transferred to the following day.

The sets, parameters and decision variables are as follows.

Sets

$N = \{1, \dots, n\}$: *Job set*

$T = \{1, \dots, t\}$: *Day set*

F: *Fragmentable jobs set* $(F \in N)$

$\bar{F}$: *Non − fragmentable jobs set* $(\bar{F} \in N)$

$N = F \cup \bar{F}$

a_i: *Jobs that can be assigned to day* $i \in T$

$\bar{a}_i$: *Jobs that cannot be assigned to day* $i \in T$

A_j: *Days that job* $j \in N$ *can be assigned to*

$\bar{A}_j$: *Days that job* $j \in N$ *cannot be assigned to*

Parameters

P_j : *The processing time of job* $j \in N$

d: *The time for a normal day shift*

o: *Overtime for a working day*

Decision variables

$$x_{ji} = \begin{cases} 1, \text{if job } j \in N \text{ is assigned to day } i \in T \\ 0, \text{otherwise} \end{cases}$$

$$\bar{x}_{ji} = \begin{cases} 1, \text{if job } j \in N \text{ is fragmented to day } i \in T \\ 0, \text{otherwise} \end{cases}$$

$$y_i = \begin{cases} 1, \text{if overtime decision is made in day } i \in T \\ 0, \text{otherwise} \end{cases}$$

z_i: *fragmented time amount to day* $i \in T$

The mathematical model of the problem is as follows.

Objective

$$Min \sum_{i=1}^{t} y_i * o$$

Constraints

$$\sum_{j=1}^{n} \bar{x}_{j1} = 0 \quad (1)$$

$$z_1 = 0 \quad (2)$$

$$\sum_{i \in A_j} x_{ji} = 1 \qquad j \in N \; (3)$$

$$\sum_{i \in \bar{A}_j} x_{ji} = 0 \qquad j \in N \; (4)$$

$$\sum_{i \in A_j} \bar{x}_{ji} \leq 1 \qquad j \in F \; (5)$$

$$\sum_{i \in \bar{A}_j} \bar{x}_{ji} = 0 \qquad j \in F \; (6)$$

$$\sum_{i=1}^{t} \bar{x}_{ji} = 0 \qquad j \in \bar{F} \; (7)$$

$$\sum_{j \in a_i} \bar{x}_{ji} \leq 1 \qquad i \in T/\{1\} \; (8)$$

$$\sum_{j \in \bar{a}_i} \bar{x}_{ji} = 0 \qquad i \in T/\{1\} \; (9)$$

$$x_{ji} \geq \bar{x}_{ji+1} \qquad j \in a_i, i \in T/\{t\} \; (10)$$

$$z_i \leq \sum_{j=1}^{n} \bar{x}_{ji} * P_j \qquad i \in T/\{1\} \; (11)$$

$$z_2 + y_1 * o \geq \sum_{j=1}^{n} x_{j1} * P_j - d \qquad (12)$$

$$y_t * o \geq z_t + \sum_{j=1}^{n} x_{jt} * P_j - d \qquad (13)$$

$$z_{(i+1)} + y_i * o \geq z_i + \sum_{j=1}^{n} x_{ji} * P_j - d \quad i \in T/\{1, t\} \qquad (14)$$

$$x_{ji}, \bar{x}_{ji}, y_i \in \{0,1\} \qquad j \in N, i \in T \; (15)$$

$$z_i \geq 0 \qquad i \in T \; (16)$$

In the model, objective function minimizes the total overtime. Constraints (1) and (2) ensure that a job cannot be fragmented before the first day of the planning horizon. Constraints (3) and (4) guarantee that jobs have to be assigned to only one day and they cannot be assigned to days that are later than their delivery dates. Constraints (5) and (6) state that if a job is fragmentable, it can be fragmented for the days that are earlier than its delivery dates. Constraints (7) guarantee that non-fragmentable jobs cannot be fragmented. Constraints (8) ensure that at most one job can be fragmented among all jobs for the day. Constraints (9) ensure that a job can not be fragmented for days to which it cannot be assigned. Constraints (10) state that a job can only be fragmented on the day after its original assigned day. Constraints (11) guarantee that the fragmented time of the day cannot be more than the processing time of the fragmented job. Constraints (12-14) ensure that the capacity of each day is not exceeded. The planning horizon can be separated into three sections by considering their special conditions while setting up the model. The first day cannot have an earlier day's remaining capacity requirement. Constraints (12) control the capacity of the first day of the planning horizon. The last day cannot have over capacity to transfer the next day. Constraints (13) control the last day of the planning horizon. Constraints (14) control the capacity of the remaining days over the planning horizon. Constraints (15) and (16) define the domain for decision variables.

4. Numerical study

This section presents the numerical study conducted to evaluate the performance of the MIP formulation on the BPPIF. The MIP model was solved using Gurobi Optimizer version 9.5.0.0rc5. A PC with a 16 GB RAM and Apple M1 processor was used to carry out all the experiments. We imposed a run time limit of 60 seconds for the MIP model.

4.1. Data generation

We construct our experiment design based on average processing time (APT), fragmentable item ratio (FIR), job number (JN), and capacity ratio (CR) parameters. In our test instances, we aim to have a nearly equal number of jobs with the same due date. To do so, day numbers are calculated parametrically as follows:

$$DN = \frac{JN * APT * CR}{DT}$$

where *DN* represents the day number, *JN* represents the job number, *APT* represents the average processing time, *CR* represents the capacity ratio and *DT* represents the day time which is the total time of normal shift time and over time per day.

We generated the processing time of jobs randomly by using the uniform distribution with mean 40. The bounds of the uniform distribution is determined by the following equations.

$$upperLimit = APT * CR$$
$$lowLimit = APT * (2 - CR)$$

In our experimental setup, we used the following set of parameters; *JN*∈{176, 352, 704, 1408}, *FI*∈{20%, 40%, 60%} and *CR*∈{110%, 160%}.

We employed a daytime duration of 704 minutes, with 554 minutes designated as normal shift time and the remaining 150 minutes allocated for overtime. To ensure statistical robustness, we generated 10 samples for each instance class. This leads us to 240 test instances in total. The average values obtained from these samples were subsequently employed in analyzing results. Finally, *DN*∈{11, 16, 22, 32, 44, 64, 88, 128} are found implicitly based on parameters given above.

4.2. Results

In this section, we present the computational results of our experiments. The results on the test instances show that the model yields optimal solutions for 90% of the 240 test instances within a time limit of 60 seconds. In only 10% of the total instances, it fails to find the optimal solution within the given time limit. The maximum gap is found as %4 while the average gap found as %3 in those instances that were not solved optimally. This result highlights the effectiveness of the proposed mathematical model in solving a significant portion of the test instances efficiently.

Table 2 presents the average, minimum and maximum solution times for the instances based on each parameters. It can be observed from the table that as the number of jobs increases, the solution time of the model also increases. The relationship between the number of jobs and the solution time can be attributed to the computational complexity of the problem. As the number of jobs increases, the problem becomes more complex and requires additional computational resources to find the optimal solution. This increase in solution time is expected due to the combinatorial nature of the problem, where the number of possible solutions grow exponentially with the number of tasks.

The effect of FI ratio, which indicates the percentage of jobs that are fragmentable can be also observed in the Table 2. It is well-known that the problem becomes trivial if there is no restriction on the item fragmentation. This indicates that one would expect to have faster computation as the ratio between fragmentable and nonfragmentable jobs approaches to 1. The results show that, the average solution time decreases when the number of fragmentable jobs in the problem increases sufficiently. Yet, we cannot observe a similar trend in the maximum solution time statistics.

Table 2. Solution times for parameters.

Group	*Value*	AST	Min	Max
JN	176	0.020	0.002	0.100
	352	0.143	0.008	1.006
	704	2.501	0.033	18.073
	1408	6.633	0.142	56.255
FI	20%	0.762	0.002	12.710
	40%	2.788	0.002	42.831
	60%	1.877	0.002	56.255
CR	110%	4.060	0.020	56.255
	160%	0.052	0.002	0.190

JN: Job number, FI: Fragmentable item ratio, CR: Capacity ratio, AST: Average solution time (seconds), Min: Minimum solution time (seconds), Max: Maximum solution time (seconds)

The CR ratio, as mentioned before, has an effect on the randomly determined processing times for jobs. As the CR ratio increases, the average total processing time of jobs that must finish prior to any day decreases. This implies that, for lower CR ratio, the daily capacity becomes tighter as compared to that of higher CR ratio. As such, the problem inherently gets more difficult. In Table 2, it can be observed that solution times dramatically improve as CR ratio increases.

Finally, the average solution times for DN with same CR are given in Table 3. CR have a direct impact on the calculation of DN. CR, in a way, indicates the underutilization of the workcenter each day. Therefore, for the same CR, the rate of utilization, i.e., daily capacity tigthness, remains steady.

Table 3. Solution times of DN for same CR.

DN	CR	AST	Min	Max
16	160%	0.002	0.002	0.002
32	160%	0.008	0.008	0.008
64	160%	0.035	0.033	0.039
128	160%	0.165	0.142	0.190
11	110%	0.039	0.002	0.100
22	110%	0.278	0.089	1.006
44	110%	4.967	0.734	18.073
88	110%	45.436	39.386	56.255

DN: Day number, CR: Capacity ratio, AST: Avereage solution time (seconds), Min: Minimum solution time (seconds), Max: Maximum solution time (seconds)

In Table 3, we report the impact of day number on the average, minimum and maximum solution time for the instances with the same underutilization level. As a result, we can see that DN has a negative impact on the average solution time. More specifically, the average solution time increases with greater DN values. This is not surprising because the number of binary variables used within the MIP model depends on DN. Therefore, greater DN values lead us to larger MIP models and this eventually increases the solution times.

5. Conclusions and future research directions

We have studied the assignment problem of multi product assembly jobs to the days. Considering the similarity of the problem with the BPPIF, we have proposed a MIP model. We have considered the additional constraint of item-bin conflict. An item can be fragmented at most once, and only to the following bin. Computational experiments have shown that the MIP model obtained optimal solutions for majority of instances within reasonable computation times. Our results provide insights for researchers and practitioners in scheduling problems with due dates and overtime constraints.

The proposed model can be used as a decision support tool in planning production assignments where sequence-dependent setup times can be ignored, and delivery times are of interest. The MIP model can be considered as a simple yet effective model for systems involving processes with less than 1000 job numbers.

Several research directions could be considered for future work. The performance of the MIP model for the BPPIF could be examined further to minimize the number of fragmented jobs. Despite extensive research on the BPPIF, several open problems and challenging variants still exist, including the BPPIF with uncertain item sizes, multiple criteria, and precedence relations. Furthermore, developing efficient algorithms, such as metaheuristics, for handling large-scale instances of the problem remains an active research area.

References

[1] Gurkan, M. E., & Tunc, H. (2021). A fix-and-optimize heuristic for the capacitated multi-item stochastic lot-sizing problem. *An International Journal of Optimization and Control: Theories & Applications*, 11(1), 41-51.

[2] Cetin, K., Tuzkaya, G., & Vayvay, O. (2020). A mathematical model for personnel task assignment problem and an application for banking sector. *An International Journal of Optimization and Control: Theories & Applications*, 10(2), 147-158.

[3] Göçgün, Y., & Bakır, N. O. (2022). Optimal matchday schedule for Turkish professional soccer league using nonlinear binary integer programming. *An International Journal of Optimization and Control: Theories & Applications*, 12(2), 113-127.

[4] Koç, Ç., Erbaş, M., & Özceylan, E. (2018). A rich vehicle routing problem arising in the replenishment of automated teller machines. *An International Journal of Optimization and Control: Theories & Applications*, 8(2), 276-287.

[5] Eilon, S., & Christofides, N. (1971). The loading problem. *Management Science*, 17(5), 259-268.

[6] Jansen, K. (1999). An approximation scheme for bin packing with conflicts. *Journal of Combinatorial Optimization*, 3(4), 363-377.

[7] Loh, K. H., Golden, B., & Wasil, E. (2008). Solving the one-dimensional bin packing problem with a weight annealing heuristic. *Computers & Operations Research*, 35(7), 2283-2291.

[8] Khanafer, A., Clautiaux, F., & Talbi, E. G. (2010). New lower bounds for bin packing problems with conflicts. *European Journal of Operational Research*, 206(2), 281-288.

[9] Crainic, T. G., Perboli, G., Rei, W., & Tadei, R. (2011). Efficient lower bounds and heuristics for the variable cost and size bin packing problem. *Computers & Operations Research*, 38(11), 1474-1482.

[10] Elhedhli, S., Li, L., Gzara, M., & Naoum-Sawaya, J. (2011). A branch-and-price algorithm for the bin packing problem with conflicts. *INFORMS Journal on Computing*, 23(3), 404-415.

[11] Fleszar, K., & Charalambous, C. (2011). Average-weight-controlled bin-oriented heuristics for the one-dimensional bin-packing problem. *European Journal of Operational Research*, 210(2), 176-184.

[12] Bertazzi, L., Golden, B., & Wang, X. (2019). The bin packing problem with item fragmentation: a worst-case analysis. *Discrete Applied Mathematics*, 261, 63-77.

[13] Ekici, A. (2021). Bin packing problem with conflicts and item fragmentation. *Computers & Operations Research*, 126, 105113.

[14] Casazza, M., & Ceselli, A. (2014). Mathematical programming algorithms for bin packing problems with item fragmentation. *Computers & Operations Research*, 46, 1-11.

[15] LeCun, B., Mautor, T., Quessette, F., & Weisser, M. A. (2015). Bin packing with fragmentable items: Presentation and approximations. *Theoretical Computer Science*, 602, 50-59.

[16] Byholm, B., & Porres, I. (2018). Fast algorithms for fragmentable items bin packing. *Journal of Heuristics*, 24, 697-723.

[17] Dokeroglu, T., & Cosar, A. (2014). Optimization of one-dimensional bin packing problem with island parallel grouping genetic algorithms. *Computers & Industrial Engineering*, 75, 176-186.

[18] Casazza, M. (2019). New formulations for variable cost and size bin packing problems with item fragmentation. *Optimization Letters*, 13(2), 379-398.

[19] Ekici, A. (2022). Variable-sized bin packing problem with conflicts and item fragmentation. *Computers & Industrial Engineering*, 163, 107844.

[20] Arbib, C., & Marinelli, F. (2017). Maximum lateness minimization in one-dimensional bin packing. *Omega*, 68, 76-84.

[21] Khanafer, A., Clautiaux, F., Hanafi, S., & Talbi, E. G. (2012). The min-conflict packing problem. *Computers & Operations Research*, 39(9), 2122-2132.

Mustafa Ustuncelik *is an Industrial Engineer and serves as a Planning and Control Assistant Manager at Hidromek Construction Equipment Company located in Thailand. He received his B.S. in Industrial Engineering from Eskisehir Osmangazi University in 2013 and his M.S. in Business Administration from Social Sciences University of Ankara in 2023.*

http://orcid.org/0009-0008-3385-7808

Cagri Koc *is an Associate Professor in the Department of Business Administration at Social Sciences University of Ankara. He received his Ph.D. degree (2015) in Operational Research/Management Science from the Southampton Business School of University of Southampton. He worked as a Postdoctoral Fellow at HEC Montreal and at CIRRELT. His research mainly focuses on the application of mathematical and metaheuristic optimization techniques to logistics and supply chain management problems.*

https://orcid.org/0000-0002-7377-204X

Huseyin Tunc *is an Associate Professor in the Department of Business Administration at Social Sciences University of Ankara. He received his Ph.D. in Industrial and Systems Engineering from Mississippi State University in 2012. He joined the Social Sciences University of Ankara in 2019. He worked at Hacettepe University, Swiss Federal Institute of Technology in Lausanne (EPFL), and Mississippi State University.*

https://orcid.org/0000-0001-5508-3702

An International Journal of Optimization and Control: Theories & Applications (http://ijocta.balikesir.edu.tr)

An International Journal of Optimization and Control: Theories & Applications
ISSN:2146-0957 eISSN:2146-5703
Vol.14, No.1, pp.41-49 (2024)
http://doi.org/10.11121/ijocta.1392

RESEARCH ARTICLE

On the upper bounds of Hankel determinants for some subclasses of univalent functions associated with sine functions

Muhammet Kamali*, Alina Riskulava,

Department of Mathematics, Faculty of Sciences, Kyrgyz-Türkish Manas University, Chyngz Aitmatov Avenue Bishkek, Kyrgyz Recuplic
muhammet.kamali@manas.edu.kg, alinka.ryskulova97@gmail.com

ARTICLE INFO

Article History:
Received 13 April 2023
Accepted 15 July 2023
Available Online 12 December 2023

Keywords:
Analytic functions
Coefficient estimates
Subordination
Hankel determinant
Starlike functions
Convex function
Sine function

AMS Classification 2010:
30C45; 30C50

ABSTRACT

Let a normalized analytic function be given on the open unit disk. In this paper, we define and consider some familiar subsets of analytic functions associated with sine functions in the region of unit disk on the complex plane. For these classes, we aim to find the upper bounds of the modules of the Hankel determinants obtained from the coefficients of the functions belonging to some classes defined by subordination.

1. Introduction

Let A be the family of functions of the form

$$f(z) = z + \sum_{n=2}^{\infty} a_n z^n, \quad z \in E \tag{1}$$

which are analytic in the open unit disk $E = \{z \in C : |z| < 1\}$ and let S denote the subclass of A consisting of all univalent functions in E. With a view to recalling the principal of subordination between analytic functions, let $f(z)$ and $g(z)$ be analytic functions in E. Then we say that the function $f(z)$ is subordinate to $g(z)$ in E, if there exits a Schwarz function $w(z)$, analytic in E with

$$w(0) = 0 \text{ and } |w(z)| < 1, (z \in E)$$

such that $f(z) = g(w(z))$. We denote this subordination by

$$f(z) \prec g(z).$$

If g is a univalent function in E, then

$$f(z) \prec g(z) \Leftrightarrow f(0) = g(0) \text{ and } f(E) \subset g(E).$$

The famous coefficient conjucture Beiberbach conjucture for the functions $f \in S$ of the form (1) was first presented by Beiberbach [1] in 1916 and proven by de-Branges [2] in 1985. In between the years 1916 and 1985, many mathematicians worked to prove Beiberbach's conjucture. Consequently, they defined several subclasses of S connected with different image domains. Among these, the families S^*, C and K of starlike functions, convex functions, and close-to-convex functions, respectively, are the most fundamental subclasses of S and have a

*Corresponding Author

nice geometric interpretation. These families are defined as follows:

$$S^* = \left\{ f \in S : \frac{zf'(z)}{f(z)} \prec \frac{1+z}{1-z}, (z \in E) \right\} \quad (2)$$

$$C = \left\{ f \in S : 1 + \frac{zf''(z)}{f'(z)} \prec \frac{1+z}{1-z}, (z \in E) \right\} \quad (3)$$

$$K = \left\{ f \in S : \frac{zf'(z)}{g(z)} \prec \frac{1+z}{1-z}, g(z) \in S^*, (z \in E) \right\}. \quad (4)$$

We recall here which are connected with trigonometric functions and are defined as folows:

$$S^*_{\sin} = \left\{ f \in S : \frac{zf'(z)}{f(z)} \prec 1 + \sin(z), (z \in E) \right\} \quad (5)$$

$$C_{\sin} = \left\{ f \in S : 1 + \frac{zf''(z)}{f'(z)} \prec 1 + \sin(z), (z \in E) \right\} \quad (6)$$

$$R_{\sin} = \left\{ f \in S : f'(z) \prec 1 + \sin(z), (z \in E) \right\} \quad (7)$$

The class $S^*_{\sin}$ of analytic function defined in (5) was introduced by Cho et al. [3].

In the 1960s Pommerenke [4], [5] defined the Hankel determinant $H_{q,n}(f)$for a given f of the form (1) f as follows

$$H_{q,n}(f) = \begin{vmatrix} a_n & a_{n+1} & \cdots & a_{n+q-1} \\ a_{n+1} & a_{n+2} & \cdots & a_{n+q} \\ \vdots & \vdots & \cdots & \vdots \\ a_{n+q-1} & a_{n+q} & \cdots & a_{n+2q-2} \end{vmatrix}, \quad (8)$$

where $q, n \in N = \{1, 2, 3, ...\}$. In particular,

$$H_{2,1}(f) = \begin{vmatrix} 1 & a_2 \\ a_2 & a_3 \end{vmatrix} = a_3 - a_2^2,$$

$$H_{2,2}(f) = \begin{vmatrix} a_2 & a_3 \\ a_3 & a_4 \end{vmatrix} = a_2 a_4 - a_3^2$$

and

$$H_{3,1}(f) = \begin{vmatrix} 1 & a_2 & a_3 \\ a_2 & a_3 & a_4 \\ a_3 & a_4 & a_5 \end{vmatrix}$$

$$= a_3 \left(a_2 a_4 - a_3^2\right) + a_4 \left(a_2 a_3 - a_4\right) + a_5 \left(a_3 - a_2^2\right).$$

The studies on Hankel determinants are concentrated on estimating $H_{2,2}(f)$ and $H_{3,1}(f)$ for different subclasses of S.The absolute sharp bounds of the functional $H_{2,2}(f)$ were found in [6], [7] for each of the families S^*,C, and R, where the family$R$ contains functions of bounded turning. In [7] , Janteng et al. proved that $|H_{2,2}(f)| \leq 1$ for $S^*$and $|H_{2,2}(f)| \leq \frac{1}{8}$ for K,where $S^*$and $K$are very well known classes of starlike and convex functions. The estimation of the determinant $|H_{3,1}(f)|$ is very hard as compared to deriving the bound of $|H_{2,2}(f)|$. The paper on $|H_{3,1}(f)|$ was given in 2010 by Babalola [8], in which he obtained the upper bound of $H_{3,1}(f)$ for the families of S^*,C, and R. Later on, many authors published their work regarding $|H_{3,1}(f)|$ for different subclasses of univalent functions; see [9–16]. In 2017, Zaprawa [17] improved the results of Babalola. In 2018, Kowalczyk et al. [18] and Lecko et al. [19] obtained the sharp inequalities:

$$|H_{3,1}(f)| \leq \frac{4}{35} \text{ and } |H_{3,1}(f)| \leq \frac{1}{9}$$

for the recognizable families K and $S^*\left(\frac{1}{2}\right)$, respectively , where the symbol $S^*\left(\frac{1}{2}\right)$ stands for the family of starlike functions of order $\frac{1}{2}$. Arif M. et al. [20] obtained the upper bound of $|H_{3,1}(f)|$for the subclasses $S^*_{\sin}$,$C_{\sin}$ and $R_{\sin}$ in 2019. In 2019, Shi et al. [21] investigated the estimate of $|H_{3,1}(f)|$for the subclasses S^*_{car},C_{car} and R_{car}in of analytic functions connected with the cardioid domain. In 2019, Zaprawa [22] studied the Hankel Determinant for Univalent Functions Related to the Exponential Function.

For $f \in A$,$n \in N = \{0, 1, 2, , 3, ...\}$, the operator $D^n f$ is defined by $D^n : A \to A$ [23]

$$D^0 f(z) = f(z)$$
$$D^{n+1} f(z) = z\left[D^n f(z)\right]', z \in E.$$

If $f \in A$, $f(z) = z + \sum_{k=2}^{\infty} a_k z^k$, then $D^n f(z) = z + \sum_{k=2}^{\infty} k^n a_k z^k$, $z \in E$.

Let $n \in N = \{0, 1, 2, , 3, ...\}$ and $\lambda \geq 0$. We let D^n_λ denote [24] the operator defined by

$$D^n_\lambda : A \to A, D^0_\lambda f(z) = f(z),$$
$$D^1_\lambda f(z) = (1-\lambda) D^0_\lambda f(z) + \lambda z \left(D^0_\lambda f(z)\right)'$$
$$= (1-\lambda) f(z) + \lambda z f'(z),$$
$$\cdots$$
$$D^{n+1}_\lambda f(z) = (1-\lambda) D^n_\lambda f(z) + \lambda z \left(D^n_\lambda f(z)\right)'.$$

We observe that D^n_λ is a linear operator and for $f(z) = z + \sum_{k=2}^{\infty} a_k z^k$, we have [25]

$$D_\lambda^n f(z) = z + \sum_{k=2}^{\infty} [1 + \lambda(k-1)]^n a_k z^k .$$

Now, we define a subclass of analytic functions as follows:

Definition 1. *Let $\lambda \geq 0$, $n \in N = \{0, 1, 2, 3, ...\}$ and $f(z)$ is defined by (1). We define the classes of $S^*_{(\lambda,n)}$ and $C_{(\lambda,n)}$ in the following way*

$$S^*_{(\lambda,n)} = \left\{ f \in S : \frac{z\left(D_\lambda^n f(z)\right)'}{D_\lambda^n f(z)} \prec 1 + \sin(z) \right\} \tag{9}$$

and

$$C_{(\lambda,n)} = \left\{ f \in S : 1 + \frac{z\left(D_\lambda^n f(z)\right)''}{\left(D_\lambda^n f(z)\right)'} \prec 1 + \sin(z) \right\}. \tag{10}$$

In this present article, our aim is to investigate the estimate of $|H_{2,2}(f)|$ and $|H_{3,1}(f)|$ for the subclasses $S^*_{(\lambda,n)}$ and $C_{(\lambda,n)}$ of analytic functions related with sine function.

2. Auxiliary lemmas

Let P denote the family of all functions p which are analytic in E with $Re\ p(z) > 0$ and has the following series representation

$$p(z) = 1 + p_1 z + p_2 z^2 + p_3 z^3 + ... = 1 + \sum_{n=1}^{\infty} p_n z^n \ (z \in E). \tag{11}$$

Here $p(z)$ is called the Caratheodory function [26].

Lemma 1. *([27]) Let $p(z) \in P$. Then $|p_n| \leq 2$, $n = 1, 2, ...$.*

Lemma 2. *([28], [29]) Let the function $p(z) \in P$ be given by (11), then*

$$2p_2 = p_1^2 + x\left(4 - p_1^2\right) \tag{12}$$

for some x, $|x| \leq 1$, and

$$4p_3 = p_1^3 + 2p_1\left(4 - p_1^2\right)x - p_1\left(4 - p_1^2\right)x^2 + 2\left(4 - p_1^2\right)\left(1 - |x|^2\right)\eta \tag{13}$$

for some complex value η, $|\eta| \leq 1$.

Lemma 3. *([20], [30]) Let $p(z) \in P$ and has the form (11) then*

$$\left| p_2 - \frac{p_1^2}{2} \right| \leq 2 - \frac{|p_1|^2}{2} \tag{14}$$

$$\left| p_{n+2k} - \mu p_n p_k^2 \right| \leq 2(1 + 2\mu) \ \ for\ \mu \in R, \tag{15}$$

$$|p_{n+k} - \eta p_n p_k| < 2, \quad \text{for } 0 \leq \eta \leq 1, \tag{16}$$

$$|p_m p_n - p_k p_l| \leq 4 \quad \text{for } m + n = k + l, \tag{17}$$

and for complex number λ, we have

$$\left| p_2 - \lambda p_1^2 \right| \leq \max\{2, 2|\lambda - 1|\}. \tag{18}$$

For the results in (14),(15),(16),(17) see ([31], [32]) for the inequality (18).

Lemma 4. *([20]) Let $p(z) \in P$ and has the form (11),then*

$$\left| Jp_1^3 - Kp_1p_2 + Lp_3 \right| \leq 2|J| + 2|K - 2J| + 2|J - K + L|. \tag{19}$$

3. Main results

3.1. The upper bound of the modules of Hankel's determinants for the coefficients of functions belonging to class $S^*_{(\lambda,n)}$

Theorem 1. *If the function $f(z) \in S^*_{(\lambda,n)}$ and of the form (1), then*

$$|a_2| \leq \frac{1}{(1+\lambda)^n}, |a_3| \leq \frac{1}{2(1+2\lambda)^n},$$
$$|a_4| \leq \frac{13}{36(1+3\lambda)^n}, |a_5| \leq \frac{7}{24(1+4\lambda)^n}.$$

Proof. From the definition of the class $S^*_{(\lambda,n)}$, we have

$$\frac{z\left(D_\lambda^n f(z)\right)'}{D_\lambda^n f(z)} = 1 + \sin(w(z)) \tag{20}$$

where w is analytic in E with $w(0) = 0$ and $|w(z)| < 1, z \in E$. Consider a function p such that

$$p(z) = \frac{1 + w(z)}{1 - w(z)} = 1 + p_1 z + p_2 z^2 + ...$$

then $p \in P$. This implies that

$$w(z) = \frac{p(z) - 1}{p(z) + 1} = \frac{p_1 z + p_2 z^2 + p_3 z^3 + ...}{2 + p_1 z + p_2 z^2 + p_3 z^3 + ...}.$$

From (1), we can write

$$\frac{z\left(D_{\lambda}^{n}f\left(z\right)\right)'}{D_{\lambda}^{n}f\left(z\right)} = 1+\left(1+\lambda\right)^{n}a_{2}z + \left[2\left(1+2\lambda\right)^{n}a_{3}-\left(1+\lambda\right)^{2n}a_{2}^{2}\right]z^{2} + [3\left(1+3\lambda\right)^{n}a_{4}- 3\left(1+2\lambda\right)^{n}\left(1+\lambda\right)^{n}a_{2}a_{3}+\left(1+3\lambda\right)^{3n}a_{2}^{3}\Big]z^{3} + [4\left(1+4\lambda\right)^{n}a_{5}-4\left(1+3\lambda\right)^{n}\left(1+\lambda\right)^{n}a_{2}a_{4} + 4\left(1+2\lambda\right)^{n}\left(1+\lambda\right)^{2n}a_{2}^{2}a_{3}-2\left(1+2\lambda\right)^{2n}a_{3}^{2} - \left(1+\lambda\right)^{4n}a_{2}^{4}\Big]z^{4}+... \tag{21}$$

After some simple calculations, we obtain

$$1+\sin\left(w\left(z\right)\right)=1+w\left(z\right)-\frac{\left(w\left(z\right)\right)^{3}}{3!}+\frac{\left(w\left(z\right)\right)^{5}}{5!} -\frac{\left(w\left(z\right)\right)^{7}}{7!}+... = 1+\tfrac{1}{2}p_{1}z+\left(\tfrac{p_{2}}{2}-\tfrac{p_{1}^{2}}{4}\right)z^{2}+\left(\tfrac{5}{48}p_{1}^{3}+\tfrac{p_{3}}{2}-\tfrac{p_{1}p_{2}}{2}\right)z^{3}+ \left(\frac{p_{4}}{2}+\frac{5}{16}p_{1}^{2}p_{2}-\frac{p_{1}^{4}}{32}-\frac{p_{1}p_{3}}{2}-\frac{p_{2}^{2}}{4}\right)z^{4}+... \tag{22}$$

From (20), (21) and (22), it follows that

$$a_{2}=\frac{p_{1}}{2\left(1+\lambda\right)^{n}} \tag{23}$$

$$a_{3}=\frac{p_{2}}{4\left(1+2\lambda\right)^{n}} \tag{24}$$

$$a_{4}=\frac{1}{6\left(1+3\lambda\right)^{n}}\left(p_{3}-\frac{p_{1}p_{2}}{4}-\frac{p_{1}^{3}}{24}\right) \tag{25}$$

$$a_{5}=\frac{1}{8(1+4\lambda)^{n}}\left(p_{4}-\frac{p_{1}p_{3}}{3}+\frac{5p_{1}^{4}}{144}-\frac{p_{1}^{2}p_{2}}{24}-\frac{p_{2}^{2}}{4}\right). \tag{26}$$

Applying Lemma 1 in (23) and (24), we obtain

$$\left|a_{2}\right|=\left|\frac{p_{1}}{2\left(1+\lambda\right)^{n}}\right|\leq\frac{1}{\left(1+\lambda\right)^{n}}\text{ and}$$
$$\left|a_{3}\right|=\left|\frac{p_{2}}{4\left(1+2\lambda\right)^{n}}\right|\leq\frac{1}{2\left(1+2\lambda\right)^{n}}.$$

If the expression (25) is calculated by taking $J=-\frac{1}{24},\ K=\frac{1}{4},\ L=1$ in the inequality (19), we obtain

$$\left|a_{4}\right|=\frac{1}{6(1+3\lambda)^{n}}\left|-\frac{1}{24}p_{1}^{3}-\frac{1}{4}p_{1}p_{2}+p_{3}\right| \tag{27}$$
$$\leq\frac{1}{6\left(1+3\lambda\right)^{n}}\left\{2\left|-\frac{1}{24}\right|+2\left|\frac{1}{4}+\frac{1}{12}\right|+2\left|-\frac{1}{24}-\frac{1}{4}+1\right|\right\}$$
$$\leq\frac{1}{6\left(1+3\lambda\right)^{n}}\left\{\frac{1}{12}+\frac{2}{3}+\frac{17}{12}\right\}\leq\frac{13}{36\left(1+3\lambda\right)^{n}}.$$

If the expression (26) is calculated using the Lemma 1 and (16) inequality, we have

$$\left|a_{5}\right|\leq\frac{1}{8\left(1+4\lambda\right)^{n}} \tag{28}$$
$$\left\{\frac{1}{2}\left|p_{4}-\frac{2}{3}p_{1}p_{3}\right|+\frac{1}{2}\left|p_{4}-\frac{1}{2}p_{2}^{2}\right|+\frac{\left|p_{1}\right|^{2}}{24}\left|p_{2}-\frac{5}{6}p_{1}^{2}\right|\right\}$$
$$<\frac{7}{24\left(1+4\lambda\right)^{n}}.$$

Taking $\lambda=0,n=0$ in Theorem 1, we obtain the following Corollary 1. □

Corollary 1. *If the function $f\left(z\right)\in S_{(0,0)}^{*}=S^{*}$ and of the form (1), then $\left|a_{2}\right|\leq 1\left|a_{3}\right|\leq\frac{1}{2},\left|a_{4}\right|\leq\frac{13}{36},\left|a_{5}\right|<\frac{7}{24}$.*

Theorem 2. *If the function $f\left(z\right)\in S_{(\lambda,n)}^{*}$ and of the form (1), then*

$$\left|a_{3}-a_{2}^{2}\right|\leq\frac{1}{2\left(1+2\lambda\right)^{n}} \tag{29}$$

Proof. To obtain the (29) inequality, we will use the expression (18). If equations (23) and (24) are used,we can write

$$\left|a_{3}-a_{2}^{2}\right| = \left|\frac{p_{2}}{4\left(1+2\lambda\right)^{n}}-\left[\frac{p_{1}}{2\left(1+\lambda\right)^{n}}\right]^{2}\right|$$
$$=\left|\frac{p_{2}}{4\left(1+2\lambda\right)^{n}}-\frac{p_{1}^{2}}{4\left(1+\lambda\right)^{2n}}\right|$$
$$=\frac{1}{4\left(1+2\lambda\right)^{n}}\left|p_{2}-\frac{\left(1+2\lambda\right)^{n}}{\left(1+\lambda\right)^{2n}}p_{1}^{2}\right|$$
$$\leq\frac{1}{4\left(1+2\lambda\right)^{n}}\max\left\{2,2\left|\frac{\left(1+2\lambda\right)^{n}}{\left(1+\lambda\right)^{2n}}-1\right|\right\}.$$

Here, considering that

$$\frac{\left(1+2\lambda\right)^{n}}{\left(1+\lambda\right)^{2n}}\leq 1\Rightarrow\left(1+2\lambda\right)^{n}\leq\left(1+\lambda\right)^{2n}$$
$$\Rightarrow 1+2\lambda\leq 1+2\lambda+\lambda^{2}\Rightarrow\lambda^{2}\geq 0,$$
$$\left|a_{3}-a_{2}^{2}\right|\leq\frac{1}{2\left(1+2\lambda\right)^{n}}$$

is written. □

Theorem 3. *If the function $f\left(z\right)\in S_{(\lambda,n)}^{*}$ and of the form (1), then*

$$\left|a_{2}a_{3}-a_{4}\right| \tag{30}$$

$$\leq \begin{cases} \frac{1}{2(1+\lambda)^n(1+2\lambda)^n} - \frac{1}{9(1+3\lambda)^n}, & 0 \leq \lambda \leq \frac{3\nu+\sqrt{9\nu^2+8v}}{4} \\ \frac{13}{36(1+3\lambda)^n}, & \lambda \geq \frac{3\nu+\sqrt{9\nu^2+8v}}{4} \end{cases}.$$

Here, it is defined as $\nu = \left(\frac{18}{17}\right)^{\frac{1}{n}} - 1$.

Proof. From (23), (24) and (25), it follows that

$$|a_2a_3 - a_4| = \left| \begin{array}{c} \frac{p_1^3}{144(1+3\lambda)^n} + \\ \left(\frac{1}{8(1+\lambda)^n(1+2\lambda)^n} + \frac{1}{24(1+3\lambda)^n}\right) p_1p_2 \\ -\frac{p_3}{6(1+3\lambda)^n} \end{array} \right|. \tag{31}$$

If the expression (31) is calculated by taking

$$\begin{aligned} J &= \frac{1}{144(1+3\lambda)^n}, \\ K &= -\left(\frac{1}{8(1+\lambda)^n(1+2\lambda)^n} + \frac{1}{24(1+3\lambda)^n}\right), \\ L &= -\frac{1}{6(1+3\lambda)^n} \end{aligned}$$

in the inequality (19),we obtain

$$\begin{aligned} |a_2a_3 - a_4| \leq & \frac{1}{72(1+3\lambda)^n} \\ & + 2\left|\frac{1}{8(1+\lambda)^n(1+2\lambda)^n} + \frac{1}{18(1+3\lambda)^n}\right| \\ & + 2\left|\frac{1}{8(1+\lambda)^n(1+2\lambda)^n} - \frac{17}{144(1+3\lambda)^n}\right| \end{aligned}$$

Now, Let's Look at the sign of $\frac{1}{8(1+\lambda)^n(1+2\lambda)^n} - \frac{17}{144(1+3\lambda)^n}$ expression. Let's assume that

$$\frac{1}{8(1+\lambda)^n(1+2\lambda)^n} - \frac{17}{144(1+3\lambda)^n} \leq 0.$$

With a simple calculation, we write

$$\begin{aligned} & \tfrac{1}{8(1+\lambda)^n(1+2\lambda)^n} \leq \tfrac{17}{144(1+3\lambda)^n} \\ & \Rightarrow 144(1+3\lambda)^n \leq 136\left[(1+\lambda)(1+2\lambda)\right]^n \Rightarrow \\ & 18(1+3\lambda)^n \leq 17\left(1+3\lambda+2\lambda^2\right)^n \\ & \Rightarrow \left(\tfrac{18}{17}\right)^{\frac{1}{n}} \leq 1 + \tfrac{2\lambda^2}{1+3\lambda} \Rightarrow \left(\tfrac{18}{17}\right)^{\frac{1}{n}} - 1 \leq \tfrac{2\lambda^2}{1+3\lambda}. \end{aligned}$$

If $\left(\frac{18}{17}\right)^{\frac{1}{n}} - 1 = \nu$, then $\left(\frac{18}{17}\right)^{\frac{1}{n}} - 1 \geq 0$. Thus, we obtain $\nu \leq \frac{2\lambda^2}{1+3\lambda} \Rightarrow 2\lambda^2 - 3\nu\lambda - \nu \geq 0$.

If this inequality is solved, we fınd

$$\lambda_1 = \frac{3\nu - \sqrt{9\nu^2 + 8v}}{4} \text{ and } \lambda_2 = \frac{3\nu + \sqrt{9\nu^2 + 8v}}{4}.$$

Thus, since $\lambda \geq 0$ must be, we get $|a_2a_3 - a_4| \leq$

$$\begin{cases} \frac{1}{2(1+\lambda)^n(1+2\lambda)^n} - \frac{1}{9(1+3\lambda)^n}, & 0 \leq \lambda \leq \frac{3\nu+\sqrt{9\nu^2+8v}}{4} \\ \frac{13}{36(1+3\lambda)^n}, & \lambda \geq \frac{3\nu+\sqrt{9\nu^2+8v}}{4} \end{cases}.$$

□

Theorem 4. *If the function* $f(z) \in S^*_{(\lambda,n)}$ *and of the form (1), then*

$$\begin{aligned} |H_{2,2}(f)| &= \left|a_2a_4 - a_3^2\right| \\ &\leq \frac{13}{36(1+\lambda)^n(1+3\lambda)^n} + \frac{1}{4(1+2\lambda)^{2n}}. \end{aligned} \tag{32}$$

Proof. From (23), (24) and (25), it follows that

$$\begin{aligned} & \left|a_2a_4 - a_3^2\right| \\ = & \left| \begin{array}{c} \frac{p_1p_3}{12(1+\lambda)^n(1+3\lambda)^n} - \frac{p_1^2p_2}{48(1+\lambda)^n(1+3\lambda)^n} \\ -\frac{p_1^4}{288(1+\lambda)^n(1+3\lambda)^n} - \frac{p_2^2}{16(1+2\lambda)^{2n}} \end{array} \right|. \end{aligned}$$

If the triangle inequality is applied to this last equation, we obtain

$$\begin{aligned} & \left|a_2a_4 - a_3^2\right| \\ \leq & \left\{ \begin{array}{c} \frac{|p_1|}{12(1+\lambda)^n(1+3\lambda)^n}\left|p_3 - \frac{p_1p_2}{4} - \frac{p_1^3}{24}\right| \\ + \left|\frac{p_2^2}{16(1+2\lambda)^{2n}}\right| \end{array} \right\}. \end{aligned}$$

(19) according to inequality, we can write

$$\begin{aligned} & \left|p_3 - \frac{p_1p_2}{4} - \frac{p_1^3}{24}\right| \\ \leq & \left\{ \begin{array}{c} 2\left|-\frac{1}{24}\right| + 2\left|\frac{1}{4} + \frac{1}{12}\right| \\ +2\left|-\frac{1}{24} - \frac{1}{4} + 1\right| \end{array} \right\} \\ \leq & \frac{13}{6}. \end{aligned}$$

Thus , we obtain $\left|a_2a_4 - a_3^2\right| \leq$

$$\begin{aligned} & \left\{\frac{2}{12(1+\lambda)^n(1+3\lambda)^n} \cdot \frac{13}{6} + \frac{1}{4(1+2\lambda)^{2n}}\right\} \\ & \leq \frac{13}{36(1+\lambda)^n(1+3\lambda)^n} + \frac{1}{4(1+2\lambda)^{2n}}. \end{aligned}$$

□

Theorem 5. *If the function* $f(z) \in S^*_{(\lambda,n)}$ *and of the form (1), then*

$$|H_3(1)| < \begin{cases} \frac{13}{36(1+3\lambda)^n(1+\lambda)^n(1+2\lambda)^n} \\ +\frac{1}{8(1+2\lambda)^{3n}} \\ -\frac{13}{324(1+3\lambda)^{2n}} \\ +\frac{7}{48(1+4\lambda)^n(1+2\lambda)^n}; 0 \le \lambda \le \frac{3\nu+\sqrt{9\nu^2+8v}}{4} \\ \frac{13}{72(1+3\lambda)^n(1+\lambda)^n(1+2\lambda)^n} \\ +\frac{1}{8(1+2\lambda)^{3n}} \\ +\frac{169}{1296(1+3\lambda)^{2n}} \\ +\frac{7}{48(1+4\lambda)^n(1+2\lambda)^n}; \lambda \ge \frac{3\nu+\sqrt{9\nu^2+8v}}{4} \end{cases} \quad (33)$$

Here, it is defined as $\nu = \left(\frac{18}{17}\right)^{\frac{1}{n}} - 1$.

Proof. If the absolute value of both sides of the expression

$$H_3(1) = a_3\left(a_2a_4 - a_3^2\right) - a_4\left(a_4 - a_2a_3\right) + a_5\left(a_3 - a_2^2\right)$$

is taken and the triangle inequality is applied, we can write

$$|H_3(1)| \le |a_3|\left|a_2a_4 - a_3^2\right| + |a_4|\left|a_4 - a_2a_3\right| + |a_5|\left|a_3 - a_2^2\right|.$$

In this last inequality, if the upper bound expressions discussed in Theorem 1, Theorem 2, Theorem 3, and Theorem 4, are written instead of and necessary operations are done, we obtain

$$|H_3(1)| < \begin{cases} \frac{13}{36(1+3\lambda)^n(1+\lambda)^n(1+2\lambda)^n} \\ +\frac{1}{8(1+2\lambda)^{3n}} \\ -\frac{13}{324(1+3\lambda)^{2n}} \\ +\frac{7}{48(1+4\lambda)^n(1+2\lambda)^n}; 0 \le \lambda \le \frac{3\nu+\sqrt{9\nu^2+8v}}{4} \\ \frac{13}{72(1+3\lambda)^n(1+\lambda)^n(1+2\lambda)^n} \\ +\frac{1}{8(1+2\lambda)^{3n}} \\ +\frac{169}{1296(1+3\lambda)^{2n}} \\ +\frac{7}{48(1+4\lambda)^n(1+2\lambda)^n}; \lambda \ge \frac{3\nu+\sqrt{9\nu^2+8v}}{4} \end{cases}.$$

Here, it is defined as $\nu = \left(\frac{18}{17}\right)^{\frac{1}{n}} - 1$. □

3.2. The upper bound of the modules of Hankel's determinants for the coefficients of functions belonging to class $C_{(\lambda,n)}$.

Theorem 6. *If the function* $f(z) \in C_{(\lambda,n)}$ *and of the form (1), then* $|a_2| \le \frac{1}{2(1+\lambda)^n}, |a_3| \le \frac{1}{6(1+2\lambda)^n}, |a_4| \le \frac{13}{144(1+3\lambda)^n}, |a_5| \le \frac{7}{120(1+4\lambda)^n}$.

Proof. From the definition of the class $C_{(\lambda,n)}$, we have

$$1 + \frac{z\left(D_\lambda^n f(z)\right)''}{\left(D_\lambda^n f(z)\right)'} = 1 + \sin(w(z)) \quad (34)$$

where w is analytic in E with $w(0) = 0$ and $|w(z)| < 1, z \in E$.

From (1), we can write

$$\begin{aligned} 1 + \frac{z\left(D_\lambda^n f(z)\right)''}{\left(D_\lambda^n f(z)\right)'} &= 1 + 2(1+\lambda)^n a_2 z \\ &+ \left[6(1+2\lambda)^n a_3 - 4(1+\lambda)^{2n} a_2^2\right] z^2 \\ &+ [12(1+3\lambda)^n a_4 \\ &-18(1+\lambda)^n(1+2\lambda)^n a_2a_3 \\ &+8(1+\lambda)^{3n} a_2^3\Big] z^3 + [20(1+4\lambda)^n a_5 \\ &-32(1+\lambda)^n(1+3\lambda)^n a_2a_4 \\ &-18(1+2\lambda)^{2n} a_3^2 \\ &+48(1+\lambda)^{2n}(1+2\lambda)^n a_2^2a_3 \\ &-16(1+\lambda)^{4n} a_2^4\Big] z^4 + ... \end{aligned} \quad (35)$$

From (23) and (35) , it follows that

$$a_2 = \frac{p_1}{4(1+\lambda)^n} \quad (36)$$

$$a_3 = \frac{p_2}{12(1+2\lambda)^n} \quad (37)$$

$$a_4 = \frac{1}{24(1+3\lambda)^n}\left(p_3 - \frac{p_1p_2}{4} - \frac{p_1^3}{24}\right) \quad (38)$$

$$a_5 = \frac{1}{40(1+4\lambda)^n}\left(p_4 - \frac{p_1p_3}{3} + \frac{5p_1^4}{144} - \frac{p_1^2p_2}{24} - \frac{p_2^2}{4}\right). \quad (39)$$

Applying Lemma 1 in (36) and (37), we obtain

$$|a_2| \le \left|\frac{p_1}{4(1+\lambda)^n}\right| \le \frac{1}{2(1+\lambda)^n} \quad (40)$$

and

$$|a_3| \le \left|\frac{p_2}{12(1+2\lambda)^n}\right| \le \frac{1}{6(1+2\lambda)^n}. \quad (41)$$

If the expression (38) is calculated by taking $J = -\frac{1}{24}$, $K = \frac{1}{4}$, $L = 1$ in the inequality (19), we obtain

$$\begin{aligned} |a_4| &\le \frac{1}{24(1+3\lambda)^n}\left|-\frac{1}{24}p_1^3 - \frac{1}{4}p_1p_2 + p_3\right| \\ &\le \frac{13}{144(1+3\lambda)^n}. \end{aligned}$$

If the expression (39) is calculated using the Lemma 1 and (16) inequality, we have

$$|a_5| \leq \frac{1}{40(1+4\lambda)^n} \left\{ \begin{array}{c} \frac{1}{2}\left|p_4 - \frac{2}{3}p_1p_3\right| \\ +\frac{1}{2}\left|p_4 - \frac{1}{2}p_2^2\right| + \frac{|p_1|^2}{24}\left|p_2 - \frac{5}{6}p_1^2\right| \end{array} \right\} = \frac{7}{120(1+4\lambda)^n}. \tag{42}$$

□

Theorem 7. *If the function $f(z) \in C_{(\lambda,n)}$ and of the form (1), then*

$$\left|a_3 - a_2^2\right| \leq \frac{1}{6(1+2\lambda)^n}. \tag{43}$$

Proof. To obtain the inequality (43) we will use the expression (18). If equations (36) and (37) are used,we can write

$$\begin{aligned} &\left|a_3 - a_2^2\right| \\ = &\left|\frac{p_2}{12(1+2\lambda)^n} - \left[\frac{p_1}{4(1+\lambda)^n}\right]^2\right| \\ \leq &\frac{1}{12(1+2\lambda)^n}\max\left\{2, 2\left|\frac{3(1+2\lambda)^n}{4(1+\lambda)^{2n}} - 1\right|\right\}. \end{aligned}$$

Here , $\frac{3(1+2\lambda)^n}{4(1+\lambda)^{2n}} \leq 1$. Thus, since $\max\left\{2, 2\left|\frac{3(1+2\lambda)^n}{4(1+\lambda)^{2n}} - 1\right|\right\} = 2$, the desired result is obtained in the form of $\left|a_3 - a_2^2\right| \leq \frac{1}{6(1+2\lambda)^n}$. □

Theorem 8. *If the function $f(z) \in C_{(\lambda,n)}$ and of the form (1), then*

$$|a_2a_3 - a_4| \leq \frac{1}{12(1+\lambda)^n(1+2\lambda)^n} + \frac{13}{144(1+3\lambda)^n}. \tag{44}$$

Proof. From (36), (37) and (38), it follows that

$$\begin{aligned} &|a_2a_3 - a_4| \\ = &\left| \begin{array}{c} \frac{p_1p_2}{48(1+\lambda)^n(1+2\lambda)^n} \\ +\frac{1}{24(1+3\lambda)^n}\left(\frac{p_1^3}{24} + \frac{p_1p_2}{4} - p_3\right) \end{array} \right|. \end{aligned}$$

If the triangle inequality is applied to this last equation, we write

$$\begin{aligned} &|a_2a_3 - a_4| \\ \leq &\frac{|p_1||p_2|}{48(1+\lambda)^n(1+2\lambda)^n} \\ &+\frac{1}{24(1+3\lambda)^n}\left|\frac{p_1^3}{24} + \frac{p_1p_2}{4} - p_3\right|. \end{aligned}$$

According to the (19) inequality, it is thought that

$$\begin{aligned} &\left|\frac{p_1^3}{24} + \frac{p_1p_2}{4} - p_3\right| \\ \leq &\left\{ \begin{array}{c} 2\left|\frac{1}{24}\right| + 2\left|-\frac{1}{4} - \frac{1}{12}\right| \\ +2\left|\frac{1}{24} + \frac{1}{4} - 1\right| \end{array} \right\} \\ \leq &\frac{13}{6} \end{aligned}$$

can be written and if Lemma 1 is taken into account, we find

$$\begin{aligned} &|a_2a_3 - a_4| \\ \leq &\frac{|p_1||p_2|}{48(1+\lambda)^n(1+2\lambda)^n} + \frac{1}{24(1+3\lambda)^n}\left|\frac{p_1^3}{24} + \frac{p_1p_2}{4} - p_3\right| \\ \leq &\frac{1}{12(1+\lambda)^n(1+2\lambda)^n} + \frac{13}{144(1+3\lambda)^n}. \end{aligned}$$

□

Theorem 9. *If the function $f(z) \in C_{(\lambda,n)}$ and of the form (1), then*

$$\left|a_2a_4 - a_3^2\right| \leq \frac{13}{288(1+\lambda)^n(1+3\lambda)^n} + \frac{1}{36(1+2\lambda)^{2n}}. \tag{45}$$

Proof. From (36), (37) and (38), it follows that

$$\begin{aligned} &\left|a_2a_4 - a_3^2\right| \\ = &\left| \begin{array}{c} \frac{p_1p_3}{96(1+\lambda)^n(1+3\lambda)^n} - \frac{p_1^2p_2}{384(1+\lambda)^n(1+3\lambda)^n} \\ -\frac{p_1^4}{2304(1+\lambda)^n(1+3\lambda)^n} - \frac{p_2^2}{144(1+2\lambda)^{2n}} \end{array} \right|. \end{aligned}$$

If the triangle inequality is applied to this last equation, we write

$$\begin{aligned} &\left|a_2a_4 - a_3^2\right| \\ \leq &\left\{ \begin{array}{c} \frac{|p_1|}{96(1+\lambda)^n(1+3\lambda)^n} \\ \left|p_3 - \frac{p_1p_2}{4} - \frac{p_1^3}{24}\right| + \left|\frac{p_2^2}{144(1+2\lambda)^{2n}}\right| \end{array} \right\}. \end{aligned}$$

According to the (19) inequality, it is thought that

$$\begin{aligned} &\left|p_3 - \frac{p_1p_2}{4} - \frac{p_1^3}{24}\right| \\ \leq &\left\{2\left|-\frac{1}{24}\right| + 2\left|\frac{1}{4} + \frac{1}{12}\right| + 2\left|-\frac{1}{24} - \frac{1}{4} + 1\right|\right\} \\ \leq &\frac{13}{6} \end{aligned}$$

can be written and if Lemma 1. is taken into account, we find

$$\begin{aligned} &\left|a_2a_4 - a_3^2\right| \\ \leq &\left\{\frac{2}{96(1+\lambda)^n(1+3\lambda)^n} \cdot \frac{13}{6} + \frac{1}{36(1+2\lambda)^{2n}}\right\} \\ \leq &\frac{13}{288(1+\lambda)^n(1+3\lambda)^n} + \frac{1}{36(1+2\lambda)^{2n}}. \end{aligned}$$

□

Theorem 10. *If the function $f(z) \in C_{(\lambda,n)}$ and of the form (1), then*

$$|H_3(1)| \le \frac{13}{864(1+3\lambda)^n(1+\lambda)^n(1+2\lambda)^n} + \frac{1}{216(1+2\lambda)^{3n}} + \frac{169}{20736(1+3\lambda)^{2n}} + \frac{7}{720(1+4\lambda)^n(1+2\lambda)^n}.$$

Proof. The proof of this theorem is similar to the one in Theorem 5. □

References

[1] Bieberbach, L. (1916). Über die Koeffizienten derjenigen Pottenzreihen, welche eine schlichte Abbildung des Einheitskreises vermitteln. Sitzungsberichte Preussische Akademie der Wissenschaften, 138, pp. 940-955.

[2] De-Branges, L. (1985). A proof of the Beiberbach conjecture. *Acta Mathematica*, 154, 137-152.

[3] Cho, N.E., Kumar, V., Kumar, S.S. & Ravichandran, V. (2019). Radius problems for starlike functions associated with the sine function. *Bulletin of the Iranian Mathematical Society*, 45, 213–232.

[4] Pommerenke, C. (1975). On the coefficients and Hankel determinants of univalent functions. *Journal of the London Mathematical Society*, 41, 111–122.

[5] Pommerenke, C. (1967). On the Hankel determinants of univalent functions. *Mathematika*, 14, 108–112.

[6] Janteng, A., Halim, S.A. & Darus, M. (2006). Coefficient inequality for a function whose derivative has a positive real part. *Journal of Inequalities in Pure and Applied Mathematics*, 7, 1-5.

[7] Janteng, A., Halim, S.A. & Darus, M. (2007). Hankel determinant for starlike and convex functions. *International Journal of Mathematical Analysis*, 1, 619-625.

[8] Babalola, K.O. (2010). On Hankel determinants for some classes of univalent functions. *Inequality Theory and Applications*, 6, 1-7.

[9] Altınkaya, S. & Yalçın, S. (2016). Third Hankel determinant for Bazilevic functions. *Advances in Mathematics*, 5, 91-96.

[10] Bansal, D., Maharana, S. & Prajapat, J.K. (2015). Third order Hankel determinant for certain univalent functions. *Journal of Korean Mathematical Society*, 52, 1139–1148.

[11] Krishna, D.V., Venkateswarlu, B. & RamReddy, T. (2015). Third Hankel determinant for bounded turning functions of order alpha. *Journal of the Nigerian Mathematical Society*, 34, 121–127.

[12] Raza, M. & Malik, S.N. (2013). Upper bound of third Hankel determinant for a class of analytic functions related with lemniscate of Bernoulli. *Journal of Inequalities and Applications*, 412.

[13] Shanmugam, G., Stephen, B.A. & Babalola, K.O. (2014). Third Hankel determinant for α- starlike functions. *Gulf Journal of Mathematics*, 2, 107–113,

[14] Zhang, H.Y., Tang, H. & Ma, L.N. (2017). Upper bound of third Hankel determinant for a class of analytic functions. *Pure and Applied Mathematics*, 33(2), 211- 220.

[15] Breaz, D., Cataş, A. & Cotırla, L. (2022). On the upper bound of the third Hankel determinant for certain class of analytic functions related with exponential function. *Analele Stiintifice ale Universitatii ''Ovidius Constanta. Seria Mathematica*, 30(1), 75-89.

[16] Orhan, H., Çağlar, M. & Cotırla, L. (2023). Third Hankel determinant for a subfamily of holomorphic functions related with lemniscate of Bernoulli. *Mathematics*, 11, 1147.

[17] Zaprawa, P. (2019). Third Hankel determinants for subclasses of univalent functions. *Mediterranean Journal of Mathematics*, 14, 19.

[18] Kowalczyk, B., Lecko, A. & Sim,Y.J. (2018). The sharp bound of the Hankel determinant of the third kind for convex functions. *Bulletin of the Australian Mathematical Society*, 97, 435–445.

[19] Lecko,A., Sim, Y.J. & Smiarowska, B. (2018).The sharp bound of the Hankel determinant of the third kind for starlike functions of order. *Complex Analysis and Operator Theory*, 1–8.

[20] Arif, M., Raza, M., Tang, H., Hussain, S. & Khan, H. (2019). Hankel determinant of order three for familiar subsets of analytic functions related with sine function. *Open Mathematics*, 17, 1615-1630.

[21] Shi, L., Ali, I., Arif ,M., Cho ,N.E., Hussain ,S. & Khan, H. (2019). A Study of third Hankel determinant problem for certain subfamilies of analytic functions involving cardioid domain, *Mathematics*, 7, 418.

[22] Zaprawa, P. (2019). Hankel Determinant for univalent functions related to the exponential function. *Symmetry*, 11, 1211.

[23] Salagean, G. (1983). *Subclasses of Univalent Functions.* Lecture Notes in Mathematics. Springer-Verlag, Berlin, 1013, 362-372.

[24] Al-Oboudi, F.M. (2004). On univalent functions defined by a generalized Salagean operator. *Indian Journal of Mathematics and Mathematical Sciences*, 25-28, 1429-1436.

[25] Oros, I.O. & Oros, G. (2008). On a class of univalent functions defined by a generalized Salagean operator. *Complex Variables and Elliptic Equations*, 53(9), 869-877.

[26] Caratheodory, C. (1911). Uber den variabilitatsbereich der Fourier'schen Konstanten Von Positiven harmonischen. *Rendiconti del Circolo Mathematico di Palermo*, 32, 193–217.

[27] Duren, P.L. (1983). Univalent functions, (Springer-Verlag), 114–115. *Mathematicheskii Sbornik*, 37 (79), 471–476.

[28] Libera, J. & Zlotkiewicz, E.J. (1982). Early coefficients of the inverse of a regular convex Function. *Proceedings of American Mathematical Society*, 85(2), 225–230.

[29] Libera, J. & Zlotkiewicz, E.J. (1983). Coefficient bounds for the inverse of a function with derivative in P. *Proceedings of American Mathematical Society*, 87(2), 251–257,

[30] Ayınla, R.O.B. & Risikat, A. (2021). Toeplitz determinants for a subclass of analytic functions. *Journal of Progressive Research in Mathematics*, 18(1), 99-106.

[31] Keough, F. & Merkes, E. (1996). A coefficient inequality for certain subclasses of analytic functions. *Proceedings of American Mathematical Society*, 20, 8–12.

[32] Pommerenke, C. (1975). Univalent Functions, *Studia Mathematica Mathematische Lehrbucher*, Vandenhoeck & Ruprecht, Gottingen, vol. 25.

Muhammet Kamali *received his doctoral degree from Atatürk University. Currently, he is serving as a professor in the Department of Mathematics at Kyrgyz-Turkish Manas University. His area of interest is complex analysis.*
https://orcid.org/0000-0002-6230-6836

Alina Riskulava *received his master's degree from Kyrgyz-Turkish Manas University. His area of interest is complex analysis.*
https://orcid.org/0009-0000-1311-892X

An International Journal of Optimization and Control: Theories & Applications
ISSN:2146-0957 eISSN:2146-5703
Vol.14, No.1, pp.50-61 (2024)
http://doi.org/10.11121/ijocta.1369

RESEARCH ARTICLE

Mathematical modelling of fiber optic cable with an electro-optical cladding by incommensurate fractional-order differential equations

Büşra Ersoy[a], Bahatdin Daşbaşı[b], Ekin Aslan[a*]

[a] *Department of Electrical and Electronics Engineering, Kayseri University, Turkey*
[b] *Department of Engineering Basic Sciences, Kayseri University, Turkey*
bsrersoy38@gmail.com, bdasbasi@kayseri.edu.tr, ekinaslan@kayseri.edu.tr

ARTICLE INFO

Article History:
Received 3 February 2023
Accepted 11 September 2023
Available Online 12 December 2023

Keywords:
Electro-optical fiber
Fractional-order differential equations (FODEs)
Mathematical model
Stability analysis

AMS Classification 2010:
26A33; 78A05

ABSTRACT

In this study, the mathematical model through incommensurate fractional-order differential equations in Caputo meaning are presented for time-dependent variables given as the numerical aperture, critical angle, and acceptance angle characteristics of a fiber optic cable with electro-optical cladding. The qualitative analysis including the existence and stability of the equilibrium points of the proposed model has been made according to the used parameters, and then, the results obtained from this analysis are supported through numerical simulations by giving the possible values that can be obtained from experimental studies to these parameters in the model. In this way, a stable equilibrium point of the system for the core refractive index, cladding refractive index and electrical voltage is obtained according to the threshold parameter. Thus, the general formulas for the critical angle, acceptance angle and numerical aperture have been obtained when this fixed point is stable.

1. Introduction

Optical fibers are referred to as the waveguide used for light transmission [1]. The light signal includes modulated information and is carried over the glass surface due to the structure of the fiber [2]. Modern optical fibers consist of two coaxial glass cylinders, consisting of the outer layer called cladding and the inner layer called the essence with a larger refractive index [3]. The structure of the optical fiber is depicted in Figure 1.

The phenomenon of total internal reflection is a necessary condition for the transmission of light within the waveguide. Otherwise, efficient transmission does not occur, that is, the light passes to the external environment. Furthermore, gauges such as optical fibers' refractive index profiles, structures, the number of modes they support, signal processing capabilities, distribution, and polarization can also classify them. The phenomenon of total reflection can be explained by Snell's law, which represents the phenomenon of beam optics at the interface separating two different media [1] and is expressed as $n_1 \sin\emptyset_1 = n_2 \sin\emptyset_2$.

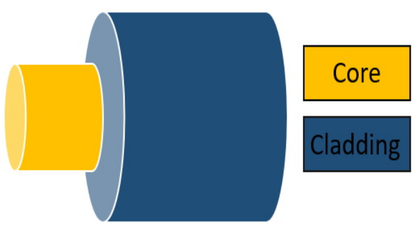

Figure 1. The basic structure of the optical fiber.

When a light beam encounters an interface separating two different environments, some of the

*Corresponding Author

light is reflected in the first environment and the rest passes to the second medium. This is because the speed of light is different in the two environments. Figure 2 shows the behavior of the light beam when it encounters the interface. Here, the relationship between refractive indices is $n_1 > n_2$ [4–6].

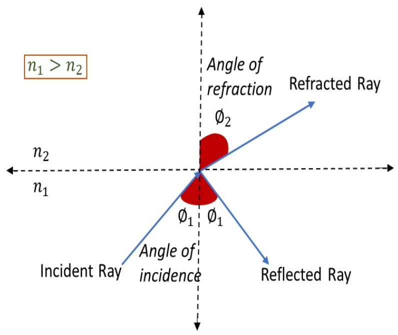

Figure 2. The behavior of the light beam encountering an interface.

Assuming that the angle of refraction is 90^o, the expression $\emptyset_c = \sin^{-1}\left(\frac{n_2}{n_1}\right)$ is reached and $\emptyset_c$ is known as the critical angle [7,8]. If the angle of $\emptyset_1$ made by the incoming beam with the normal of the interface is greater than the critical angle, the total internal reflection criterion is met and the light is reflected back to the initial environment at exactly the same angle [7–9]. The refractive indices, critical angle, acceptance angle, and acceptance cone of the core, cladding, and external environment on the fiber optic cable operating on the total reflection principle are stated are Figure 3.

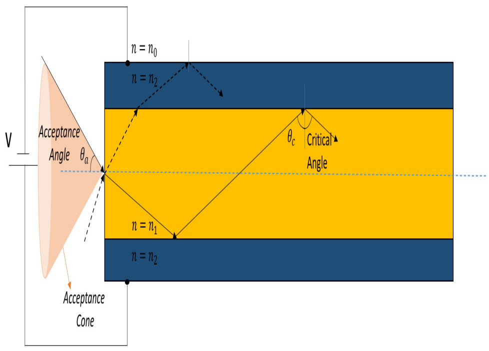

Figure 3. The refractive indices, critical angle, acceptance angle and acceptance cone of the core, cladding and external environment on the fiber optic cable.

One of the parameters that determine the performance of optical fibers is the numerical aperture (NA), whose formula is $NA = n_0 \sin\theta_a = \left(n_1^2 - n_2^2\right)^{1/2}$ [7]. Here θ_a is the angle of acceptance [8]. NA is the capacity to capture light rays of different angles entering the fiber optic cable. The larger the NA magnitude, the more light beams travel through the fiber. Fibers have a certain angle of acceptance, and this angle varies depending on the refractive index of the core, cladding, and medium from which the light comes. Fiber optic cable can only transmit incoming light rays within the limits of the acceptance cone angle, and another performance criterion, the acceptance angle is half the acceptance cone angle. NA grows as the difference between the core and cladding indices of fiber optic cable grows [7,8,10].

The development of optical fibers is possible through close cooperation between both waveguide and materials engineering [11,12]. Functionality can be added to fiber optic cables with the adjustable behavior of materials. A variation in refractive indices of electro-optical (EO) materials, whose optical effects can be adjusted, can be observed with an externally applied electric field. In this context, there are many studies on EO waveguide modulators and optical fibers in the literature. The first study on EO polymer optical fiber (POF) has been proposed by Kuzyk et all [13–19]. Here, high electrical strength has been obtained with an optical fiber consisting of cladding with two parallel indium electrodes, doped EO cores and poly (methyl methacrylate) (PMMA) cladding.

In another study, a few important factors related to the creation and sustainability of EO effect in POF have been examined experimentally and several EO POF designs have been presented. One of the designs is a dual-core-planar cladding while the other designs are a dual-core design with one EO core and an H-shaped cladding in section. In the study, the EO effect of the structure has been measured and the change of this effect in different conditions has been examined. In the same article, it is emphasized that many device applications are based on the EO effect and it is also stated that they plan to improve liquid crystal doped POFs [13].In this study, the refractive index change caused by the EO effect of the material with the external electric field applied to the cladding from the outside is defined in the proposed mathematical model.

A mathematical model is an abstract model made using mathematical symbols and objects to explain the behavior of a real-life situation. This type of modeling can help make better decisions and examine functional relationships by making predictions about a particular process [20].It can be submitted in many different versions, such as mathematical models, statistical models, and differential equations. Differential equation models are used in many fields of science to determine the dynamic perspectives of systems. Fractional calculus has been an ancient but increasingly important subject of mathematics since the 17th century. Fractional integral and differential operators can be thought of as generalized forms of integral and derivative operators with non-integer order [21]. The memory notion for fractional calculus is significant. In memory systems, it has to remember previous values of the input to indicate the current value of the output. Considering the modeling of various memory phenomena, it is generally stated that a memory process is composed two phases, a short-term situation with permanent retention and a situation through fractional derivative [22]. Recently, an increasing number of studies and applications of fractional order systems have been presented in many fields of science and engineering [23–26].

The innovation in this study is to propose the fractional-order differential equation model for the fiber optic consisting of EO cladding, such that the dependent variables are the external electric field applied externally to the cladding and the changes in refractive index caused by the EO effect of the material.

Therefore, the structure of this article is formatted in the following order. In Section 2, we submit some mathematical definitions and notations regarding fractional-order differential equations adopted in the article. In Section 3, the mathematical model for an electro-optic cladding fiber optic cable is introduced and then it has been carried out the qualitative analysis of this model. Also, the formulas for the structural parameters of optical fiber waveguides have been updated, when the system is in equilibrium. The proposed method is numerically examined by a sample in Section 4. Finally, the results and discussion are drawn in Section 5.

2. Preliminaries of fractional-order derivative

This section reviews the fundamental definitions, theorems, concepts, and results that we will use throughout the remainder of this paper.

Definition 1. *(Riemann–Liouville fractional integral) Let* $t_0 \in \mathbb{R}_+ = [0,\infty)$ *be the initial time. Let* $L_1^{loc}(J,\mathbb{R}^n)$ *be the linear space of all locally Lebesgue integrable functions* $m : J \to \mathbb{R}^m,\ J \subset \mathbb{R}$. *Let* $||.||$ *be a norm in* $\mathbb{R}^n$. *Riemann–Liouville fractional integral of order* $\alpha \in (0,1)$

$$ {}_{t_0}I_t^{\alpha} m(t) = \frac{1}{\Gamma(\alpha)} \int_{t_0}^{t} \frac{m(s)}{(t-s)^{1-\alpha}} ds,\ t \geq t_0, \tag{1}$$

where $m \in L_1^{loc}([t_0,\infty),\mathbb{R})$ *and* $\Gamma(.)$ *is the Gamma function [27].*

Definition 2. *(Caputo fractional derivative) The Caputo fractional-order differential operator of the function* X *can be stated as*

$$ {}_{t_0}^{C}D_t^{\alpha} X(t) = \begin{cases} \frac{1}{\Gamma(m-\alpha)} \int_a^t \frac{X^{(m)}(\tau)}{(t-\tau)^{\alpha-m+1}} d\tau & \text{for } m-1<\alpha<m, \\ X^{(m)}(\tau) & \text{for } \alpha = m, \end{cases} \tag{2}$$

where $t_0 \leq t$, $m \in \mathbb{Z}^+$ *[27].*

Lemma 1. *(Generalized mean value theorem) Assume that* $X(t) \in C([a,b])$ *and* ${}_{t_0}^{C}D_t^{\alpha} X(t) \in C([a,b])$, *such that* $0 < \alpha \leq 1$, *then:*

$$ X(t) = X(a) + \frac{1}{\Gamma(\alpha)} {}_{t_0}^{C}D_t^{\alpha} X(\xi)(t-a)^{\alpha}, \tag{3}$$

with $a \leq \xi \leq t$, *for all* $t \in (a,b]$ *[28, 29].*

Definition 3. *(Incommensurate fractional order system) The multi-order fractional differential equation system reads as*

$$ {}_{t_0}^{C}D_t^{\alpha} X(t) = F(t,X),\ X(0) = X_0 \tag{4}$$

where $X(t) = [x_1(t),\ x_2(t), \ldots, x_n(t)]^T \in \mathbb{R}^n$, $F = [f_1, f_2, \ldots, f_n]^T \in \mathbb{R}^n$, $f_i : [0,+\infty) \times \mathbb{R}^n \to \mathbb{R}$, $i = 1,2,\ldots,n$. $\alpha = [\alpha_1, \alpha_2, \ldots, \alpha_n]$ *is the multi-order of system (4), if all* α_i *are equal to a constant, then (4) is the generally considered model.* ${}_{t_0}^{C}D_t^{\alpha} = \left[{}_{t_0}^{C}D_t^{\alpha_1}, {}_{t_0}^{C}D_t^{\alpha_2}, \ldots, {}_{t_0}^{C}D_t^{\alpha_n}\right]^T$, ${}_{t_0}^{C}D_t^{\alpha_i}$ *denotes* α_i *th-order fractional derivative in the Caputo sense.* ${}_{t_0}^{C}D_t^{\alpha} X(t)$ *refers to the "direct product" of linear operator* ${}_{t_0}^{C}D_t^{\alpha}$ *and vector* $X(t)$, *i.e.* ${}_{t_0}^{C}D_t^{\alpha} X(t) = \left[{}_{t_0}^{C}D_t^{\alpha_1} x_1(t), {}_{t_0}^{C}D_t^{\alpha_2} x_2(t), \ldots, {}_{t_0}^{C}D_t^{\alpha_n} x_n(t)\right]^T$ *[30]. The multiple order can be any real vector, even a complex one. In this study, it is only accepted the real case of order.*

If $\alpha = \alpha_1 = \alpha_2 = \ldots = \alpha_n$, *then the system is called a commensurate order system, otherwise system denotes an incommensurate order system (IFOS), which is more general than the other [31].*

Definition 4. *The equilibrium points of system (4) are calculated by solving the following equation* $F(X) = 0$ *and we have been supposed that* $X^* = (x_1^*,\ x_2^*, \ldots, x_n^*)$ *is an equilibrium point of system (4).*

Lemma 2. *Eigenvalues* λ_i *for* $i = 1,2,\ldots,\ \rho(\alpha_1 +\ \alpha_2 + \cdots + \alpha_n)$ *of system (4)* *are calculated by the charasteristical polynomial obtained from* $\det\left(\operatorname{diag}\left(\lambda^{\rho\alpha_1},\ \lambda^{\rho\alpha_2},\ldots,\lambda^{\rho\alpha_n}\right)-\ J\left(X^*\right)\right) = 0$ *such that* ρ *is the least common multiple of the denominators of rational numbers* $\alpha_1,\ \alpha_2,\ldots,\ \alpha_n$ *and* $J\left(X^*\right) = \frac{\partial F}{\partial X}\big|_{X=X^*}$. *If all eigenvalues* λ_i *satisfy* $\left|arg\left(\lambda_i\right)\right| > \frac{\pi}{2\rho}$, *then* X^* *is locally asymtotically stable (LAS) for system (4) [32, 33].*

3. The mathematical model for an electro-optic cladding fiber optic cable

This section of the paper purposes to suggest a model based on the memorability nature of the Caputo fractional-order derivative. Let the $t\ (\geq 0)$ value represent the time parameter. It is denoted the voltage of the electric field by v, the refractive index of the core of the fiber optic cable by n_1, and the cladding refractive index by n_2. Also, it is $v = v\left(t\right),\ n_1 = n_1\left(t\right),\ n_2 = n_2\left(t\right)$ such that $v,\ n_1,\ n_2 > 0$. Our recommended model described the changes in the refractive indexes of fiber optic cable with electro-optic cladding is expressed by the following IFOS

$$\begin{aligned}
&{}_0^C D_t^{\alpha_1} v\left(t\right) = \mathit{\Lambda} - \beta v\\
&{}_0^C D_t^{\alpha_2} n_1\left(t\right) = r_1 n_1\left(1-\tfrac{n_1}{C}\right)\\
&{}_0^C D_t^{\alpha_3} n_2\left(t\right) = r_2 n_2\left(1-\tfrac{n_2}{n_1}\right) - \delta v + n_0
\end{aligned}\tag{5}$$

with positive initial conditions $v\left(0\right) = v_0,\ n_1\left(0\right) = n_{10}, n_2\left(0\right) = n_{20}$. In addition that, the derivative orders are α_i for $i = 1, 2, 3$ such that $0 < \alpha_i \leq 1$ and the parameters have the properties given as

$$\mathit{\Lambda},\ \beta, r_1, C,\ r_2,\ \delta, n_0 > 0. \tag{6}$$

The model has the following assumptions. The voltage is supplied by the fixed amount of $\mathit{\Lambda}$ and it is decreasing by a ratio β. It is also assumed that the inequality

$$\tfrac{n_0}{\delta} \geq v \tag{7}$$

exists for v. For the refractive index of the core of the fiber optic cable (n_1) and the refractive index of the cladding (n_2), their sizes vary according to the logistic rules. The rate of increase of n_1 is r_1 and its maximum magnitude (the mathematically well-known the carrying capacity term) is C. Also, it is always $n_1 > n_2$. Therefore, the maximum magnitude of the refractive index of the cladding is up to or smaller than the refractive index of the core of the fiber optic cable. The growth rate of the refractive index of the cladding is r_2. Also, n_2 decreases by its δ ratio as it is affected by the voltage of the electric field. Since n_0, which is the refractive index of the medium outside the fiber optic cable, is smaller than n_2, n_0 has been added to the cladding refractive index.

3.1. The existence and uniqueness of the solution of system (5)

In this section, the existence and uniqueness of the solutions for FOS in Eqs (5) is examined.

Lemma 3. *With each non-negative initial conditions, there exists a unique solution of fractional-order system in Eqs (3). For every non-negative initial condition, there is a unique solution of fractional-order system in Eqs (5).*

Proof. Existence and uniqueness of system (3) will be indicated in the region $\mathit{\Omega}\times(0;\ T]$ where $\mathit{\Omega} = \left\{(v, n_1, n_2)\in\mathbb{R}_+^3 : \max\left(\left|v\right|, \left|n_1\right|, \left|n_2\right|\right)\leq\zeta\right\}$. Here, it is followed the approach used in [32]. We express $X = (v, n_1, n_2)$ and $\overline{X} = (\overline{v}, \overline{n_1}, \overline{n_2})$. Consider a mapping

$$G\left(X\right) = \left(G_1\left(X\right), G_2\left(X\right), G_3\left(X\right)\ \right)$$

and

$$\begin{aligned}
G_1\left(X\right) &= \mathit{\Lambda} - \beta v,\\
G_2\left(X\right) &= r_1 n_1\left(1-\tfrac{n_1}{C}\right),\\
G_3\left(X\right) &= r_2 n_2\left(1-\tfrac{n_2}{n_1}\right) - \delta v + n_0.
\end{aligned}\tag{8}$$

For any $X,\ \overline{X}$, it follows from (8) that $\left\|G(X)-G(\bar{X})\right\| = \left|\Lambda-\beta v-\Lambda+\beta\bar{v}\right| + \left|r_1 n_1(1-\frac{n_1}{C}) - r_1\bar{n}_1(1-\frac{\bar{n}_1}{C})\right| + \left|r_2 n_2(1-\frac{n_2}{n_1}) - \delta v + n_0 - r_2\bar{n}_2(1-\frac{\bar{n}_2}{\bar{n}_1}) + \delta\bar{v} - n_0)\right| = \beta\left|v-\bar{v}\right| + \left|r_1(n_1-\bar{n}_1) - \frac{r_1}{C}(n_1-\bar{n}_1)(n_1+\bar{n}_1)\right| + \left|r_2(n_2-\bar{n}_2) - r_2(n_2\frac{n_2}{n_1} - \bar{n}_2\frac{\bar{n}_2}{\bar{n}_1}) - \delta(v-\bar{v})\right|$,

$\left\|G(X)-G(\bar{X})\right\| \leq \beta\left|v-\bar{v}\right| + r_1\left|(n_1-\bar{n}_1)\right| + \frac{r_1}{C}\left|(n_1-\bar{n}_1)\right|\left|(n_1+\bar{n}_1)\right| + \left|r_2(n_2-\bar{n}_2)\right| + r_2\left|(n_2\frac{n_1}{n_2} - \bar{n}_2\frac{\bar{n}_1}{\bar{n}_2})\right| + \delta\left|(v-\bar{v})\right|$,

$\left\|G(X)-G(\bar{X})\right\| \leq (\beta+\delta)\left|v-\bar{v}\right| + (r_1 + \frac{r_1}{C}\left|(n_1+\bar{n}_1)\right|)\left|n_1-\bar{n}_1\right| + r_2\left|n_2-\bar{n}_2\right| + r_2\left|(\frac{n_2^2}{n_1} - \frac{\bar{n}_2}{\bar{n}_1})\right|$.

We said that the logistic growth rule is valid for n_1. If the non-negative initial condition $(n_1\left(0\right))$ is less than the carrying capacity, it will approach its capacity (C) by increasing, if not, it will approach its capacity by decreasing. For example, let $max\left\{n_1, \overline{n_1}\right\} = n_1$. In this case we have have $\left|\frac{n_2^2}{n_1} - \frac{\overline{n_2}^2}{\overline{n_1}}\right| \leq \left|\frac{n_2^2-\overline{n_2}^2}{n_1}\right| \leq \frac{\left|n_2-\overline{n_2}\right|\left|n_2+\overline{n_2}\right|}{\underbrace{n_1\left(0\right)}_{or\ C}}$. Therefore, it is

$$\left\|G\left(X\right)-G\left(\bar{X}\right)\right\| \leq \varphi_1\left|v-\bar{v}\right|+\varphi_2\left|n_1-\bar{n}_1\right| + \varphi_3\left|n_2-\bar{n}_2\right|, \tag{9}$$

where

$$\begin{gathered}\varphi_1=(\beta+\delta)\\ \varphi_2=\left(r_1+2\zeta\frac{r_1}{C}\right)\\ \varphi_3=\left(r_2+r_2\frac{2\zeta}{n_1(0)}\right)\end{gathered} \tag{10}$$

Therefore, it is obtained $\left\|G\left(X\right)-G\left(\overline{X}\right)\right\| \leq L\left\|X-\overline{X}\right\|$ where $L=\max\left(\varphi_1,\varphi_2,\varphi_3\right)$. $G(X)$ satisfies the Lipschitz condition. In this sense, it is indicated the existence and uniqueness of the solutions of Eqs (5) □

3.2. Boundedness and non-negativity of the solutions of system(5)

Solutions of Eqs. (5) are non-negative and bounded since they have densities of interacting variables. This case is examined here.

Lemma 4. *The solutions of (3) which start in $\mathbb{R}_+^3$ are uniformly bounded and non-negative.*

Proof. It is adopted the manner of approaching which is used in [34]. Therefore, we have follows ${}_{t_0}^{C}D_t^{\alpha}v\left(t\right)=\Lambda-\beta v \Rightarrow v\left(t\right)=v\left(0\right)E_{\alpha}\left(-\beta(t)^{\alpha}\right)+\Lambda(t)^{\alpha}E_{\alpha,\alpha+1}\left(-\beta(t)^{\alpha}\right)$,

${}_{t_0}^{C}D_t^{\alpha}n_1 \leq r_1 n_1\left(1-\frac{n_1}{C}\right)$ and ${}_{t_0}^{C}D_t^{\alpha}n_1+r_1n_1 \leq 2r_1n_1-\frac{r_1}{C}{n_1}^2 = -\frac{r_1}{C}\left(\overbrace{{n_1}^2-2n_1C+C^2}^{(n_1-C)^2}-C^2\right) \leq r_1C \Rightarrow n_1\left(t\right) \leq n_1\left(0\right)E_{\alpha}\left(-r_1(t)^{\alpha}\right)+r_1C(t)^{\alpha}E_{\alpha,\alpha+1}\left(-r_1(t)^{\alpha}\right)$

$$\lim_{t\to\infty} n_1\left(t\right) \leq C \tag{11}$$

and ${}_{t_0}^{C}D_t^{\alpha}n_2 = r_2n_2\left(1-\frac{n_2}{n_1}\right)-\delta v+n_0$ and ${}_{t_0}^{C}D_t^{\alpha}n_2+r_2n_2 \leq -\frac{r_2}{n_1}\left(n_2^2-2n_2n_1+n_1^2-n_1^2-\frac{n_0}{\frac{r_2}{n_1}}\right) = \left(-\frac{r_2}{n_1}\left(n_2-n_1\right)^2+r_2\left(n_1+\frac{n_0}{r_2}\right)\right) \leq r_2\left(C+\frac{n_0}{r_2}\right) \Rightarrow n_2\left(t\right) \leq n_2\left(0\right)E_{\alpha}\left(-r_2(t)^{\alpha}\right)+r_2\left(C+\frac{n_0}{r_2}\right)(t)^{\alpha}E_{\alpha,\alpha+1}\left(-r_2(t)^{\alpha}\right)$

$$\lim_{t\to\infty} n_2\left(t\right) \leq \left(C+\frac{n_0}{r_2}\right). \tag{12}$$

Hence, the solutions of FOS starting in $\mathbb{R}_+^3$ are uniformly bounded in the region Ω.

From the system (5), we have

$$\begin{gathered}{}_0^CD_t^{\alpha_1}v\left(t\right)\Big|_{v=0}=\Lambda\geq 0\\ {}_0^CD_t^{\alpha_2}n_1\left(t\right)\Big|_{n_1=0}=0\\ {}_0^CD_t^{\alpha_3}n_2\left(t\right)\Big|_{n_2=0}=n_0-\delta v\geq 0 \text{ (Due to (7))}\end{gathered} \tag{13}$$

for all $t\in[0,T]$. With respect to Lemma 1, we can accomplish that the solution $X(t)=\left(v\left(t\right),\ n_1\left(t\right),n_2\left(t\right)\right)^T$ of system (5) belongs to $\mathbb{R}_+^3$, and this completes the proof. □

Definition 5. ***(Threshold Parameter)*** *To examine the local stability of equilibrium point of Eqs (5), threshold parameter called basic reproduction number has been introduced given as*

$$\mathcal{R}_0=\frac{\left(\delta\frac{\Lambda}{\beta}-n_0\right)}{\frac{Cr_2}{4}}. \tag{14}$$

The stability for equilibrium values of the electric field voltage, the core refractive index of fiber optic cable, and the cladding refractive index of fiber optic cable is defined according to the threshold parameter.

Lemma 5. *Considering equilibrium points of the proposed model in (5) with reference to threshold parameter definited in (14), it is satisfied the followings:*

i. *If $\mathcal{R}_0 \leq 1$, then there is always $E_1\left(\frac{\Lambda}{\beta},\ C, C\frac{1+\sqrt{(1-\mathcal{R}_0)}}{2}\right)$,*

ii. *If $0<\mathcal{R}_0\leq 1$, then there are both $E_1\left(\frac{\Lambda}{\beta},\ C, C\frac{1+\sqrt{(1-\mathcal{R}_0)}}{2}\right)$ and $E_2\left(\frac{\Lambda}{\beta},\ C, C\frac{1-\sqrt{(1-\mathcal{R}_0)}}{2}\right)$.*

Proof. We have assumed that $E\left(\overline{v},\ \overline{n_1},\overline{n_2}\right)$ represent the equilibrium point of the system (5), such that

$$\overline{v},\ \overline{n_1},\overline{n_2}>0. \tag{15}$$

The steadiness points of system (5) are achieved by deciphering the following system of equations: $Dv^{\alpha_1}=Dn_1^{\alpha_2}=Dn_2^{\alpha_3}=0$. Therefore, we have

$$\begin{aligned}&\Lambda-\beta v=0\\ &r_1n_1\left(1-\frac{n_1}{C}\right)=0\\ &r_2n_2\left(1-\frac{n_2}{n_1}\right)-\delta v+n_0=0\end{aligned} \tag{16}$$

From the first two equations of (16), $\overline{n_1}=C$ and $\overline{v}=\frac{\Lambda}{\beta}$ are obtained. By substituting these values in the last equation, it is obtained the 2nd degree polynomial given as

$$\overline{n_2}^2-C\overline{n_2}+\frac{C}{r_2}\left(\delta\frac{\Lambda}{\beta}-n_0\right)=0 \tag{17}$$

for the equilibrium value showing the refractive index of the cladding. The discriminant of this equation is $\Delta = C^2(1-\mathcal{R}_0)$ according to (14). If $\mathcal{R}_0 > 1$, a suitable $\overline{n_2}$ value cannot be found due to $\Delta < 0$.

(i) Let $\mathcal{R}_0 \leq 1$. In this case, $(\overline{n_2})_{1,2} = C\frac{1\pm\sqrt{(1-\mathcal{R}_0)}}{2}$ for roots of Eq.(17) are obtained. Since it is obvious $(\overline{n_2})_1 > 0$, the equilibrium point $E_1\left(\frac{A}{\beta},\ C, C\frac{1+\sqrt{(1-\mathcal{R}_0)}}{2}\right)$ is reached.

(ii) Also, the equilibrium point $E_2\left(\frac{A}{\beta},\ C, C\frac{1-\sqrt{(1-\mathcal{R}_0)}}{2}\right)$ occurs too, when $\mathcal{R}_0 > 0$.

□

Lemma 6. *The LAS conditions of equilibrium points for the system (5) are as follows.*

(i) *Let* $\mathcal{R}_0<1$*. In this case,* $E_1\left(\frac{A}{\beta},\ C, C\frac{1+\sqrt{(1-\mathcal{R}_0)}}{2}\right)$ *is LAS.*

(ii) *The equilibrium point* $E_2\left(\frac{A}{\beta},\ C, C\frac{1-\sqrt{(1-\mathcal{R}_0)}}{2}\right)$ *existing for* $0 < \mathcal{R}_0 \leq 1$ *is always unstable.*

Proof. Let $\mathcal{R}_0 \leq 1$. The Jacobian matrix of the system (5) at $E(\overline{v},\ \overline{n_1}, \overline{n_2})$ for E_1 and/or E_2 is given by

$$J\left(E\left(\overline{v},\ \overline{n_1},\overline{n_2}\right)\right) =$$

$$\begin{pmatrix} -\beta & 0 & 0 \\ 0 & r_1 - \frac{2r_1\overline{n_1}}{C} & 0 \\ -\delta & \frac{r_2\overline{n_2}^2}{\overline{n_1}^2} & r_2 - \frac{2r_2\overline{n_2}}{\overline{n_1}} \end{pmatrix} \tag{18}$$

From the equation $\det\left(diagonal\left(\lambda^{\rho\alpha_1}, \lambda^{\rho\alpha_2}, \lambda^{\rho\alpha_3}\right) - J\left(E\left(\overline{v},\ \overline{n_1},\overline{n_2}\right)\right)\right) = 0$, the characteristic equation is

$$(\lambda^{\rho\alpha_1}+\beta)(\lambda^{\rho\alpha_2}-(r_1-\tfrac{2r_1\overline{n_1}}{C}))(\lambda^{\rho\alpha_3}-(r_2-\tfrac{2r_2\overline{n_2}}{\overline{n_1}}))=0 \tag{19}$$

where ρ is the least common multiple of the denominators of the derivative orders $\alpha_1, \alpha_2, \alpha_3$ in the system (5). Considering Lemma 2, the LAS condition of $E(\overline{v},\ \overline{n_1}, \overline{n_2})$ is that the λ eigenvalues to be obtained from (19) satisfy the inequalities $arg(\lambda) > \frac{\pi}{2\rho}$. Also, if λ is real number ($\in \mathbb{R}$), it must be $\lambda < 0$ to satisfy the stability conditions of the equilibrium point. Therefore, it is

$$\lambda^{\rho\alpha_1} = -\beta \tag{20}$$

$$\lambda^{\rho\alpha_2} = r_1 - \frac{2r_1\overline{n_1}}{C} \tag{21}$$

$$\lambda^{\rho\alpha_3} = r_2 - \frac{2r_2\overline{n_2}}{\overline{n_1}} \tag{22}$$

where $\lambda^{\rho\alpha_1}, \lambda^{\rho\alpha_2}, \lambda^{\rho\alpha_3} \in \mathbb{R}$ and $\lambda^{\rho\alpha_1} \in \mathbb{R}^-$ due to inequalities in (6) and (15). Let us consider (20). Therefore, the equations

$$\lambda_j = \beta^{\frac{1}{\rho\alpha_1}} \operatorname{cis}\frac{(2j-1)\pi}{\rho\alpha_1},\ \text{for } j = 1, 2, 3, \ldots, \rho\alpha_1 \tag{23}$$

is obtained by means of the De-Moivre rules such that it is $\operatorname{cis}\pi = \cos\pi + i\sin\pi$ for $i = \sqrt{-1}$. We have

$$|Arg(\lambda_j)| = \frac{\pi}{\rho\alpha_1}, \frac{3\pi}{\rho\alpha_1}, \ldots, \frac{(2\rho\alpha_1-1)\pi}{\rho\alpha_1} \tag{24}$$

If the stability conditions in Lemma 2 are applied; then

$$\frac{\pi}{\rho\alpha_1}, \frac{3\pi}{\rho\alpha_1}, \ldots, \frac{(2\rho\alpha_1-1)\pi}{\rho\alpha_1} > \frac{\pi}{2\rho}$$

and so,

$$\frac{1}{\alpha_1}, \frac{3}{\alpha_1}, \ldots, \frac{(2\rho\alpha_1-1)}{\alpha_1} > \frac{1}{2}$$

$$\alpha_1 < min\left\{2, 6, \ldots, 2\left(2\rho\alpha_1 - 1\right)\right\} \tag{25}$$

are obtained. In the introduction of proposed model in the system (5), it is stated that $\alpha_i \in (0, 1]$ for $i = 1, 2, 3$. Therefore, Eqs. (23) for (20-a) are already satisfied. This means that the stability conditions for the equilibrium point $E(\overline{v},\ \overline{n_1}, \overline{n_2})$ are not disturbed.

Thus, it should be examined whether the equations in (20-b) and (20-c) satisfy the stability conditions. Consider that $\overline{n_1} = C$ for the equilibrium points both E_1 and E_2, the equations in (20-b) and (20-c) have the following forms:

$$\lambda^{m\alpha_2} = -r_1 \tag{26}$$

$$\lambda^{m\alpha_3} = r_2 - \frac{2r_2\overline{n_2}}{C}. \tag{27}$$

Since $-r_1 < 0$ due to inequality in (6), it is clear that (26) does not disturb the stability conditions when it is considered similarly to (20). From (27), if

$$\overline{n_2} > \tfrac{C}{2}, \tag{28}$$

then the equilibrium point is stable, since $\lambda^{\rho\alpha_3} \in \mathbb{R}^-$. Thus, the following results are achieved.

(i) Let $\mathcal{R}_0 \leq 1$. It is $\overline{n_2} = C\frac{1+\sqrt{(1-\mathcal{R}_0)}}{2}$ for E_1. The LAS conditions in terms of (25) are fulfilled, when $\mathcal{R}_0 < 1$. Therefore, E_1 is LAS.

(ii) Let $0 < \mathcal{R}_0 \leq 1$. In this case, we have $\overline{n_2} = C\frac{1-\sqrt{(1-\mathcal{R}_0)}}{2}$ for E_2. Considering (25), E_2 is unstable point.

The abovementioned results regarding the equilibrium points are submitted in Table 1.

Table 1. LAS conditions of equilibrium points of the system(5).

Equilibrium Point	Existence Condition	Stability Condition
$E_1\left(\frac{\Lambda}{\beta}, C, C\frac{1+\sqrt{(1-\mathcal{R}_0)}}{2}\right)$	If $\mathcal{R}_0 \leq 1$,	If $\mathcal{R}_0 < 1$
$E_2\left(\frac{\Lambda}{\beta}, C, C\frac{1-\sqrt{(1-\mathcal{R}_0)}}{2}\right)$	If $0 < \mathcal{R}_0 \leq 1$,	Unstable point

$\square$

4. Numerical studies

In this section, the parameters used in the system (5) are given numerical values and this system is analyzed numerically to be compatible with the outcomes of the qualitative analysis. The parameter values are as shown in Table 2.

Table 2. The considered values of parameters in the proposed model (5) and their interpretations.

Parameters	Definitions	Values
Λ	Applied voltage constant	10.5
β	Decrease rate of voltage constant	1
r_1	Growth rate of core refractive index	0.2
C	Maximum magnitude of the cladding refractive index	15
r_2	Growth rate of cladding refractive index	0.25
δ	The rate of voltage-dependent decrease in cladding refractive index	0.8
n_0	Environmental refractive index	8
$(\alpha_1, \alpha_2, \alpha_3)$	Fractional-orders	$(1,1,1)$ $(0.9,0.9,0.9)$ $(0.75,0.75,0.75)$ $(0.7,0.8,0.9)$ $(0.9,0.8,0.7)$
(v_0, n_{10}, n_{20})	Initial conditions	$(16,12,9)$

The following figures show the stability of the equilibrium point $E_1\,(10.5,\ 15, 13.17890832929182)$, since $0 \leq \mathcal{R}_0 = 0.42666667 < 1$.

Table 3. Sensitivity indices of $\mathcal{R}_0$ according to Table (2).

Parameters	Sensitivity index $\left(^{(S)}\right)$	Elasticity
r_2	$^{(S)}\mathcal{R}^1_{0r_2} = \frac{-4}{Cr_2^2}\left(\delta\frac{\Lambda}{\beta} - n_0\right) = \frac{-1}{r_2}\mathcal{R}_0$	-1.7066
δ	$^{(S)}\mathcal{R}^1_{0\delta} = \frac{4}{Cr_2}\left(\delta\frac{\Lambda}{\beta} - n_0\right) = \frac{4}{Cr_2}\frac{\Lambda}{\beta}$	11.2
Λ	$^{(S)}\mathcal{R}^1_{0\Lambda} = \frac{4}{Cr_2}\left(\delta\frac{\Lambda}{\beta} - n_0\right) = \frac{4}{Cr_2}\frac{\delta}{\beta}$	0.8533
β	$^{(S)}\mathcal{R}^1_{0\beta} = \frac{4}{Cr_2}\left(\delta\frac{\Lambda}{\beta} - n_0\right) = \frac{-4}{Cr_2}\delta\frac{\Lambda}{\beta^2}$	-8.96
C	$^{(S)}\mathcal{R}^1_{0C} = \frac{-4}{C^2r_2}\left(\delta\frac{\Lambda}{\beta} - n_0\right) = \frac{-1}{C}\mathcal{R}_0$	-0.0284
n_0	$^{(S)}\mathcal{R}^1_{0n_0} = \frac{4}{Cr_2}\left(\delta\frac{\Lambda}{\beta} - n_0\right) = -\frac{4}{Cr_2}$	-1.0666

The parameter with the greatest positive effect on $\mathcal{R}_0$ is δ, while the parameter with the greatest negative effect is β. If δ is increased (or decreased) by 1%, then the value of $\mathcal{R}_0$ will increase (or decrease) by 10.6667%. Similarly, if β is increased (or decreased) by 1%, then the value of $\mathcal{R}_0$ will decrease (or increase) by 8%.

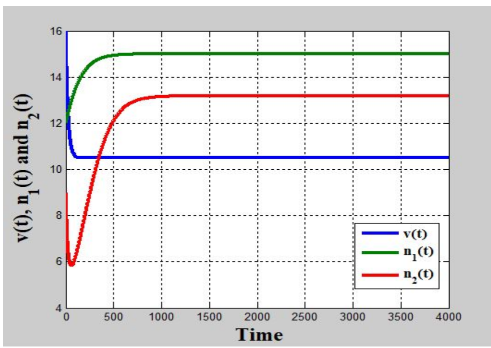

Figure 4. Stabilities of variables for derivative orders given by (1,1,1).

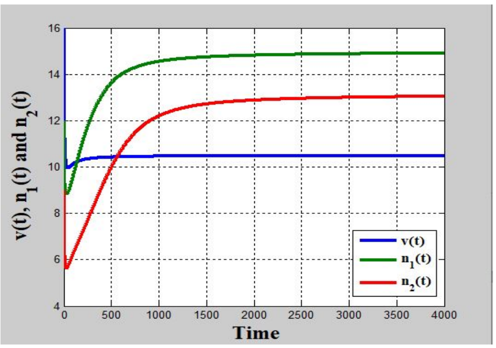

Figure 5. Stabilities of variables for derivative orders given by (.9,.9,.9).

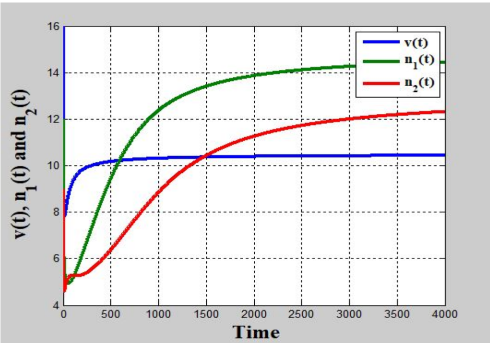

Figure 6. Stabilities of variables for derivative orders given by (.75,.75,.75).

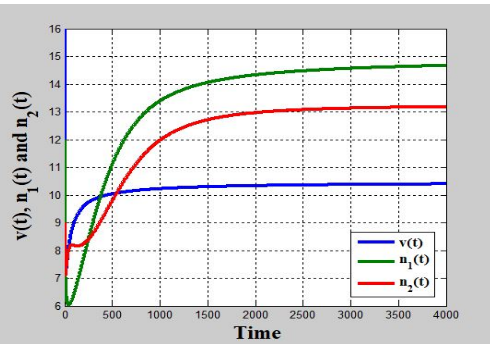

Figure 7. Stabilities of variables for derivative orders given by (.7,.8,.9).

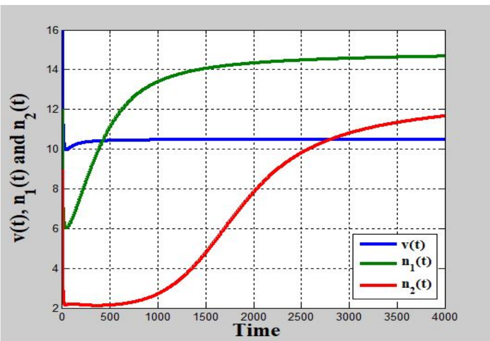

Figure 8. Stabilities of variables for derivative orders given by (.9,.8,.7).

5. Conclusion

In this study, which proposes optical fiber with EO cladding unlike the literature, a mathematical model in the IFOS form in the Caputo meaning including optical fiber variables, given as numerical aperture, critical angle and acceptance angle are presented. The stability analysis consequences of system have been shown with simulations and it has been seen that they are consistent with respect to qualitative analysis.

In the following results as a contribution to the literature, the structural parameters including numerical aperture, critical angle and acceptance angle of optical fiber waveguides are mentioned. In the light of the information given in Table 1, the necessary calculations were made for the stable equilibrium point $E_1\left(\frac{A}{\beta},\ C, C\frac{1+\sqrt{(1-\mathcal{R}_0)}}{2}\right)$ at $\mathcal{R}_0 < 1$.

Result 1 Since the critical angle formula is $\emptyset_c = \arcsin\left(\frac{n_2}{n_1}\right)$, this value evaluated at the LAS E_1 is obtained as

$$\overline{\emptyset_c} = \arcsin\left(\frac{1+\sqrt{(1-\mathcal{R}_0)}}{2}\right) \quad \text{for } 0 \le \mathcal{R}_0 < 1, \tag{29}$$

such that $-\frac{\pi}{2} \le \overline{\emptyset_c} \le \frac{\pi}{2}$.

Result 2 Let us consider that the numerical aperture formula given as $NA = n_0 \sin\theta_a = \sqrt{n_1^2 - n_2^2}$. When E_1 is LAS, this formula is

$$\overline{NA} = \frac{C}{2}\sqrt{2+\mathcal{R}_0 - 2\sqrt{(1-\mathcal{R}_0)}} \text{ for } 0 \le \mathcal{R}_0 < 1. \tag{30}$$

Result 3 Acceptance angle for the LAS $E_1$is obtained as

$$\overline{\theta_a} = \arcsin\left(\frac{C}{2n_0}\sqrt{2+\mathcal{R}_0 - 2\sqrt{(1-\mathcal{R}_0)}}\right)$$
$$\text{for } 0 \le \mathcal{R}_0 < 1. \tag{31}$$

such that $-\frac{\pi}{2} \le \overline{\theta_a} \le \frac{\pi}{2}$.

Consider the point E_1 for $\mathcal{R}_0 < 1$, the results obtained above are summarized in the table below.

Table 4. The obtained results of the proposed system in (5) for $0 \leq \mathcal{R}_0 < 1$.

The LAS equilibrium point	$E_1\left(\frac{A}{\beta},\ C, C\frac{1+\sqrt{(1-\mathcal{R}_0)}}{2}\right)$
The critical angle formula for E_1	$\overline{\emptyset_c} = \arcsin\left(\frac{1+\sqrt{(1-\mathcal{R}_0)}}{2}\right)$
The numerical aperture formula for E_1	$\overline{NA} = \frac{C}{2}\sqrt{2+\mathcal{R}_0 - 2\sqrt{(1-\mathcal{R}_0)}}$
The acceptance angle formula for E_1	$\overline{\theta_a} = \arcsin\left(\frac{C}{2n_0}\sqrt{2+\mathcal{R}_0 - 2\sqrt{(1-\mathcal{R}_0)}}\right)$

Considering the values in Table 2, the values in Table 3 are obtained as follows:

- Threshold parameter: $0 \leq \mathcal{R}_0 = 0.42666667 < 1$,
- The LAS equilibrium point: $E_1(10.5, 15, 13.1789)$,
- The critical angle: $\overline{\emptyset_c} = \arcsin(0.8785) = 61.46194534^o$,
- The numerical aperture formula: $\overline{NA} = 7.163544880024326$,
- The acceptance angle: $\overline{\theta_a} = \arcsin(0.8954) = 63.55985484^o$.

As a result, considering these assumptions, the fiber optic cable, the numerical aperture, the critical angle, and the acceptance angle values can be accordingly recalculated by the obtained formulas. In addition, the above-mentioned structural parameter values can be easily found according to the parameter values of the system.

In the scope of our study, we introduced an innovative approach by proposing the utilization of an electro-optic material, previously unconsidered, for the protective sheath of the fiber optic cable. Subsequently, we mathematically modeled the phenomena associated with light behavior. As a result of this analysis, we put forth the proposition that, instead of employing a general formula, calculations for these parameters could be conducted using the novel equations derived from our mathematical modeling.

In the future, such works will be able to guide the mathematical modeling of fibers designed with materials with the proposed adjustable cladding index and will be able to shed light on material development in line with this modeling. The types of materials to be developed in this way can be the subject of research in many fields, especially in materials engineering. The results obtained can be revolutionary in many fields.

References

[1] Addanki, S., Amiri, I. S., & Yupapin, P. (2018). Review of optical fibers-introduction and applications in fiber lasers. *Results in Physics*, 10, 743-750.

[2] Sharma, P., Pardeshi, S., Arora, R.K. & Singh, M. (2013). A Review of the Development in the Field of Fiber Optic Communication Systems. *International Journal of Emerging Technology and Advanced Engineering*, 3(5), 2250-2459.

[3] Chu, P.L. (2009). *Fiber Optic Devices and Systems.Electrical Engineering - Volume II 113.* EOLSS Publications.

[4] Born, M., Wolf, E. (1999). *Principles of Optics: Electromagnetic Theory of Propagation, Interference and Diffraction of Light.* 6th ed. Cambridge University Press.

[5] Shirley, J.W. (2005). An Early Experimental Determination of Snell's Law. *American Journal of Physics*, 19(9), 507.

[6] Bryant, F. (1958). Snell's Law of Refraction. *Physics Bulletin*, 9(12), 317.

[7] Martın-Fernandez, M.L., Tynan, C.J., & Webb, S.E.D. (2013). A 'pocket guide' to total internal reflection fluorescence. *Journal of Microscopy*, 252(1), 16-22.

[8] Senior, J. M. (2009). *Optical Fiber Communications Principles and Practice Third Edition.* Kirby Street, London

[9] Axelrod, D., Burghardt, T. P. & Thompson, N. L. (1984) Total internal reflection fluorescence. *Annual Review of Biophysics and Bioengineering*, 13(1),247–268.

[10] Wadsworth, W.J., Percival, R.M., Bouwmans, G., Knight, J.C., Birks, T.A., Hedley, T.D., & Russell, P. St J. (2004). Very High Numerical Aperture Fibers.*IEEE Photonics Technology Letters*,16(3),843–845.

[11] Dragic, P.D., Cavillon, M., & Ballato, J. (2018). Materials for optical fiber lasers: A review.*Applied Physics Reviews*, 5(4), 041301.

[12] Kao, K. C. & Hockham, G.A.(1997). Dielectric-fibre surface waveguides for optical frequencies. *Elektron*, 14(5), 11–12.

[13] Peng, G.D., Ji, P., & Chu, P.L. (2002). Electro-optic polymer optical fibers and their device applications. *SPIE*, 4459, 101–117.

[14] Welker, D.J., Garvey,D.W., Breckon, C. D., & Kuzyk, M.G.(1999). Single-mode Electrooptic Polymer Optical Fiber. *Organic Thin Films for Photonic Applications*, SaC1.

[15] Welker, D.J., Tostenrude, J., Garvey, D.W., Canfield, B.K. & Kuzyk, M.G. (1998).Fabrication and characterization of single-mode electro-optic polymer optical fiber. *Optics Letters*, 23(23), 1826.

[16] Singer,K. D., Kuzyk,M. G., Holland, W. R., Sohn, J.E., Lalama,S.J., Comizzoli, R.B., Katz, H.E., & Schilling,M. L. (1998). Electro-optic phase modulation and optical second-harmonic generation in corona-poled polymer films. *Applied Physics Letters*, 53(19), 1800.

[17] Canfield, B.K., Kuzyk, M.G., & Welker, D.J. (1999). Nonlinear characterization of polymer electro-optic fiber. *In Organic Nonlinear Optical Materials*, 3796, 313-319. https://doi.org/10.1117/12.368289.

[18] Kuzyk, M.G., Garvey, D.W., Canfield, B.K., Vigil, S.R., Welker, D.J., Tostenrude, J., & Breckon, C. (1999). Characterization of single-mode polymer optical fiber and electrooptic fiber devices. *Chemical Physics*, 245(1-3), 327-340.

[19] Garvey, D.W. & Kuzyk, M.G. (1999). Nonlinear optics in polymer optical fibers. (1999). *In Organic Nonlinear Optical Materials*, https://doi.org/10.1117/12.368283, 3796, 13-20.

[20] Ali, Z., Rabiei, F., Rashidi, M.M., & Khodadadi, T. (2022). A fractional-order mathematical model for COVID-19 outbreak with the effect of symptomatic and asymptomatic transmissions. *The European Physical Journal Plus*, 137(3), 1-20.

[21] Delavari, H., Baleanu, D., & Sadati, J.(2012).Stability analysis of Caputo fractional-order nonlinear systems revisited. *Nonlinear Dynamics*, 67(4), 2433–2439.

[22] Du, M., Wang, Z. & Hu,H. (2013). Measuring memory with the order of fractional derivative. *Scientific Reports*, 3(1), 1–3.

[23] Xie, L., Shi, J., Yao, J., & Wan, D. (2022). Research on the Period-Doubling Bifurcation of Fractional-Order DCM Buck-Boost Converter Based on Predictor-Corrector Algorithm. *Mathematics*, 10(12), 1993.

[24] Baleanu, B., Guvenc, Z.B., & Machado,J.A.T. (2010). New Trends in Nanotechnology and Fractional Calculus Applications. *New Trends in Nanotechnology and Fractional Calculus Applications*, 10, 978-90, New York: Springer.

[25] Abro, K.A. (2021). Role of fractal–fractional derivative on ferromagnetic fluid via fractal Laplace transform: A first problem via fractal–fractional differential operator.*European Journal of Mechanics - B/Fluids*, 85, 76-81.

[26] Abro, K.A. & Atangana, A. (2020). Mathematical analysis of memristor through fractal-fractional differential operators: A numerical study.*Mathematical Methods in the Applied Sciences*, 43(10), 6378–6395.

[27] Podlubny, I. (1999). *Fractional differential equations: an introduction to fractional derivatives, fractional differential equations, to methods of their solution and some of their applications.* Academic Press, San Diego

[28] Odibat, Z.M., Shawagfeh, N.T. (2007). Generalized Taylor's formula. *Applied Mathematics and Computation*, 186(1), 286–293.

[29] Daşbaşı, B. (2023). Fractional order bacterial infection model with effects of anti-virulence drug and antibiotic. *Chaos, Solitons & Fractals* , 170, 113331.

[30] Deng, W., Li, C., & Guo, Q. (2007). Analysis of fractional differential equations with multi-orders. *Fractals*, 15(2), 173–182.

[31] Tavazoei, M., Asemani, M.H. (2020). Robust stability analysis of incommensurate fractional-order systems with time-varying interval uncertainties. *Journal of the Franklin Institute*, 357(18), 13800-13815.

[32] Daşbaşı, B. (2020). Stability analysis of the hiv model through incommensurate fractional-order nonlinear system. *Chaos, Solitons & Fractals*, 137(109870),

[33] Daşbaşı, B., & Daşbaşı, T. (2017). Mathematical analysis of Lengyel-Epstein chemical reaction model by fractional-order differential equation's system with multi-orders. *International Journal of Science and Engineering Investigations*, 6(70), 78-83.

[34] Li, H. L., Zhang, L., Hu, C., Jiang, Y. L., & Teng, Z. (2017). Dynamical analysis of a fractional-order predator-prey model incorporating a prey refuge. *Journal of Applied Mathematics and Computing*, 54, 435-449,

Büşra Ersoy *was born on March 8, 1997, in Kayseri. She took English preparatory education for one year in the 2015-2016 academic year. Then she received a BS degree from the Electrical and Electronics Engineering Department of Erciyes University, Kayseri in 2020. In 2021, she started her Master's Education in the Electronics Engineering Department at Kayseri University. She is currently working as a researcher assistant in the research project titled "Design, Fabrication, and Characterization of Meta-Lenses for Infrared and Visible Wavelengths" and has a Graduate Research Scholarship supported by the Scientific and Technological Research Council of Turkey (TUBİTAK-ARDEB-121E518).*

https://orcid.org/0000-0003-1383-3311

Bahatdin Daşbaş *received a BS degree in Mathematics from Ankara University in 2002, the MS degree in the field of applied statistic in Mathematics department from the Niğde University in 2005 and a Ph.D. degree in the field of applied mathematics in mathematics department from the Erciyes University in 2016. He also has the title of Associate Professor in Mathematics since 2021. He is still working as an associate professor at the Department of Basic Engineering Sciences, Faculty of Engineering, Architecture and Design, Kayseri University. His current research interests include fractional order differential equations, mathematical modeling, stability analysis, and artificial neural networks.*

https://orcid.org/0000-0001-8201-7495

Ekin Aslan *received the BS degree in 2004 from the Electronics Engineering Department of Erciyes University, MS degree in 2011 from the Electrical and Electronics Engineering of Mustafa Kemal University,* *and PhD degree in 2017 from the Electrical and Electronics Engineering Department of Erciyes University. Dr. Aslan was a recipient of the Doctoral Research Fellowship from the Scientific and Technological Research Council of Turkey (TUBITAK) (2214-A). She worked as an Assistant Professor in the Departments of Electrical and Electronics Engineering at Nuh Naci Yazgan University and Hatay Mustafa Kemal University. She is currently working as an Associate Professor in the Electrical and Electronics Engineering Department of Kayseri University. Her research interests include integrated plasmonic systems for bio-detection, vibrational spectroscopy, plasmonic metamaterials, computational and experimental electromagnetics, and nanophotonic devices.*

https://orcid.org/0000-0003-0933-7796

Appendix A

Matlab codes used for graphics are:

memory.m

```

function [yo] = memory(r, c, k)
temp = 0;
for j=1:k-1
temp = temp + c(j)*r(k-j);
end
yo = temp;
```

fiber_optic_function.m

```
function [T, Y] = fiber\_optic\_function(parameters, orders, TSim, Y0)
h = .04;
n = round(TSim/h);
q1 = orders(1); q2 = orders(2);  q3 = orders(3);
a\_1 = parameters,(1); b = parameters(2); r\_1 = parameters(3);
C = parameters(4); r\_2 = parameters (5); a\_2 = parameters(6);
n\_3 = parameters(7);
cp1 = 1; cp2 = 1; cp3 = 1;
for j = 1:n
c1(j) = (1-(1+q1)/j)*cp1;
c2(j) = (1-(1+q2)/j)*cp2;
c3(j) = (1-(1+q3)/j)*cp3;
cp1 = c1(j); cp2 = c2(j); cp3 = c3(j);
end

x(1) = Y0(1); y(1) = Y0(2); z(1) = Y0(3);

for i = 2:n
x(i) = (a\_1-b*x(i-1))*h$\mathrm{\wedge}$q1 - memory(x, c1, i);
y(i) = (r\_1*y(i-1)*(1-y(i-1)/C))*h$\mathrm{\wedge}$q2 -memory(y, c2, i);
z(i) = (r\_2*z(i-1)*(1-z(i-1)/y(i-1))-a\_2*x(i-1)+n\_3)*h$\mathrm{\wedge}$q3 - memory(z, c3, i);
end

for j = 1:n
Y(j,1) = x(j); Y(j,2) = y(j); Y(j,3) = z(j);
end

T = 0:h:TSim;
```

run.m

```
close all; clear all; clc;
A = 1:4000;
A = A';
```

```
[t, y] = fiber\_optic\_function ([10.5 1 .2 15 .25 .8 8], [1 1 1], 160, [16 12 9]);
figure; plot(A,y(:,1), A,y(:,2),A,y(:,3));
xlabel('{\textbackslash}bf Time', 'fontsize', 10); ylabel('{\textbackslash}bf v(t), n\_1(t) and n\_2(t)', 'fontsize', 10); grid;
legend('v(t)','n\_1(t)','n\_2(t)');
title('Stabilities of variables for derivative orders given by (1,1,1)');

[t, y] = fiber\_optic\_function ([10.5 1 .2 15 .25 .8 8], [.9 .9 .9], 160, [16 12 9]);
figure; plot(A,y(:,1), A,y(:,2),A,y(:,3));
xlabel('{\textbackslash}bf Time', 'fontsize', 10); ylabel('{\textbackslash}bf v(t), n\_1(t) and n\_2(t)', 'fontsize', 10); grid;
legend('v(t)','n\_1(t)','n\_2(t)');
title('Stabilities of variables for derivative orders given by (.9,.9,.9)');

[t, y] = fiber\_optic\_function ([10.5 1 .2 15 .25 .8 8], [.75 .75 .75], 160, [16 12 9]);
figure; plot(A,y(:,1), A,y(:,2),A,y(:,3));
xlabel('{\textbackslash}bf Time', 'fontsize', 10); ylabel('{\textbackslash}bf v(t), n\_1(t) and n\_2(t)', 'fontsize', 10); grid;
legend('v(t)','n\_1(t)','n\_2(t)');
title('Stabilities of variables for derivative orders given by (.75,.75,.75)');

[t, y] = fiber\_optic\_function ([10.5 1 .2 15 .25 .8 8], [.7 .8 .9], 160, [16 12 9]);
figure; plot(A,y(:,1), A,y(:,2),A,y(:,3));
xlabel('{\textbackslash}bf Time', 'fontsize', 10); ylabel('{\textbackslash}bf v(t), n\_1(t) and n\_2(t)', 'fontsize', 10); grid;
legend('v(t)','n\_1(t)','n\_2(t)');
title('Stabilities of variables for derivative orders given by (.7,.8,.9)');

[t, y] = fiber\_optic\_function ([10.5 1 .2 15 .25 .8 8], [.9 .8 .7], 160, [16 12 9]);
figure; plot(A,y(:,1), A,y(:,2),A,y(:,3));
xlabel('{\textbackslash}bf Time', 'fontsize', 10); ylabel('{\textbackslash}bf v(t), n\_1(t) and n\_2(t)', 'fontsize', 10); grid;
legend('v(t)','n\_1(t)','n\_2(t)');
title('Stabilities of variables for derivative orders given by (.9,.8,.7)');
```

An International Journal of Optimization and Control: Theories & Applications
ISSN:2146-0957 eISSN:2146-5703
Vol.14, No.1, pp.62-73 (2024)
http://doi.org/10.11121/ijocta.1424

RESEARCH ARTICLE

Numerical solution of coupled system of Emden-Fowler equations using artificial neural network technique

Ashish Kumar[a], Manoj Kumar[b*], Pranay Goswami[a]

[a] *School of Liberal Studies, Dr. B. R. Ambedkar University Delhi, Delhi, India*
[b] *Department of Applied Sciences and Humanities, Indira Gandhi Delhi Technical University for Women, Delhi, India*
ashish2.20@stu.aud.ac.in, manojkumar7281@gmail.com, pranay@aud.ac.in

ARTICLE INFO

Article History:
Received 12 July 2023
Accepted 27 November 2023
Available Online 10 January 2024

Keywords:
Coupled system of Emden-Fowler equations
Numerical method
Deep neural network technique

AMS Classification 2010:
34K37; 34K28

ABSTRACT

In this paper, a deep artificial neural network technique is proposed to solve the coupled system of Emden-Fowler equations. A vectorized form of algorithm is developed. Implementation and simulation of this technique is performed using Python code. This technique is implemented in various numerical examples, and simulations are conducted. We have shown graphically how accurately this method works. We have shown the comparison of numerical solution and exact solution using error tables. We have also conducted a comparative analysis of our solution with alternative methods, including the Bernstein collocation method and the Homotopy analysis method. The comparative results are presented in error tables. The efficiency and accuracy of this method are demonstrated by these graphs and tables.

1. Introduction

Differential equations are used to model natural phenomena in many fields of science, including biology, ecology, physics, engineering, chemistry, etc. Due to the vast applications of these differential equations in many branches of science([1], [2]), there is a great need to solve these kinds of equations. The Emden-Fowler equation is also an important differential equation in astrophysics and physics. It is also very difficult to solve this equation numerically due to the singularity behavior of the equation at the point $\zeta = 0$. This equation arises in the study of stellar structure [3], which involves the evolution of a star under the laws of physics. Stars' gravity balances the stars' core radiations. This balance is called hydrostatic equilibrium. The Emden-Fowler equation arises when this equilibrium state is modeled while studying the stellar structure. In 1870, Jonathan Lane [4] introduced the equation, and Jacob Emden [5] generalized it further. Lane - Emden equation is given as

$$\frac{d^2\omega}{d\zeta^2} + \frac{2}{\zeta}\frac{d\omega}{d\zeta} + \omega^n = 0, \tag{1}$$

where n is the polytropic index. Many astrophysicists were interested in the behavior of the solution of these equations under some initial conditions. Fowler studied the these equations during 1914-1931. The more general form of (1) is

$$\frac{d^2\omega}{d\zeta^2} + \frac{\vartheta}{\zeta}\frac{d\omega}{d\zeta} + \varphi(\omega) = \psi(\zeta), \tag{2}$$

where $\varphi(\omega)$ is a linear or non-linear function. Emden-Fowler equation is also used in chemical reactors, fluid mechanics, and gas dynamics.
There are many variants of Emden-Fowler equations including coupled system of Emden-Fowler equations that reads as follows-

$$\begin{aligned} \frac{d^2\omega_1}{d\zeta^2} + \frac{\vartheta_1}{\zeta}\frac{d\omega_1}{d\zeta} &= \varphi_1(\zeta, \omega_1, \omega_2), \\ \frac{d^2\omega_2}{d\zeta^2} + \frac{\vartheta_2}{\zeta}\frac{d\omega_2}{d\zeta} &= \varphi_2(\zeta, \omega_1, \omega_2), \end{aligned} \tag{3}$$

*Corresponding Author

where $\vartheta_1 > 0$, $\vartheta_2 > 0$ are real constants. φ_1 and φ_2 are nonlinear functions of ζ, ω_1 and ω_2.
The groundwork of artificial neural network(ANN) was started in 1943 when McCulloch and Pitts modeled a neuron as a switch that receives input from other neurons and, depending on total weighted input, is either activated or remains inactive. Thus, artificial neural networks are inspired by sensory processing of the brain. ANN can be created by simulating a network of model neurons in a computer. The structure comprises input layer, output layer, and hidden layers. Every layer contains neurons. By using an algorithm we can make the network learn to solve mathematical problems. A model neuron receives the input from other units, weighs each unit and add them up. If the total input is above a threshold we get the output.
When a structure has multiple hidden layers, deep neural networks (DNNs) are used. Deep neural networks have been proposed as a way to produce more predictive models. Combining a large number of layers endows the model with high prediction power.

2. Related work

Machine learning techniques such as deep neural networks have a wide range of applications such as speech recognition, image classification [6], computer vision tasks [7], machine translation, drug design, climate science, cybersecurity ([8], [9]). DNN is also very useful in automated driving. Automative researchers are able to detect stop signs, traffic lights, pedestrians that helps lower accidents. The deep layers in DNN capture more variances.
The main issues of deep neural networks are robustness, stability and adversarial perturbation which are discussed in ([10], [11], [12], [13]). The source of instability arises from the high depth of neural networks, where a "shattered gradient" effect was observed [14]. More advances in the applications of deep neural networks are presented in ([15], [16]).
Solving differential equations using optimization strategies has been very popular for quite some time in the form of least squares method ([17], [18]) and Galerkin methods [19]. These techniques are also used in neural networks. Nowadays researchers are using ANN to solve differential equations. ANN solutions are in closed-analytic form and are differentiable. Solving a differential equation was first described by Lagaris et al. [20]. Lee sen ten [21] solved ODEs with modified back propagation(mBP) with multilayer perception neural network (MPNN) as ANN technique. Craig Michoski et. al. [22] Solved PDEs using deep neural networks (DNNs) They discussed and analyzed the sod shocktube solution to the compressible Euler equations. Jiequen Han [23] also used deep learning to solve high-dimensional PDEs such as Black-Scholes equation, Allen-cahn equations, Bellman equation. Sabir et al. [24] solved fourth order Emden-Fowler equation using heuristic computing technique. Raja et al. [25] used Neuro-swarms intelligent computing techinque using kernel to solve Emden-Fowler equations. Sabir et al. [26] also discussed the applications of neural networks in COVID-19 model using the effects of lockdown. Fernandez [27] used a feedforward neural algorithm to solve linear ordinary differential equations using a limit activation function to construct a feedforward neural network. Fotiadis (1998) also solved ODEs and PDEs using ANN and compared the solution with a numerical method like the finite element method. Aarts and Ven Der (2001) [28] solved PDEs with boundary and initial conditions using neural networks. They used single hidden layers with multiple inputs and a single output. They tested their method on physics and geological problems. Sadogi Yazdi (2011) [29] implemented an ANN technique with kernel mean square algorithm to solve Ordinary differential equations. Asady and Nazarlue (2014) [30] solved the Fredholm integral equation using ANN with great precision. Nystorm (2018) [31] solved PDEs in complex geometries using deep feedforward artificial neural networks. Viana (2020) [32] introduced the recurrent neural networks to integrate ordinary differential equations. For more related works we can check Rackauckas [33], Wang Huan [34].

3. Neural network architecture and working

We are using vectorized algorithm (given in [35]) to solve the system of Emden-Fowler equations using deep neural networks (DNN).

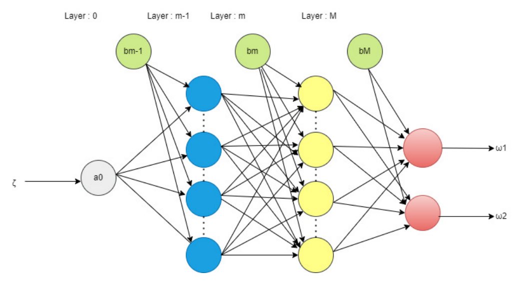

Figure 1. Deep ANN schematic diagram.

As indicated in Figure 1, the network has input layer containing one neuron as an independent variable for system of equations and n neurons in output layer. We form a matrix $T = \left[\zeta^1, ..., \zeta^r\right] \in R^{1\times r}$ using r sample points from domain and take $\mathrm{N} \in R^{n\times r}$ as output matrix. For example, $\mathrm{N}_\lambda(\zeta^\tau, Q_\lambda)$ is the λth output corresponding to τth point, where Q_λ is related to the weights and bias parameters. For each $\zeta \in [a, b]$ a trial solution, which is an extension of trial solution given in [35], is considered as

$$\widehat{\omega}_j(\zeta, Q_j) =$$

$$a_j + (\zeta - a)\mathrm{N}_j(\zeta, Q_j) + \frac{(\zeta - a)^2}{2!}\mathrm{N}_j(\zeta, Q_j) + ..., \quad (4)$$

where $j = 1, 2, ..., n$. This trial solution satisfies the initial conditions. The total cost function is

$$\mathrm{H} = \sum_{\tau=1}^{r}\sum_{j=1}^{n}\left(\frac{d^2\widehat{\omega}_j}{d\zeta^2} + \frac{\vartheta_j}{\zeta}\frac{d\widehat{\omega}_j}{d\zeta} - \varphi_j\right)^2, \quad (5)$$

converges to 0, $\varphi_j = \varphi_j(\zeta^\tau, \widehat{\omega}_j, Q_j)$.

Forward propagation

We represent $m-1$ and m layer node by s and j respectively. The value that goes into jth node,

$$u_j^m = \sum_{s=1}^{d} y_{js}^m a_s^{m-1} + b_s^m, \quad (6)$$

In the mth layer, the variable d represents the number of neurons. The equation (6) can be expressed in matrix form as follows:

$$u^m = Y^m a^{m-1} + b^m, \quad (7)$$

where Y^m contains all the weights and b^m is the bias. An appropriate activation function passes The values to the next hidden layer. For consistency, we select the identical activation function for all nodes within a layer. The values for the subsequent layer are as follows:

$$a^m = \pi^m(u^m) = \pi^m(Y^m a^{m-1} + b^m), \quad (8)$$

where π^m is activation function. For the r grid points, where $\tau = 1, 2, \ldots, r$, we proceed with the following steps. In the initial hidden layer,

$$u^{1(\tau)} = Y^1 z^\tau + b^1,$$
$$a^{1(\tau)} = \pi^1(u^{1(\tau)}),$$

at the second hidden layer,

$$u^{2(\tau)} = Y^2 a^{1(\tau)} + b^2,$$
$$a^{2(\tau)} = \pi^2(u^{2(\tau)}),$$

similarly the output layer,

$$u^{M(\tau)} = Y^M a^{M-1(\tau)} + b^M,$$
$$a^{M(\tau)} = \pi^M(u^{M(\tau)}).$$

So we have the matrix form as

$$U^1 = Y^1 Z + b^1,$$
$$A^1 = \pi^1(Y^1),$$

for second layer

$$U^2 = Y^2 A^1 + b^2,$$
$$A^2 = \pi^2(Y^2),$$

and so on. The output layer

$$U^M = Y^M A^{M-1} + b^M,$$
$$A^M = \pi^M(Y^M),$$

The algorithm

Step 1 : Take r distinct points and form a vector $T = \left[\zeta^1, ..., \zeta^r\right] \in R^{1\times r}$.

Step 2 : We define the structure of neural networks such as number of layers M, input layer having one unit, $M-2$ hidden layers with g^m units, and an output layer with n units, where n corresponds to the number of unknowns in the system.

Step 3 : Initialize the parameters such as weights and bias, Q_j, $j = 1, 2, ..n$, where n denotes number of neurons. *Step 4 :* Use forward propagation

- Assign $A^0 = Z$ in input layer.
- In hidden layers
  $$U^m = Y^m A^{m-1} + b^m,$$
  $$A^m = \pi^m(Y^m),$$
  where $m = 1, ...M-1$, π^m is the activation function for mth hidden layer.
- For output layer,
  $$U^M = Y^M A^{M-1} + b^M,$$
  $$A^M = \pi^M(Y^M),$$
- We use trial solution of order four in (4). We need to initialize sets of parameters to find an unknown function.

Step 5 : Use (5) to calculate the cost, gradients, and learning parameters. Apply the automatic differentiation [36].

Step 6 : Utilize gradient descent or any other optimization method to update the parameters. We update the parameters according to following rule

$$Q_j^{r+1} = Q_j^r - \varepsilon\nabla\mathrm{H}(Q_j^r),$$

where ε is learning rate and r denotes iteration.

There are many advanced methods we can choose instead of the gradient descent method such as the moment method, which is a modification of the gradient method. The updating role is

$$\begin{aligned} Q_j^{r+1} &= Q_j^r + L_j^{r+1}, \\ L_j^{r+1} &= \gamma L_j^r - \varepsilon \nabla \mathrm{H}(Q^r), \end{aligned}$$

where γ is a coefficient between 0 and 1, we call it momentum. L_j is a velocity parameter starting from 0 corresponding to each unknown.
Another method is Nesterov accelerated gradient obtained from the moment method with update rule

$$\begin{aligned} Q_j^{r+1} &= Q_j^r + L_j^{r+1}, \\ L_j^{r+1} &= \gamma L_j^r - \varepsilon \nabla \mathrm{H}(Q^r + \gamma L_j^r). \end{aligned}$$

The adaptive gradient method is

$$\begin{aligned} L_j^r &= L_j^{r-1} + (\nabla \mathrm{H}(Q^r))^2, \\ Q_j^{r+1} &= Q_j^r - \frac{\varepsilon}{\sqrt{L_j^r + c}} \nabla \mathrm{H}(Q^r), \end{aligned}$$

where c is a minimal number to avoid division by 0. Clearly, the learning rate is decaying because of it.
The update rule for root mean square propagation is

$$\begin{aligned} L_j^r &= \rho L_j^{r-1} + (1-\rho)(\nabla \mathrm{H}(Q^r))^2, \\ Q_j^{r+1} &= Q_j^r - \frac{\varepsilon}{\sqrt{L_j^r + c}} \nabla \mathrm{H}(Q^r), \end{aligned}$$

where $\rho \in (0,1)$ is forgetting factor. Another method is the Adam adaptive method which is a combination of the last two methods with updating rule

$$\begin{aligned} F_j^r &= \rho_1 F_j^{r-1} + (1-\rho_1)\nabla \mathrm{H}(Q^r), \\ L_j^r &= \rho_2 L_j^{r-1} + (1-\rho_2)(\nabla \mathrm{H}(Q^r))^2, \\ \widehat{F_j^r} &= \frac{F_r}{1-{\rho_1}^r}, \widehat{L_j^r} = \frac{L_r}{1-{\rho_2}^r}, \\ Q_j^{r+1} &= Q_j^r - \frac{\varepsilon}{\sqrt{\widehat{L_j^r} + c}} \widehat{F_j^r}, \end{aligned}$$

where ρ_1 and ρ_2, both belonging to the interval $[0,1)$, represent the rates of decay for moment estimation. Initially, we set the parameters F_r and L_r to 0.

4. Numerical illustrations

This section presents the implementation of an algorithm designed to solve known systems of second-order nonlinear differential equations. The initial step involves experimenting to determine the appropriate number of layers and neurons within the layer. The algorithm's accuracy is then validated by comparing the analytic and numerical solutions obtained using conventional methods. To achieve this objective, we simulate the problems related to systems of second-order nonlinear differential equations as follows:

Example 1. *Let us consider a problem of Emden-Fowler equations documented in [37].*

$$\begin{aligned} \frac{d^2\omega_1}{d\zeta^2} + \frac{3}{\zeta}\frac{d\omega_1}{d\zeta} &= -(3+\omega_2^2)\omega_1^5, \\ \frac{d^2\omega_2}{d\zeta^2} + \frac{4}{\zeta}\frac{d\omega_2}{d\zeta} &= (4\omega_1^{-2}+1)\omega_2^{-3}, \end{aligned} \tag{9}$$

with the initial conditions (ICs)

$$\omega_1(0) = \omega_2(0) = 1 \text{ and } \omega_1'(0) = \omega_2'(0) = 0.$$

The exact solutions to the problem are $\omega_1(\zeta) = \frac{1}{\sqrt{1+\zeta^2}}$ *and* $\omega_2(\zeta) = \sqrt{1+\zeta^2}$.

4.1. Investigating the network via experimentation for solving (9)

We performed an experiment to determine how many neurons are in a layer. We examined how the number of hidden layers, the number of neurons, and the number of iterations affected the cost function. We have taken the trial solution up to $n = 4$. During the simulation, we varied the number of hidden neurons, specifically using sizes $h = 4$, 13, 27, 60, 90, and 180. We then compared the convergence of the cost function across these different sizes by plotting it against the number of iterations. In addition, we recorded the corresponding cost values and calculation times for each neuron size at the end of the iterations. It is worth noting that all other parameters remained constant throughout the experiment.

The findings illustrated in Figures 2(a)-(c) demonstrate that achieving the necessary level of accuracy is feasible with only one neuron in the hidden layer. However, many iterations are required when working with a smaller number of neurons, which can pose computational challenges. Increasing the number of neurons can improve the model's performance, but it is not always necessary. For example, when comparing a hidden layer with $h = 60$ neurons to one with $h = 180$ neurons, both achieve similar accuracy, but the former requires less computational time.
In our next experiment, we investigated the impact of the number of hidden layers on the model's performance. Previous research by Saeed et al. (2023) [38] demonstrated that to solve nonlinear singular fractional differential equations, increasing the number of hidden layers results in improved performance in terms of error. Similarly, Panghal and Kumar (2021) [39] observed improved accuracy when simulating a delay and

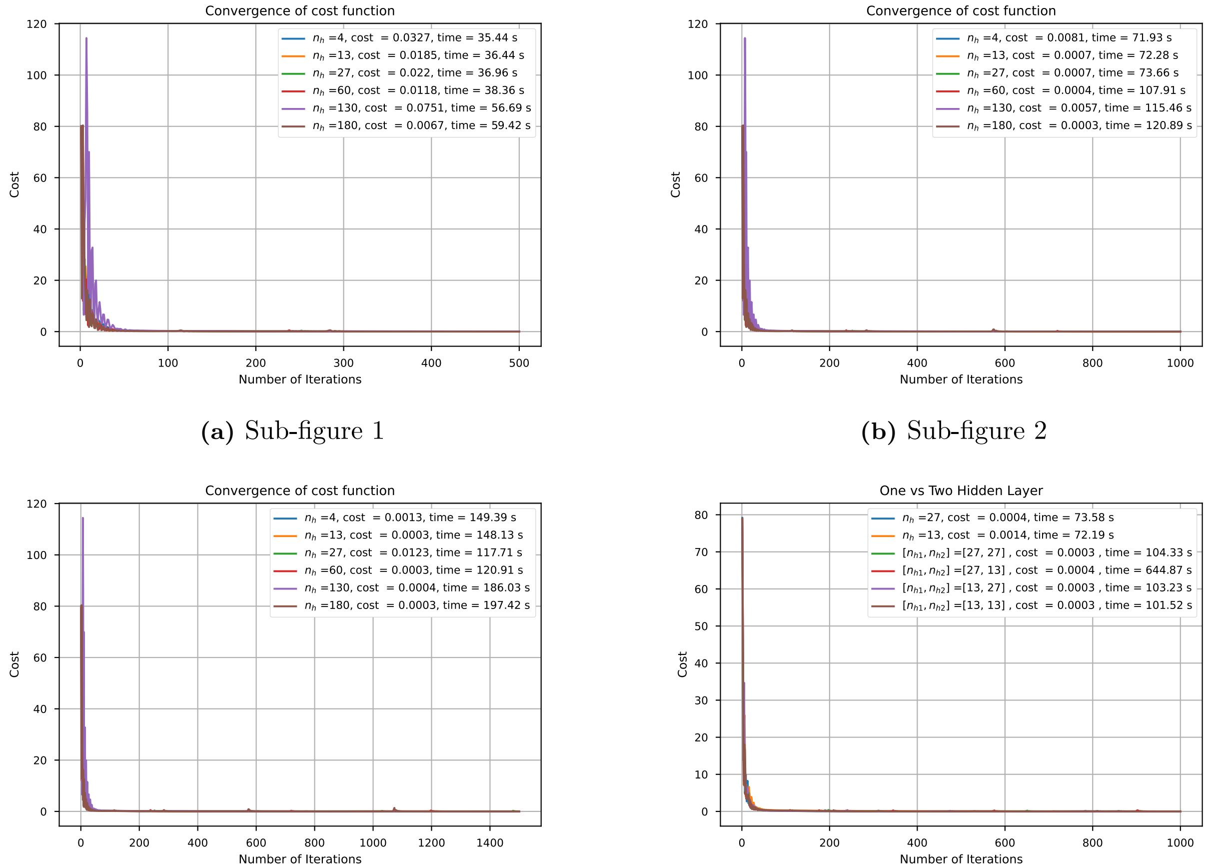

(a) Sub-figure 1

(b) Sub-figure 2

(c) Sub-figure 2

(d) Sub-figure 2

Figure 2. Comparison of loss functions for ANN models with one vs two hidden layers.

first-order differential equation system with multiple hidden layers. However, Dufera (2021) [35] denied more than one hidden layer does not lead to better performance in his experiments when solving first-order a system of differential equations. We conducted numerous experiments to evaluate the performance of neural networks with one hidden layer against those with two hidden layers. The experiments involved varying the number of neurons in the hidden layers. All other parameters and activation functions, such as Tanh, remained the same in all experiments. The results, depicted in Figure 2(d), show that for a system of 2nd order differential equations (9), adding more hidden layers with an appropriate number of neurons leads to improved performance.

4.2. Numerical solutions for solving (9)

We opted for two hidden layers comprising 13 and 27 neurons (tuning in the plus-minus range was not expected to have a significant impact). We set $m = 11$ for this experiment and sampled uniform grid points within the given interval. ANN and analytic solutions are presented in Figure 3. Table 1 contains the numerical values, and Table 2 shows the error resulting from our approach.

4.3. Advantages of using ANN over a large number of data points for solving (9)

We operate uniform grid points of size (m=6, 11, 21, 55, 100) over the domain [0, 2] and [0, 3] to calculate solutions of the ODEs system using the ANN method. As shown by the mean absolute error (MAE) in Table 3, one major advantage of ANN techniques is that they maintain solution accuracy compared to smaller or larger grid points.

Similarly, experiments have been organized for the problems (10)-(13). Using this architecture, we compared the numerical and exact solution in Tables (4)-(11) for each example. We have also compared numerical and exact solution graphically with their error plots in Figure 4 and Figure 5.

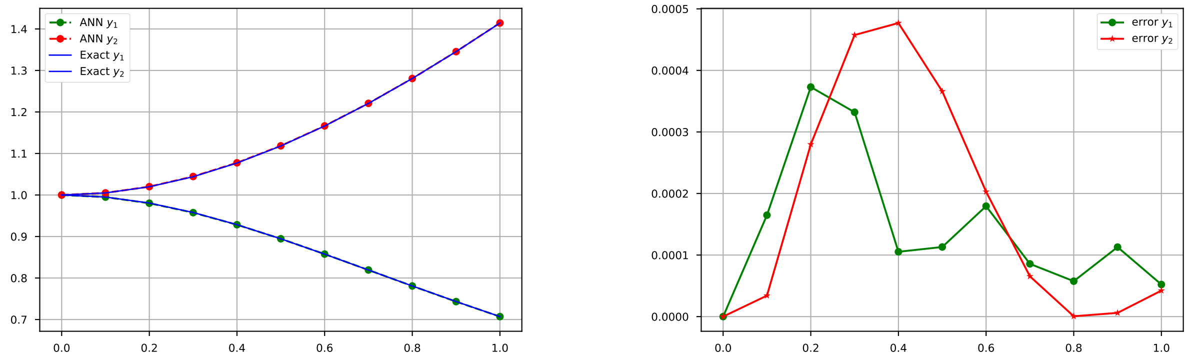

Figure 3. Comparison of ANN and exact solutions for system (9) with error plot.

Table 1. ANN and analytical solutions for system (9).

Grid point	ANN ω_1	Analytic ω_1	ANN ω_2	Analytic ω_2	BCM ω_1 [37]	BCM ω_2 [37]
0.0	1.000000	1.000000	1.000000	1.000000	1.000000	1.000000
0.1	0.994872	0.995037	1.005022	1.004988	0.996045	1.005800
0.2	0.980208	0.980581	1.020084	1.019804	0.981491	1.020560
0.3	0.957494	0.957826	1.044488	1.044031	0.958620	1.044698
0.4	0.928371	0.928477	1.077510	1.077033	0.929146	1.077590
0.5	0.894540	0.894427	1.118400	1.118034	0.894959	1.118473
0.6	0.857672	0.857493	1.166393	1.166190	0.857883	1.166515
0.7	0.819318	0.819232	1.220721	1.220656	0.819498	1.220874
0.8	0.780811	0.780869	1.280624	1.280625	0.781042	1.280750
0.9	0.743181	0.743294	1.345368	1.345362	0.743387	1.345412
1.0	0.707055	0.707107	1.414256	1.414214	0.707106	1.414213

Table 2. Computing the absolute difference between ANN and exact solutions for system (9).

Grid point	error ω_1	error ω_2
0.0	0.000000	0.000000
0.1	1.65e-04	3.407319e-05
0.2	3.73e-04	2.797772e-04
0.3	3.32e-04	4.574576e-04
0.4	1.05e-04	4.769526e-04
0.5	1.13e-04	3.659818e-04
0.6	1.79e-04	2.029116e-04
0.7	8.6e-05	6.545180e-05
0.8	5.8e-05	5.426605e-07
0.9	1.13e-004	6.053325e-06
1.0	5.2e-05	4.223276e-05

Example 2. *Let us consider a problem of Emden-Fowler equations documented in [40].*

$$\begin{aligned} \frac{d^2\omega_1}{d\zeta^2} + \frac{2}{\zeta}\frac{d\omega_1}{d\zeta} &= -6(e^{\frac{\omega_2}{3}} + 4)e^{\frac{2\omega_1}{3}}, \\ \frac{d^2\omega_2}{d\zeta^2} + \frac{2}{\zeta}\frac{d\omega_2}{d\zeta} &= 6(e^{\frac{-\omega_1}{3}} + 4)e^{\frac{-2\omega_2}{3}}, \end{aligned} \tag{10}$$

with ICs

$$\omega_1(0) = -3\log(2), \omega_2(0) = 3\log(2), \omega_1'(0) = \omega_2'(0) = 0.$$

The exact solutions to the problem are $\omega_1(\zeta) = -3\log(2+\zeta^2)$ *and* $\omega_2(\zeta) = 3\log(2+\zeta^2)$.

Example 3. *Let us consider a problem of Emden-Fowler equations documented in [40].*

$$\begin{aligned} \frac{d^2\omega_1}{d\zeta^2} + \frac{5}{\zeta}\frac{d\omega_1}{d\zeta} &= -8e^{\omega_1} - 16e^{\frac{-2\omega_2}{2}}, \\ \frac{d^2\omega_2}{d\zeta^2} + \frac{3}{\zeta}\frac{d\omega_2}{d\zeta} &= 8e^{-\omega_2} + 8e^{\frac{\omega_1}{2}}, \end{aligned} \tag{11}$$

with ICs

$$\omega_1(0) = \omega_2(0) = 0, \omega_1'(0) = \omega_2'(0) = 0.$$

The exact solutions to the problem are $\omega_1(\zeta) = -2\log(1+\zeta^2)$ *and* $\omega_2(\zeta) = 2\log(1+\zeta^2)$.

Table 3. MAE for different grid points over intervals.

End points	$t \in [0, 2]$		$t \in [0, 2]$	
Grid point	mae ω_1	mae ω_2	mae ω_1	mae ω_2
6	0.050588	0.051056	0.426025	0.631669
11	0.044180	0.059593	0.405198	0.763566
21	0.045351	0.032434	0.455094	0.323775
55	0.068090	0.065440	0.803243	0.848116
100	0.051830	0.031469	0.511720	0.320044

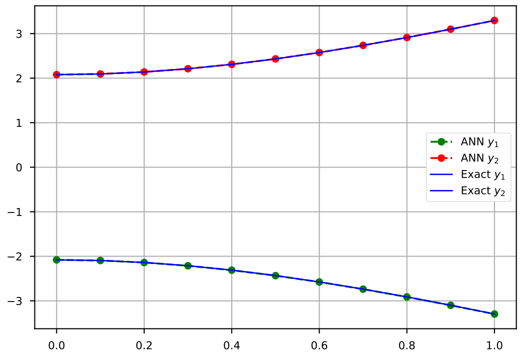

(a) Comparison of ANN and exact of system (10)

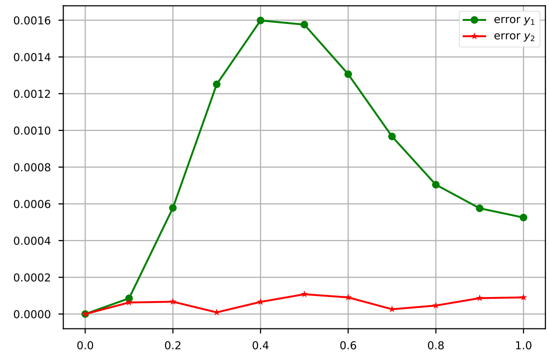

(b) Error plot of system (10)

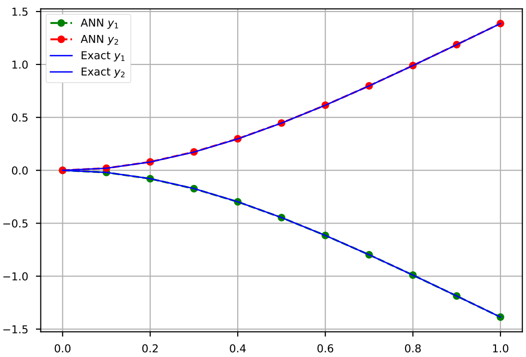

(c) Comparison of ANN and exact of system (11)

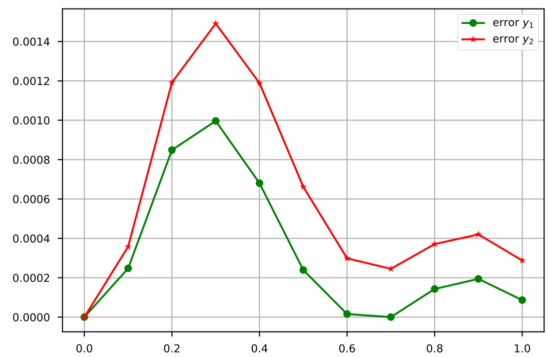

(d) Error plot of system (11)

Figure 4. Comparison of ANN and Exact Solutions of Examples with Error Plot.

Example 4. *Let us consider a problem of Emden-Fowler equations documented in [41].*

$$\begin{aligned} \frac{d^2\omega_1}{d\zeta^2} + \frac{8}{\zeta}\frac{d\omega_1}{d\zeta} &= 4\omega_1 \log(\omega_2) - 18\omega_1, \\ \frac{d^2\omega_2}{d\zeta^2} + \frac{4}{\zeta}\frac{d\omega_2}{d\zeta} &= 10\omega_2 - 4\omega_2 \log(\omega_1), \end{aligned} \tag{12}$$

with ICs

$$\omega_1(0) = \omega_2(0) = 1, \omega_1^{'}(0) = \omega_2^{'}(0) = 0.$$

The exact solutions to the problem are $\omega_1(\zeta) = e^{-\zeta^2}$ *and* $\omega_2(\zeta) = e^{\zeta^2}$.

Example 5. *Let us consider a problem of Emden-Fowler equations documented in [42].*

$$\begin{aligned} \frac{d^2\omega_1}{d\zeta^2} + \frac{1}{\zeta}\frac{d\omega_1}{d\zeta} &= (4\zeta^2 + 5)\omega_1 - \omega_1^2\omega_2, \\ \frac{d^2\omega_2}{d\zeta^2} + \frac{2}{\zeta}\frac{d\omega_2}{d\zeta} &= (4\zeta^2 - 5)\omega_2 - \omega_1\omega_2^2, \end{aligned} \tag{13}$$

with ICs

$$\omega_1(0) = \omega_2(0) = 1, \omega_1^{'}(0) = \omega_2^{'}(0) = 0.$$

The exact solutions to the problem are $\omega_1(\zeta) = e^{\zeta^2}$ *and* $\omega_2(\zeta) = e^{-\zeta^2}$.

Table 4. ANN and analytical solutions for system (10).

Grid point	ANN ω_1	Analytic ω_1	ANN ω_2	Analytic ω_2	HAM ω_1 [37]	ADM ω_1 [37]	HAM ω_2 [37]	ADM ω_2 [37]
0.0	-2.079442	-2.079442	2.079442	2.079442				
0.1	-2.094319	-2.094404	2.094467	2.094404	-2.103387	-2.138529	2.103387	2.138529
0.2	-2.139427	-2.138849	2.138916	2.138849	-2.147076	-2.180143	2.147076	2.180143
0.3	-2.212743	-2.211492	2.211501	2.211492	-2.218576	-2.248419	2.218576	2.248419
0.4	-2.311923	-2.310325	2.310259	2.310325	-2.316029	-2.341807	2.316029	2.341807
0.5	-2.434367	-2.432791	2.432683	2.432791	-2.437034	-2.458259	2.437034	2.458259
0.6	-2.577291	-2.575985	2.575894	2.575985	-2.578826	-2.595353	2.578826	2.595353
0.7	-2.737815	-2.736848	2.736822	2.736848	-2.738459	-2.750419	2.738459	2.750419
0.8	-2.913041	-2.912337	2.912383	2.912337	-2.912983	-2.920675	2.912983	2.920675
0.9	-3.100129	-3.099553	3.099640	3.099553	-3.099603	-3.103358	3.099603	3.103358
1.0	-3.296362	-3.295837	3.295927	3.295837	-3.295836	-3.295836	3.295836	3.295836

Table 5. Computing the absolute difference between ANN and exact solutions for system (10).

Grid point	error ω_1	error ω_2
0.0	0.0000	0.0000
0.1	8.6e-05	6.3e-05
0.2	5.78e-04	6.7e-05
0.3	1.251e-03	9e-06
0.4	1.599e-03	6.6e-05
0.5	1.576e-03	1.08e-04
0.6	1.306e-03	9.1e-05
0.7	9.67e-04	2.6e-05
0.8	7.04e-04	4.6e-05
0.9	5.76e-04	8.7e-05
1.0	5.25e-04	9.1e-05

Table 6. Computing the absolute difference between ANN and exact solutions for system (11).

Grid point	error y_1	error y_2
0.0	0.00000	0.00000
0.1	2.475294e-04	3.58e-04
0.2	8.486477e-04	1.192e-03
0.3	9.964365e-04	1.491e-03
0.4	6.801929e-04	1.189e-03
0.5	2.392059e-04	6.62e-04
0.6	1.564534e-05	2.99e-04
0.7	1.703470e-07	2.45e-04
0.8	1.429000e-04	3.71e-04
0.9	1.941502e-04	4.20e-04
1.0	8.640381e-05	2.87e-04

Table 7. Computing the absolute difference between ANN and exact solutions for system (12).

Grid point	error ω_1	error ω_2
0.0	0.000000	0.000000
0.1	1.3e-05	1.72e-04
0.2	2.51e-04	9.3e-05
0.3	4.09e-04	1.0e-04
0.4	4.04e-04	8.4e-05
0.5	2.76e-04	8.1e-05
0.6	1.09e-04	9.9e-05
0.7	1.10e-05	6.2e-05
0.8	3.50e-05	9.0e-05
0.9	3.0e-05	6.8e-05
1.0	1.07e-04	5.0e-05

5. Conclusions and future directions

In this paper, we used a vectorized algorithm that employs the ANN method for solving systems of ordinary differential equations (ODEs). We have compared the numerical and exact solution. Results show the stability between target and predicted results, this validates the model. Through various experiments with Python code and accompanying graphical simulations, we gained insight into the nature of the model architecture.

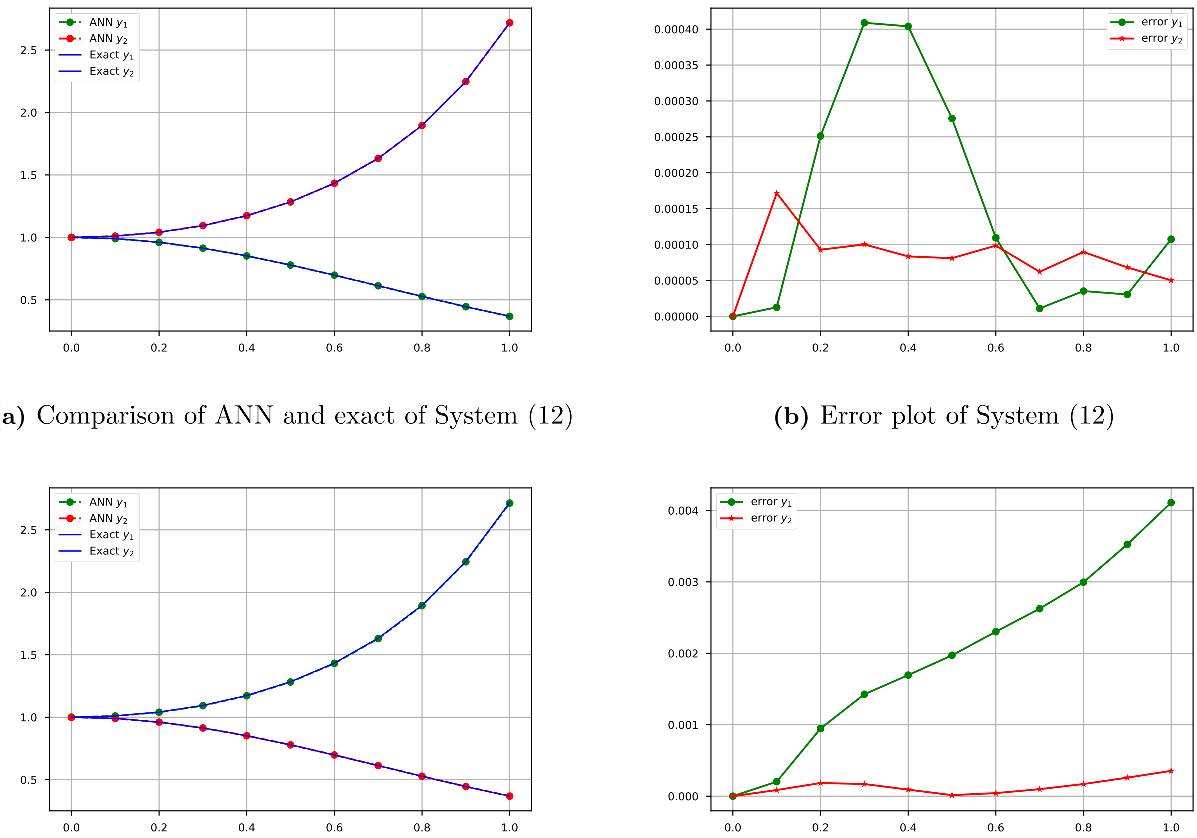

(a) Comparison of ANN and exact of System (12)

(b) Error plot of System (12)

(c) Comparison of ANN and exact of system (13)

(d) Error plot of system (13)

Figure 5. Comparison of ANN and exact solutions of examples with error plot.

Table 8. ANN and analytical solutions for system (11).

Grid point	ANN ω_1	Analytic ω_1	ANN ω_2	Analytic ω_2	HAM ω_1 [40]	HAM ω_2 [40]
0.0	0.000000	-0.000000	0.000000	0.000000		
0.1	-0.020148	-0.019901	0.020259	0.019901	-0.037713	0.054825
0.2	-0.079290	-0.078441	0.079633	0.078441	-0.093487	0.109631
0.3	-0.173352	-0.172355	0.173847	0.172355	-0.183502	0.198153
0.4	-0.297520	-0.296840	0.298029	0.296840	-0.303739	0.316521
0.5	-0.446526	-0.446287	0.446949	0.446287	-0.449283	0.459979
0.6	-0.614954	-0.614969	0.615268	0.614969	-0.614869	0.623398
0.7	-0.797552	-0.797552	0.797797	0.797552	-0.795395	0.801766
0.8	-0.989535	-0.989392	0.989763	0.989392	-0.986339	0.990600
0.9	-1.186848	-1.186654	1.187074	1.186654	-1.184086	1.186262
1.0	-1.386381	-1.386294	1.386582	1.386294	-1.386294	1.386294

Specifically, we found that for specific problems, even a single neuron in the hidden layer can achieve the necessary accuracy. In contrast, more significant numbers of neurons provide greater precision at the cost of increased parameter learning iterations. However, we caution against arbitrary increases in neuron size and recommend selecting an optimal size based on the underlying problem.

This study suggests the possibility of developing neural software that automatically adjusts the number of hidden layers and neurons based on the problem. Future research should focus on conducting additional analytical investigations to enhance the theoretical underpinnings of DNNs

Table 9. ANN and analytical solutions for system (12).

Grid point	ANN ω_1	Analytic ω_1	ANN ω_2	Analytic ω_2
0.0	1.000000	1.000000	1.000000	1.000000
0.1	0.990037	0.990050	1.009879	1.010050
0.2	0.960538	0.960789	1.040718	1.040811
0.3	0.913522	0.913931	1.094274	1.094174
0.4	0.851740	0.852144	1.173594	1.173511
0.5	0.778525	0.778801	1.283944	1.284025
0.6	0.697567	0.697676	1.433231	1.433329
0.7	0.612637	0.612626	1.632378	1.632316
0.8	0.527328	0.527292	1.896571	1.896481
0.9	0.444828	0.444858	2.247840	2.247908
1.0	0.367772	0.367879	2.718332	2.718282

Table 10. ANN and analytical solutions for system (13).

Grid point	ANN ω_1	Analytic ω_1	ANN ω_2	Analytic ω_2
0.0	1.000000	1.000000	1.000000	1.000000
0.1	1.009847	1.010050	0.989964	0.990050
0.2	1.039864	1.040811	0.960605	0.960789
0.3	1.092748	1.094174	0.913761	0.913931
0.4	1.171816	1.173511	0.852052	0.852144
0.5	1.282053	1.284025	0.778786	0.778801
0.6	1.431027	1.433329	0.697719	0.697676
0.7	1.629692	1.632316	0.612724	0.612626
0.8	1.893485	1.896481	0.527462	0.527292
0.9	2.244383	2.247908	0.445117	0.444858
1.0	2.714172	2.718282	0.368234	0.367879

Table 11. Computing the absolute difference between ANN and exact solutions for system (13).

Grid point	error ω_1	error ω_2
0.0	0.000000	0.000000
0.1	2.03e-04	8.6e-05
0.2	9.47e-04	1.84e-04
0.3	1.427e-03	1.70e-04
0.4	1.695e-03	9.2e-05
0.5	1.972e-03	1.5e-05
0.6	2.302e-03	4.3e-05
0.7	2.624e-03	9.8e-05
0.8	2.995e-03	1.70e-04
0.9	3.525e-03	2.59e-04
1.0	4.110e-03	3.54e-04

for solving systems of ODEs, encompassing areas such as delay differential equations and fractional differential equations. Such investigations would involve assessing the consistency, convergence, and suitability of DNNs in the context of solving systems of ODEs.

References

[1] Braun, M., Golubitsky, M. (1983). *Differential Equations and Their Applications* (Vol. 2). New York: Springer-Verlag.

[2] Simmons, G. F. (2016). *Differential Equations with Applications and Historical Notes.* CRC Press.

[3] Chandrasekhar, S., Chandrasekhar, S. (1957). *An Introduction to the Study of Stellar Structure* (Vol. 2). Courier Corporation.

[4] Lane, H. J. (1870). On the theoretical temperature of the sun, under the hypothesis of a gaseous mass maintaining its volume by its internal heat, and depending on the laws of gases as known to terrestrial experiment. *American Journal of Science*, 2(148), 57-74.

[5] Fowler, R. H. (1914). Some results on the form near infinity of real continuous solutions of a certain type of second order differential equation. *Proceedings of the London Mathematical Society*, 2(1), 341-371.

[6] Huang, J. T., Li, J., Gong, Y. (2015, April). An analysis of convolutional neural networks for speech recognition. *In 2015 IEEE International Conference on Acoustics, Speech and Signal Processing (ICASSP)* (pp. 4989-4993). IEEE.

[7] Seifert, C., Aamir, A., Balagopalan, A., Jain, D., Sharma, A., Grottel, S., Gumhold, S. (2017). Visualizations of deep neural networks in computer vision: A survey. *Transparent Data Mining for Big and Small Data*, 123-144.

[8] Dixit, P., Silakari, S. (2021). Deep learning algorithms for cybersecurity applications: A technological and status review. *Computer Science Review*, 39, 100317.

[9] Vigneswaran, R. K., Vinayakumar, R., Soman, K. P., Poornachandran, P. (2018, July). Evaluating shallow and deep neural networks for network intrusion detection systems in cyber security. *In 2018 9th International Conference on Computing, Communication and Networking Technologies (ICCCNT)* (pp. 1-6). IEEE.

[10] Szegedy, C., Zaremba, W., Sutskever, I., Bruna, J., Erhan, D., Goodfellow, I., Fergus, R. (2013). Intriguing properties of neural networks. *arXiv preprint arXiv*:1312.6199.

[11] Malladi, S., Sharapov, I. (2018). FastNorm: improving numerical stability of deep network training with efficient normalization.

[12] Zheng, Z., Hong, P. (2018). Robust detection of adversarial attacks by modeling the intrinsic properties of deep neural networks. *Advances in Neural Information Processing Systems*, 31.

[13] Haber, E., Ruthotto, L. (2017). Stable architectures for deep neural networks. *Inverse Problems,* 34(1), 014004.

[14] Balduzzi, D., Frean, M., Leary, L., Lewis, J. P., Ma, K. W. D., McWilliams, B. (2017, July). The shattered gradients problem: If resnets are the answer, then what is the question?. *In International Conference on Machine Learning* (pp. 342-350). PMLR.

[15] Liu, W., Wang, Z., Liu, X., Zeng, N., Liu, Y., Alsaadi, F. E. (2017). A survey of deep neural network architectures and their applications. *Neurocomputing,* 234, 11-26.

[16] Samek, W., Montavon, G., Lapuschkin, S., Anders, C. J., Müller, K. R. (2021). Explaining deep neural networks and beyond: A review of methods and applications. *Proceedings of the IEEE,* 109(3), 247-278.

[17] Björck, A. (1990) Least squares methods. *Handbook of Numerical Analysis*, Edited by P.G. Ciarlet and J.L. Lions, Volume 1, 465–652.

[18] Levenberg, K. (1944). A method for the solution of certain non-linear problems in least squares. *Quarterly of applied mathematics,* 2(2), 164-168.

[19] Fletcher, C. A., Fletcher, C. A. J. (1984). *Computational Galerkin Methods.* Springer Berlin Heidelberg, pp. 72-85

[20] Lagaris, I. E., Likas, A., Fotiadis, D. I. (1998). Artificial neural networks for solving ordinary and partial differential equations. *IEEE Transactions on Neural Networks,* 9(5), 987-1000.

[21] Tan, L. S., Zainuddin, Z., Ong, P. (2018, June). Solving ordinary differential equations using neural networks. *In AIP Conference Proceedings* (Vol. 1974, No. 1). AIP Publishing.

[22] Michoski, C., Milosavljević, M., Oliver, T., Hatch, D. R. (2020). Solving differential equations using deep neural networks. *Neurocomputing,* 399, 193-212.

[23] Han, J., Jentzen, A., E, W. (2018). Solving high-dimensional partial differential equations using deep learning. *Proceedings of the National Academy of Sciences,* 115(34), 8505-8510.

[24] Sabir, Z., Saoud, S., Raja, M. A. Z., Wahab, H. A., Arbi, A. (2020). Heuristic computing technique for numerical solutions of nonlinear fourth order Emden–Fowler equation. *Mathematics and Computers in Simulation,* 178, 534-548.

[25] Sabir, Z., Raja, M. A. Z., Arbi, A., Altamirano, G. C., Cao, J. (2021). Neuro-swarms intelligent computing using Gudermannian kernel for solving a class of second order Lane-Emden singular nonlinear model. *AIMS Mathematics*, 6(3), 2468-2485.

[26] Sabir, Z., Raja, M. A. Z., Alhazmi, S. E., Gupta, M., Arbi, A., Baba, I. A. (2022). Applications of artificial neural network to solve the nonlinear COVID-19 mathematical model based on the dynamics of SIQ. *Journal of Taibah University for Science,* 16(1), 874-884.

[27] Meade Jr, A. J., Fernandez, A. A. (1994). Solution of nonlinear ordinary differential equations by feedforward neural networks. *Mathematical and Computer Modelling,* 20(9), 19-44.

[28] Aarts, L. P., Van Der Veer, P. (2001). Neural network method for solving partial differential equations. *Neural Processing Letters,* 14, 261-271.

[29] Yazdi, H. S., Pakdaman, M., Modaghegh, H. (2011). Unsupervised kernel least mean square

algorithm for solving ordinary differential equations. *Neurocomputing,* 74(12-13), 2062-2071.

[30] Asady, B., Hakimzadegan, F., Nazarlue, R. (2014). Utilizing artificial neural network approach for solving two-dimensional integral equations. *Mathematical Sciences,* 8, 1-9.

[31] Berg, J., Nyström, K. (2018). A unified deep artificial neural network approach to partial differential equations in complex geometries. *Neurocomputing,* 317, 28-41.

[32] Nascimento, R. G., Viana, F. A. (2020). Cumulative damage modeling with recurrent neural networks. *AIAA Journal,* 58(12), 5459-5471.

[33] Innes, M., Edelman, A., Fischer, K., Rackauckas, C., Saba, E., Shah, V. B., Tebbutt, W. (2019). A differentiable programming system to bridge machine learning and scientific computing. *arXiv preprint arXiv:1907.07587.*

[34] Wang, H., Qin, C., Bai, Y., Zhang, Y., Fu, Y. (2021). Recent advances on neural network pruning at initialization. *arXiv preprint arXiv:2103.06460.*

[35] Dufera, T. T. (2021). Deep neural network for system of ordinary differential equations: Vectorized algorithm and simulation. *Machine Learning with Applications,* 5, 100058.

[36] Baydin, A. G., Pearlmutter, B. A., Radul, A. A., Siskind, J. M. (2018). Automatic differentiation in machine learning: a survey. *Journal of Marchine Learning Research,* 18, 1-43.

[37] Shahni, J., Singh, R. (2021). Numerical solution of system of Emden-Fowler type equations by Bernstein collocation method. *Journal of Mathematical Chemistry,* 59(4), 1117-1138.

[38] Althubiti, S., Kumar, M., Goswami, P., Kumar, K. (2023). Artificial neural network for solving the nonlinear singular fractional differential equations. *Applied Mathematics in Science and Engineering,* 31(1), 2187389.

[39] Panghal, S., Kumar, M. (2022). Neural network method: delay and system of delay differential equations. *Engineering with Computers,* 38(Suppl 3), 2423-2432.

[40] Singh, R., Singh, G., Singh, M. (2021). Numerical algorithm for solution of the system of Emden–Fowler type equations. *International Journal of Applied and Computational Mathematics,* 7(4), 136.

[41] Singh, R. (2018). Analytical approach for computation of exact and analytic approximate solutions to the system of Lane-Emden-Fowler type equations arising in astrophysics. *The European Physical Journal Plus,* 133(8), 320.

[42] Wazwaz, A. M. (2011). The variational iteration method for solving systems of equations of Emden–Fowler type. *International Journal of Computer Mathematics,* 88(16), 3406-3415.

Ashish kumar *received graduation degree in mathematics (Honours) from Ramjas College, University of Delhi, and Msc degree from Hindu College, University of Delhi. Currently, he is a junior research fellow at School of Liberal Studies, Dr. B.R. Ambedkar University Delhi, Delhi. His research interests include numerical analysis and applied mathematics.*
https://orcid.org/0009-0003-8968-8074

Manoj Kumar *is a visiting faculty member at the Department of Applied Sciences and Humanities, Indira Gandhi Delhi Technical University for Women, Delhi, India. He received a PhD degree in Mathematics from Dr. B. R. Ambedkar University Delhi, India. His research interests include traffic congestion modeling, machine learning, and deep learning.*
https://orcid.org/0000-0001-8218-8278

Pranay Goswami *is currently an Assistant Professor at the School of Liberal Studies, Dr. B.R. Ambedkar University Delhi. He received PhD degree in Mathematics from University of Rajasthan, India. His research interests include differential equations, fractional differential equations, numerical methods, and mathematical modeling.*
https://orcid.org/0000-0003-1205-1975

An International Journal of Optimization and Control: Theories & Applications
ISSN:2146-0957 eISSN:2146-5703
Vol.14, No.1, pp.74-80 (2024)
http://doi.org/10.11121/ijocta.1414

RESEARCH ARTICLE

An approximate solution of singularly perturbed problem on uniform mesh

Derya Arslan,[a] Ercan Celik[b*]

[a] *Department of Mathematics, University of Bitlis Eren, Turkey*
[b] *Department of Mathematics, Kyrgyz-Turkish Manas University, Kyrgyz*
d.arslan@beu.edu.tr, ercan.celik@manas.edu.kg

ARTICLE INFO

Article History:
Received 17 June 2023
Accepted 3 October 2023
Available Online 10 January 2024

Keywords:
Singularly perturbed equation
Integral boundary condition
Finite difference scheme
Uniform mesh

AMS Classification 2010:
65L10; 65L11; 65L12; 65L15; 65L20; 65L70; 34B10

ABSTRACT

In this study, we obtain approximate solution for singularly perturbed problem of differential equation having two integral boundary conditions. With this purpose, we propose a new finite difference scheme. First, we construct this exponentially difference scheme on a uniform mesh using the finite difference method. We use the quasilinearization method and the interpolating quadrature formulas to establish the numerical scheme. Then, as a result of the error analysis, we show that the method under study is convergent in the first order. Consequently, theoretical findings are supported by numerical results obtained with an example. Approximate solutions curves are compared on the chart to provide concrete indication. The maximum errors and convergence rates obtained are given on the table for different ε and N values.

1. Introduction

This study is concerned with the numerical solution the following singularly perturbed equation with integral boundary values for $0 \leq \ell_0 < \ell_1 \leq \ell$

$$\varepsilon^2 u''(t) + \varepsilon a(t) u'(t) - g(t,u) = 0, \quad 0 < t < \ell, \tag{1}$$

$$u(0) = \int_{\ell_0}^{\ell_1} u(t) f_0(t)\, dt + A, \tag{2}$$

$$u(\ell) = \int_{\ell_0}^{\ell_1} u(t) f_1(t)\, dt + B. \tag{3}$$

Here, ε is the perturbation parameter and is defined as $0 < \varepsilon \ll 1$. A and B are fixed. $a(t)$ and $g(t,u)$ are continuous functions in the interval $[0,\ell]$ and $[0,\ell] \times \mathbb{R}$, respectively. $f_0(t)$ and $f_1(t)$ are continuous functions on $[\ell_0, \ell_1]$.

When $\varepsilon = 0$ in the Eq. (1), the new equation is an algebraic equation. The boundary conditions will be unnecessary for the solution of this equation. In this case, there will be two boundary layers $t = 0$ and $t = 1$ of the problem (1-(3).

Equations with a positive parameter ε in the coefficient of the highest order derivative are called singularly perturbed equations. Solutions of these problems have thin boundary layers. In these layers, the solution changes abruptly and rapidly, while in other parts of the definition region it changes slowly and regularly. This irregularity causes the solution of singularly perturbed problems to have unlimited derivatives. Thus, serious difficulties arise in the operation of such problems. These difficulties are also evident in numerical solution. Because the approximate solution diverges from the exact solution as the mesh steps get smaller. For this reason, it is very important to establish appropriate numerical methods for the solution of problems with singular perturbations. Known classical numerical methods cannot give numerical results suitable for the exact solution. Especially in this study, an efficient numerical method such as the finite difference method, which gives uniform convergence according to ε

*Corresponding Author

is preferred for the solution of such problems [1]-[15]. Studies on problems with singular perturbations started in the 1900s. These problems are encountered in science, economics, sociology, engineering, medical science, fluids mechanics, aerodynamics, magnetic dynamics, emission theory, reaction diffusion, light emitting waves, communication lines, plasma dynamics, purified gas dynamics, motion of mass, plastics, chemical reactor theory, seismology, oceanography, meteorology, electric current, ion acoustic waves and some physical modeling [16]- [21]. Also, Bakhvalov used a special transformation in the numerical solution of boundary layer problems [22]. Bitsadze and Samarskii obtained some generalizations of linear elliptic boundary value problems [23]. Herceg and Surla found the numerical solution of the singularly perturbed problem with non-local boundary values using spline tension [24]. Gupta and Trofimchuk studied a sharper case for solving the second-order three-point boundary value problem [25]. Amiraliyev and Cakir found a uniformly convergent approach for the zeroth order reduced equation and convective singularly perturbed problem [2]. Cakir, for the three-point singularly perturbed problem, using the difference method, a second-order uniform convergence was obtained [3]. Cakir and Amiraliyev evaluated the three-point singularly perturbed boundary value problem using a Shishkin mesh [4]. In [1, 6–8, 24] and [26, 34] have been worked on the numerical solution of the singularly perturbed problem with nonlocal boundary and integral boundary conditions. The singularly perturbed problem has also been solved by different numerical methods [9, 10, 35]. There are also studies on existence and uniqueness of these problems in the literature [36]-[38].

The study of the linear state of our problem (1)-(3) is in [1], where the problem is solved with a layer-adapted mesh. The difference of this study from similar studies in the literature [6] is the use of a uniform mesh and the two integral boundary conditions of the problem (1)-(3). Although there are studies on singularly perturbed problems with two integral boundary conditions solved in Shishkin mesh as in [6], we have not come across any studies on singularly perturbed problems with two integral boundary conditions in uniform mesh. This gap, which is not in the literature, constitutes the motivation of our study.

In this paper, the difference scheme is obtained using the integral rules from [30]. In the second part, we investigated several important factors for the exact solution (1)-(3). The difference procedure for the uniform mesh of the problem (1)-(3) is given in part 3. In the fourth part, the convergence evaluation of the method is made. For the purpose of applying the theoretical procedure, an example whose exact solution is unknown is presented in Sect 5.

Throughout this study, C and C_0 will be used as positive constants that do not depend on ε and h. The norm $\|.\|$ is used to denote the maximum norm.

2. Some properties of the Exact Solution

Here we will give a Lemma and its proof, which will be needed for later parts of the study.

Lemma 1. *Let $u(t)$ be the solution of the (1)-(3), $a(t) \in C^1[0,\ell]$, $\gamma = \int_{\ell_0}^{\ell_1} (|f_0(t)| + |f_1(t)|)\,dt < 1$, $\partial g/\partial u - \varepsilon a'(t) \geq \beta_* >$ and $|\partial g/\partial t| \leqslant C$ for $t \in [0,\ell]$, then the estimations*

$$|u(t)| \leqslant C_0, \tag{4}$$

$$\left|u'(t)\right| \leqslant C\left\{1+\frac{1}{\varepsilon}\left(e^{-\frac{c_0 t}{\varepsilon}}+e^{-\frac{c_1(\ell-t)}{\varepsilon}}\right)\right\}, \tag{5}$$

hold, where $0 \leqslant t \leqslant \ell$ and

$$\begin{aligned} C_0 &= (1-\gamma)^{-1}\left(|A|+|B|+\beta^{-1}\|F\|_\infty\right), \\ c_0 &= \frac{1}{2}\left(\sqrt{a^2(0)+4\beta_*}+a(0)\right), \\ c_1 &= \frac{1}{2}\left(\sqrt{a^2(\ell)+4\beta_*}-a(\ell)\right). \end{aligned}$$

Proof. Using the mean value theorem for $g(t,u)$ in (1), we have

$$g(t,u) = \frac{\partial g(t,\xi u)}{\partial u}u(t) + g(t,0), \quad 0<\xi<1,$$

supposing of

$$b(t) = \frac{\partial g(t,\xi u)}{\partial u} > 0,\ G(t) = g(t,0).$$

Let's rewrite the (1)-(3) problem as follows to get the proof of (4)

$$\varepsilon^2 u''(t) + \varepsilon a(t)u'(t) - b(t)\,u(t) = G(t), \tag{6}$$

$$u(0) = \int_{\ell_0}^{\ell_1} f_0(x)\,u(x)\,dx + A, \tag{7}$$

$$u(\ell) = \int_{\ell_0}^{\ell_1} f_1(t)\,u(t)\,dt + B. \tag{8}$$

Here, using the maximum principle [4,39] and (6)-(8) we arrive at the following inequality:

$$|u(t)| \leq |u(0)| + |u(\ell)| + \beta^{-1}\|G\|_\infty,\ t \in [0,l]. \tag{9}$$

Now, using the boundary values (7) and (8), let's obtain the inequality (4)

$$|u(0)| \leq |A| + \int_{\ell_0}^{\ell_1} |f_0(t)| \, |u(t)| \, dt, \tag{10}$$

$$|u(\ell)| \leq |B| + \int_{\ell_0}^{\ell_1} |f_1(t)| \, |u(t)| \, dt. \tag{11}$$

If we write the inequalities (10) and (11) in the inequality (9), we get the following result:

$$\begin{aligned} |u(t)| &\leq |A| + |B| + \int_{\ell_0}^{\ell_1} |f_0(t)| \, |u(t)| \, dt \\ &+ \int_{\ell_0}^{\ell_1} |f_1(t)| \, |u(t)| \, dt + \beta^{-1} \|G\|_\infty \\ &\leq |A| + |B| + \max_{[\ell_0,\ell_1]} |u(t)| \int_{\ell_0}^{\ell_1} |f_0(t)| \, dt \\ &+ \max_{[\ell_0,\ell_1]} |u(t)| \int_{\ell_0}^{\ell_1} |f_1(t)| \, dt + \beta^{-1} \|G\|_\infty \\ &\leq |A| + |B| + \|u\|_\infty \int_{\ell_0}^{\ell_1} |f_0(t)| \, dt \\ &+ \|u\|_\infty \int_{\ell_0}^{\ell_1} |f_1(t)| \, dt + \beta^{-1} \|G\|_\infty . \end{aligned}$$

Thus, the proof of (4) is completed. Also, the proof of (5) is almost the same to that of [39]. □

3. Uniform Mesh and Construction of the difference scheme

In this part, we will obtain the difference scheme for the (1)-(3) problem. For this we will work on the uniform mesh.

$$\omega_h = \left\{ t_i = ih, i = 1, 2, \ldots, N-1 : h = \frac{\ell}{N} \right\},$$

$$\bar{\omega}_h = \omega_h \cup \{ t_0 = 0, \ t_N = \ell \} .$$

where N is the number of discretization points.

Let's give some notations for grid functions, where y_i is the approximate value for $u(t)$ at grid points t_i.

$$f_{\bar{t},i} := \frac{f_i - f_{i-1}}{h}, \quad f_{t,i} := \frac{f_{i+1} - f_i}{h},$$

$$f_{\overset{\circ}{t},i} := \frac{f_{t,i} + f_{\bar{t},i}}{2},$$

$$f_{\bar{t}t,i} := \frac{f_{i+1} - 2f_i + f_{i-1}}{h^2}, \ i = 1, 2, ..., N,$$

$$\|f\|_\infty \equiv \|f\|_{\infty,\bar{\omega}_h} := \max_{0 \leqslant i \leqslant N} |f_i| .$$

Let's start constructing the difference scheme with the following equation for $1 \leqslant i \leqslant N-1$:

$$\xi_i^{-1} h^{-1} \int_{t_{i-1}}^{t_{i+1}} Lu(t) \varphi_i(t) dt = 0, \tag{12}$$

where the functions $\{\varphi_i(t)\}_{i=1}^{N-1}$ have the form

$$\varphi_i(t) = \begin{cases} \varphi_i^{(1)}(t), & t_{i-1} < t < t_i, \\ \varphi_i^{(2)}(t), & t_i < t < t_{i+1}, \\ 0, & \text{otherwise}, \end{cases}$$

where $\varphi_i^{(1)}(t)$ and $\varphi_i^{(2)}(t)$, respectively, are the solution of the following problems:

$$\varepsilon \varphi_i^{(1)}(t) - a_i \varphi_i^{(1)}(t) = 0, \ t_{i-1} < t < t_i,$$

$$\varphi_i^{(1)}(t_{i-1}) = 0, \ \varphi_i^{(1)}(t_i) = 1,$$

$$\varepsilon \varphi_i^{(2)}(t) - a_i \varphi_i^{(2)}(t) = 0, \ t_i < t < t_{i+1},$$

$$\varphi_i^{(2)}(t_{i-1}) = 0, \ \varphi_i^{(2)}(t_i) = 1,$$

and the coefficient ξ_i^{-1} in (12) as

$$\xi_i^{-1} = \left(h^{-1} \int_{t_{i-1}}^{t_{i+1}} \varphi_i(t) dt \right)^{-1} .$$

If we rearrange (12), we get the following system

$$-\varepsilon^2 \xi_i^{-1} h^{-1} \int_{t_{i-1}}^{t_{i+1}} \varphi_i'(t) u'(t) \, dt + \varepsilon a_i^{-1} h^{-1} \int_{t_{i-1}}^{t_{i+1}} \varphi_i(t) u'(t) \, dt$$

$$-g(t_i, u_i) + R_i = 0, \quad i = 1, 2, ..., N-1, \tag{13}$$

where

$$R_i = \varepsilon \xi_i^{-1} h^{-1} \int_{t_{i-1}}^{t_{i+1}} [a(t) - a(t_i)] \varphi_i(t) u'(t) \, dt$$

$$-\xi_i^{-1} h^{-1} \int_{t_{i-1}}^{t_{i+1}} \left[\varphi_i(t) \int_{t_{i-1}}^{t_{i+1}} \frac{d}{dt} g(\xi, u(\xi)) K_{0,i}^*(t, \xi) \, d\xi \right] dt, \tag{14}$$

$$K_{0,i}^*(t, \xi) = T_0(t - \xi) - T_0(t_i - \xi) .$$

If we benefit the formulas from [5], we have the following system for $1 \leq i \leq N-1$ from (13)

$$-\varepsilon^2 \xi_i^{-1} h^{-1} \int_{t_{i-1}}^{t_i} \varphi_i'(t) u'(t) \, dt - \varepsilon^2 \xi_i^{-1} h^{-1} \int_{t_i}^{t_{i+1}} \varphi_i'(t) u'(t) \, dt$$

$$+ \varepsilon a_i \xi_i^{-1} h^{-1} \int_{t_{i-1}}^{t_i} \varphi_i(t) u'(t) \, dt$$

$$+ \varepsilon a_i \xi_i^{-1} h^{-1} \int_{t_i}^{t_{i+1}} \varphi_i(t) u'(t) \, dt - g(t_i, u_i) + R_i$$

$$= -\varepsilon^2 \xi_i^{-1} h^{-1} u_{\bar{t},i} \int_{t_{i-1}}^{t_i} \varphi_i^{(1)'}(t) dt$$

$$-\varepsilon^2\xi_i^{-1}h^{-1}u_{t,i}\int\limits_{t_i}^{t_{i+1}}\varphi_i^{(2)'}(t)dt$$

$$+\varepsilon a_i\xi_i^{-1}h^{-1}u_{\bar{x},i}\int\limits_{t_{i-1}}^{t_i}\varphi_i^{(1)}(t)dt$$

$$+\varepsilon a_i\xi_i^{-1}h^{-1}u_{t,i}\int\limits_{t_i}^{t_{i+1}}\varphi_i^{(2)}(t)dt-g(t_i,u_i)+R_i$$

$$=-\varepsilon^2\xi_i^{-1}u_{\bar{t},i}\chi_{1,i}-\varepsilon^2\xi_i^{-1}u_{t,i}\chi_{2,i}+\varepsilon a_i\xi_i^{-1}u_{\bar{x},i}\chi_{1,i}$$
$$+\varepsilon a_i\xi_i^{-1}u_{t,i}\chi_{2,i}-g(t_i,u_i)+R_i=0.$$

After the $u_{\bar{t},i}=u_{\overset{\circ}{t},i}-\frac{h}{2}u_{\bar{t}t,i}$ and $u_{t,i}=u_{\overset{\circ}{t},i}+\frac{h}{2}u_{\bar{t}t,i}$ are substituted in the above equation, the following expression is obtained:

$$\varepsilon^2\left\{\xi_i^{-1}\left(1+0.5\varepsilon^{-1}ha_i\left(\chi_{2,i}-\chi_{1,i}\right)\right)\right\}u_{\bar{t}t,i}$$
$$+\varepsilon a_i u_{\overset{\circ}{t},i}-g(t_i,u_i)+R_i=0,$$

where

$$\chi_{1,i}=h^{-1}\int\limits_{t_{i-1}}^{t_i}\varphi_i^{(1)}(t)dt,\ \chi_{2,i}=h^{-1}\int\limits_{t_i}^{t_{i+1}}\varphi_i^{(2)}(t)dt.$$

So, from the above equations, the difference scheme is defined for $1\leqslant i\leqslant N-1$:

$$\varepsilon^2\theta_i u_{\bar{t}t,i}+\varepsilon a_i u_{\overset{\circ}{t},i}-g(t_i,u_i)+R_i=0, \tag{15}$$

here

$$\theta_i=\xi_i^{-1}\left(1+\frac{(\chi_{2,i}-\chi_{1,i})}{2\varepsilon}ha_i\right). \tag{16}$$

Now, the approximations for the first and second boundary conditions need to be determined. Let t_{N_0} and t_{N_1} be the grid points nearest to ℓ_0 and ℓ_1, respectively.

$$\int_{\ell_0}^{\ell_1}f_0(t)\,u(t)\,dt=\int_{\ell_0}^{t_{N_0}}f_0(t)\,u(t)\,dt$$
$$+\int_{t_{N_0}}^{t_{N_1}}f_0(t)\,u(t)\,dt+\int_{t_{N_1}}^{\ell_1}f_0(t)\,u(t)\,dt, \tag{17}$$

and

$$\int_{t_{N_0}}^{t_{N_1}}f_0(t)\,u(t)\,dt=\sum_{i=N_0}^{N_1}\left[\int_{t_{i-1}}^{t_i}f_0(t)\,dt\right]u(t_i)+\bar{r}_0$$
$$=K_0(u)+\bar{r}_0, \tag{18}$$

where

$$K_0(u)=\sum_{i=N_0}^{N_1}\left[\int_{t_{i-1}}^{t_i}f_0(t)\,dt\right]u(t_i), \tag{19}$$

$$\bar{r}_0=\sum_{i=N_0}^{N_1}\int_{t_{i-1}}^{t_i}\left[f_0(t)\int_{t_{i-1}}^{t_i}u'(\xi)\left(T_0(t-\xi)-1\right)d\xi\right]dt.$$

Thus, we get the difference approximation corresponding to the first boundary value as:

$$u_0-K_0(u)=A+r_0, \tag{20}$$

where

$$r_0=\int_{\ell_0}^{t_{N_0}}f_0(t)\,u(t)\,dt+\int_{t_{N_1}}^{\ell_1}f_0(t)\,u(t)\,dt+\bar{r}_0. \tag{21}$$

Now we get the difference approtimation corresponding to the second boundary value as follows:

$$u_N-K_1(u)=B+r_1, \tag{22}$$

where

$$K_1(u)=\sum_{i=N_0}^{N_1}\left[\int_{t_{i-1}}^{t_i}f_1(t)\,dt\right]u(t_i), \tag{23}$$

$$r_1=\int_{\ell_0}^{t_{N_0}}f_1(t)\,u(t)\,dt+\int_{t_{N_1}}^{\ell_1}f_1(t)\,u(t)\,dt+\bar{r}_1, \tag{24}$$

$\bar{r}_1=\sum_{i=N_0}^{N_1}\int_{t_{i-1}}^{t_i}\left[f_1(t)\int_{t_{i-1}}^{t_i}u'(\xi)\left(T_0(t-\xi)-1\right)d\xi\right]dt.$

If the error values in the (14), (21) and (24) are neglected, the following difference chart is found for $1\leqslant i\leqslant N-1$:

$$\varepsilon^2\theta_i y_{\bar{t}t,i}+\varepsilon a_i y_{\overset{\circ}{t},i}-g(t_i,y_i)=0,\ , \tag{25}$$

$$y_0=K_0(y)+A, \tag{26}$$

$$y_N=K_1(y)+B. \tag{27}$$

4. Stability of the Difference Scheme

Here, we give the stability of the finite difference method with the Theorem 1 and the evaluation of the error functions with the Lemma 2.

The error term z is $z=y-u$ for $1<i<N$.

$$\varepsilon^2\theta_i z_{\bar{t}t,i}+\varepsilon a_i z_{\overset{\circ}{t},i}-\left[g(t_i,y_i)-g(t_i,u_i)\right]=R_i, \tag{28}$$

$$z_0=K_0(z)+r_0, \tag{29}$$

$$z_N=K_1(z)+r_1. \tag{30}$$

Lemma 2. *The estimates are valid for the terms R_i, r_0 and r_1 to be obtained with the help of results of Section 1 and Lemma 1*

$$\|R\|_{\infty,\omega_h}\leq Ch, \tag{31}$$

$$|r_0|\leq Ch, \tag{32}$$

$$|r_1|\leq Ch. \tag{33}$$

Proof. We have from the expression (14) for R_i on an arbitrary mesh as follows

$$|R_i| \le C \left\{ h + h + \int\limits_{t_{i-1}}^{t_{i+1}} \left(1 + \left|u'(\xi)\right|\right) d\xi \right\}.$$

This inequality and (5) enable us to write the inequality as

$$|R_i| \le C \left\{ h + \frac{1}{\varepsilon} \int\limits_{t_{i-1}}^{t_{i+1}} \left(e^{-\frac{c_0 t}{\varepsilon}} + e^{-\frac{c_1(\ell - t)}{\varepsilon}} \right) dx \right\}. \tag{34}$$

The mesh is uniform with $h = \ell N^{-1}$ for $1 \le i \le N$. So, from the above inequality, we get

$$\begin{aligned} |R_i| &\le C\left\{N^{-1} + \varepsilon^{-1} h\right\} \\ &\le Ch. \end{aligned}$$

Let us evaluate (32) using the expression (21) for r_0 as

$$|r_0| \le$$

$$\sum_{i=N_0}^{N_1} \int_{t_{i-1}}^{t_i} \left[|f_0(t)| \int_{t_{i-1}}^{t_i} \left|u'(\xi)\right| |T_0(t-\xi) - 1| \, d\xi \right] dt$$

$$+ \int_{\ell_0}^{t_{N_0}} |f_0(t)| \, |u(t)| \, dt + \int_{t_{N_1}}^{\ell_1} |f_0(t)| \, |u(t)| \, dt$$

$$\le C \max_{[t_{i-1},\, t_i]} |f_0(t)| \int_0^{\ell} \left|u'(t)\right| dt + O(h)$$

$$\le Ch. \tag{35}$$

The proof of (33) is similar to the proof of the inequality (32). All these complete the proof of Lemma 2. □

Lemma 3. *If z_i is the solution of (28)-(30) and*

$$\bar{\gamma} = \sum_{i=N_0}^{N} \int_{t_{i-1}}^{t_i} \left[|f_0(t)| + |f_1(t)|\right] dt < 1.$$

Then there is the following estimate

$$\|z\|_{\infty,\bar{\omega}_h} \le C \left(\beta^{-1} \|R\|_{\infty,\omega_h} + |r_0| + |r_1| \right). \tag{36}$$

Proof. Using Lemma 2, we easily obtain (36). □

Theorem 1. *If u be the solution of (1)-(3) and y be the solution of (25)-(27). Then, the following estimate is satisfied.*

$$\|y - u\|_{\infty,\bar{\omega}_h} \le Ch.$$

This theorem gives the result of the convergence of the proposed method with the help of Lemma 2 and Lemma 3.

5. Numerical Illustrations

Here we provide some numerical results that exemplify the current method.

By using the quasilinearization technique, the scheme (25)-(27) can be arranged as:

$$\varepsilon^2 \theta_i y_{\bar{t}t,i}^{(n)} + \varepsilon a_i y_{\overset{\circ}{t},i}^{(n)} - g\left(t_i, y_i^{(n-1)}\right) \tag{37}$$

$$-\frac{\partial g}{\partial y}\left(t_i, y_i^{(n-1)}\right)\left(y_i^{(n)} - y_i^{(n-1)}\right) = 0,$$

$$y_0^{(n)} = h \sum_{i=N_0}^{N_1} f_{0,i} y_i^{(n-1)} + A, \tag{38}$$

$$y_N^{(n)} = h \sum_{i=N_0}^{N_1} f_{1,i} y_i^{(n-1)} + B, \tag{39}$$

where $y_i^{(0)}$ for $1 \le i \le N$ and $n \ge 1$ is the initial guess.

Example 1. We apply the scheme (37)-(39) to the following singularly perturbed problem with integral boundary conditions:

$$\varepsilon^2 u'' + \varepsilon(1+t) u' = 2u - \arctan(t+u), \; 0 < t < 1,$$

$$u(0) = \int_{0.5}^{1} \cos(\pi t) u(t) \, dt + 1,$$

$$u(1) = \int_{0.5}^{1} \sin(\pi t) u(t) \, dt + 1.$$

The exact solution of the problem is unknown. For this reason, we have to use the double mesh as:

$$e_\varepsilon^N = \max_i \left| u_i^{\varepsilon,N} - \tilde{u}_{2i}^{\varepsilon,2N} \right|.$$

The rates of convergence are defined as

$$P_\varepsilon^N = \frac{\ln\left(e_\varepsilon^N / e_\varepsilon^{2N}\right)}{\ln 2}.$$

The e^N is the maximum errors as

$$e^N = \max_\varepsilon e_\varepsilon^N.$$

Table 1. Convergence rates and maximum errors for ε and N.

$\varepsilon \downarrow \rightarrow N$	16	32	64	128
2^{-10}	0.084154	0.042753	0.021547	0.010816
	0.97	0.98	0.99	
2^{-11}	0.026562	0.015689	0.008531	0.004421
	0.75	0.87	0.94	
2^{-13}	0.008590	0.004484	0.002283	0.001144
	0.93	0.97	0.99	
2^{-15}	0.002299	0.001160	0.000580	0.000288
	0.98	0.99	1.00	
2^{-17}	0.000585	0.000292	0.000145	0.000072
	p=0.99	p=1.00	p=1.01	

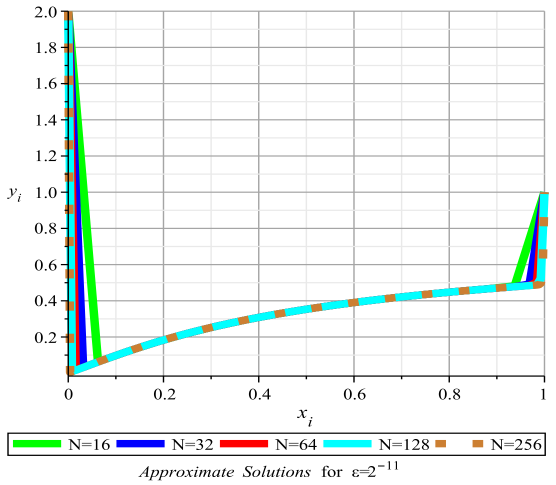

Figure 1. Numerical solution curves of Example 1.

Uniform convergence rates p and error values are given in Table 1. p values are around one. In Figure 1, the approximate solution curves have been plotted for each of the values $N = 16, 32, 64, 128, 256$ for $t = 0$. As N values increase, the approximate solution curves approach the coordinate axes around $t = 0$ and $t = 1$. Here it can be seen that the theoretical process is accurate and reliable.

6. Conclusion

In the study, the finite difference method is used to solve the problem with nonlocal conditions. The difference scheme has been established with the help of some integral forms on the uniform mesh. The difference problem was solved by the Gauss elimination method. Convergence analysis was performed. Uniform convergence was obtained from the first-order. The proposed method has been applied to a test problem. Numerical results show that the approaches described here contribute greatly to the understanding of singularly perturbed problem (see Table 1 and Figure 1). With the motivation given by this study, it is aimed to apply to nonlocal boundary condition and fuzzy problems with delay parameter with singularly perturbation feature.

Acknowledgments

The authors thanks the anonymous authors whose work largely constitutes this study.

References

[1] Cakir, M., Amiraliyev, G.M. (2005) A finite difference method for the singularly perturbed problem with nonlocal boundary condition. *Applied Mathematics and Computation*, 160, 539-549.

[2] Amiraliyev, G.M., Cakir, M. (2000). A uniformly convergent difference scheme for singularly perturbed problem with convective term and zeroth order reduced equation. *International Journal of Applied Mathematics*, 2(12), 1407-1419.

[3] Cakir, M. (2010). Uniform second-order difference method for a singularly perturbed three-point boundary value problem. *Advances in Difference Equations*, 13 pages.

[4] Cakir, M., Amiraliyev, G.M. (2010). A numerical method for a singularly perturbed three-point boundary value problem. *Journal of Applied Mathematics*, 17 pages.

[5] Amiraliyev, G.M., Mamedov, Y.D. (1995). Difference schemes on the uniform mesh for singular perturbed pseudo-parabolic equations. *Turkish Journal of Mathematics*, 19, 207-222.

[6] Arslan, D., Cakir, M. (2021). A new numerical approach for a singularly perturbed problem with two integral boundary conditions. *Computational and Applied ,mathematics*, 40(6).

[7] Arslan, D. (2020). An approximate solution of linear singularly perturbed problem with nonlocal boundary condition. *Journal of Mathematical Analysis*, 11(3), 46-58.

[8] Arslan, D. (2019). An effective numerical method for singularly perturbed nonlocal boundary value problem on Bakhvalov Mesh. *Journal of Informatics and Mathematical Sciences*, 11(3-4), 253-264.

[9] Arslan, D. (2019). A novel hybrid method for singularly perturbed delay differential equations. *Gazi University Journal of Science*, 32(1), 217-223.

[10] Arslan, D. (2019). Approximate solutions of singularly perturbed nonlinear Ill-posed and sixth-order Boussinesq equations with hybrid method. *Bitlis Eren Üniversitesi Fen Bilimleri Dergisi*, 8(2), 451-458.

[11] Negero, N.T, Duressa, G.F. (2021). A method of line with improved accuracy for singularly perturbed parabolic convection–diffusion problems with large temporal lag. *Results in Applied Mathematics*, 11, 100174.

[12] Negero, N.T. (2022). A uniformly convergent numerical scheme for two parameters singularly perturbed parabolic convection–diffusion problems with a large temporal lag. *Results in Applied Mathematics*, 16, 100338.

[13] Negero, N.T. (2023). A parameter-uniform efficient numerical scheme for singularly perturbed time-delay parabolic problems with two small parameters. *Partial Differential Equations in Applied Mathematics*, 7, 100518.

[14] Negero, N.T. (2023). A robust fitted numerical scheme for singularly perturbed parabolic reaction–diffusion problems with a general time delay. *Results in Physics*, 51, 106724.

[15] Negero, N.T. (2023). A fitted operator method of line scheme for solving two-parameter singularly perturbed parabolic convection-diffusion problems with time delay. *Journal of Mathematical Modeling*, 11(2).

[16] Nayfeh, A.H. (1985). *Perturbation Methods*. Wiley, New York.

[17] Nayfeh, A.H. (1979). *Problems in Perturbation*. Wiley, New York.

[18] Kevorkian, J., Cole, J.D. (1981). *Perturbation Methods in Applied Mathematics*. Springer, New York.

[19] O'Malley, R.E. (1991). *Singular Perturbation Methods for Ordinary Differential Equations*. Springer Verlag, New York.

[20] Miller, J.J.H., O'Riordan, E., Shishkin, G.I. (1996). *Fitted Numerical Methods for Singular Perturbation Problems*. World Scientific, Singapore.

[21] Roos, H.G., Stynes, M., Tobiska, L. (2008). *Robust Numerical Methods Singularly Perturbed Differential Equations*. Springer-Verlag, Berlin.

[22] Bakhvalov, N.S. (1969). On optimization of methods for solving boundary value problems in the presence of a boundary layer. The use of special transformation the numerical solution of boudary-layer problems. *Zhurnal Vychislitelnoi Matematiki i Matematicheskoi Fiziki*, 9(4) 841-859.

[23] Bitsadze, A.V., Samarskii, A.A. (1969). On Some Simpler Generalization of Linear Elliptic Boundary Value Problems. *Doklady Akademii Nauk SSSR*, 185, 739-740.

[24] Herceg, D., Surla, K. (1991). Solving a nonlocal singularly perturbed nonlocal problem by splines in tension. *Univ. u Novom Sadu Zb. Rad.Prirod.-Mat. Fak. Ser. Math.*, 21(2), 119-132.

[25] Gupta, C.P., Trofimchuk, S.I. (1997). A sharper condition for the solvability of a three-point second order boundary value problem. *Journal of Mathematical Analysis and Applications*, 205 586-597.

[26] Chegis, R. (1988). The numerical solution of singularly perturbed nonlocal problem (in Russian). *Lietuvas Matematica Rink*, 28, 144-152.

[27] Chegis, R. (1991). The difference scheme for problems with nonlocal conditions, *Informatica (Lietuva)*, 2, 155-70.

[28] Nahushev, A.M. (1985). On nonlocal boundary value problems (in Russian). *Differential Equations*, 21, 92-101.

[29] Sapagovas, M., Chegis, R. (1987). Numerical solution of nonlocal problems (in Russian). *Lietuvas Matematica Rink*, 27, 348-356.

[30] Xie, F., Jin, Z., Ni, M. (2010). On the step-type contrast structure of a second-order semilinear differential equation with integral boundary conditions. *Electronic Journal of Qualitative Theory of Differential Equations*, 62, 1-14.

[31] Kumar, D., Kumari, P. (2020). A parameter-uniform collocation scheme for singularly perturbed delay problems with integral boundary condition. *Journal of Applied Mathematics and Computing*, 63, 813-828.

[32] Sekar, E., Tamilselvan, A. (2019). Third order singularly perturbed delay differential equation of reaction diffusion type with integral boundary condition. *Journal of Applied Mathematics and Computational Mechanics*, 18(2), 99-110.

[33] Raja, V., Tamilselvan, A. (2019). Fitted finite difference method for third order singularly perturbed convection diffusion equations with integral boundary condition. *Arab Journal of Mathematical Science*, 25(2), 231-242.

[34] Khan, R.A. (2003). The generalized method of quasilinearization and nonlinear boundary value problems with integral boundary conditions. *Electronic Journal of Qualitative Theory of Differential Equations*, 10, 1-9.

[35] Rao, S.C.S., Kumar, M. (2007). B-spline collocation method for nonlinear singularly perturbed two-point boundary-value problems. *Journal of Optimization Theory and Applications*, 134(1), 91-105.

[36] Byszewski, L. (1991). Theorems about the existence and uniqueness of solutions of a semilinear evolution nonlocal Cauchy problem. *Journal of Mathematical Analysis and Applications*, 62, 494-505.

[37] Bougoffa, L., Khanfer, A. (2018). Existence and uniqueness theorems of second-order equations with integral boundary conditions. *Bulletin of the Korean Mathematical Society*, 55(3), 899-911.

[38] Benchohra, M., Ntouyas, S.K. (2000). Existence of solutions of nonlinear differential equations with nonlocal conditions. *Journal of Mathematical Analysis and Applications*, 252, 477-483.

[39] Samarskii, A.A. (1983). *Theory of Difference Schemes*. 2 nd ed., "Nauka", Moscow.

Derya Arslan *has obtained her PhD degree in Mathematics, Van Yuzuncu Yil University, Van, Turkey in 2016. She is currently working as an Associated Professor at the Department of Mathematics, Faculty of Arts and Sciences, University of Bitlis Eren, Bitlis, Turkey. Her fields of research are singularly perturbed problems, numerical methods, applied mathematics.*
https://orcid.org/0000-0001-6138-0607

Ercan Celik *has obtained her PhD degree in Mathematics, Atatürk University, Erzurum, Turkey in 2002. He is currently working as a Professor at the Department of Mathematics, Kyrgyz-Turkish ManasUniversity, Kyrgyz. Him fields of research are optimization, numerical analysis, applied mathematics.*
https://orcid.org/0000-0002-1402-1457

INSTRUCTIONS FOR AUTHORS

Aims and Scope

An International Journal of Optimization and Control: Theories & Applications (IJOCTA) is a scientific, peer-reviewed, open-access journal that publishes original research papers and review articles of high scientific value in all areas of applied mathematics, optimization and control. It aims to focus on multi/inter-disciplinary research into the development and analysis of new methods for the numerical solution of real-world applications in engineering and applied sciences. The basic fields of this journal cover mathematical modeling, computational methodologies and (meta)heuristic algorithms in optimization, control theory and their applications. Note that new methodologies for solving recent optimization problems in operations research must conduct a comprehensive computational study and/or case study to show their applicability and practical relevance.

Journal Topics

The topics covered in the journal are (not limited to):

Applied Mathematics, Financial Mathematics, Control Theory, Optimal Control, Fractional Calculus and Applications, Modeling of Bio-systems for Optimization and Control, Linear Programming, Nonlinear Programming, Stochastic Programming, Parametric Programming, Conic Programming, Discrete Programming, Dynamic Programming, Nonlinear Dynamics, Stochastic Differential Equations, Optimization with Artificial Intelligence, Operational Research in Life and Human Sciences, Heuristic and Metaheuristic Algorithms in Optimization, Applications Related to Optimization in Engineering.

Submission of Manuscripts

New Submissions

Solicited and contributed manuscripts should be submitted to IJOCTA via the journal's online submission system. You need to make registration prior to submitting a new manuscript (please click here to register and do not forget to define yourself as an "Author" in doing so). You may then click on the "New Submission" link on your User Home.

IMPORTANT: If you already have an account, please click here to login. It is likely that you will have created an account if you have reviewed or authored for the journal in the past.

On the submission page, enter data and answer questions as prompted. Click on the “Next” button on each screen to save your work and advance to the next screen. The names and contact details of at least four internationally recognized experts who can review your manuscript should be entered in the "Comments for the Editor" box.

You will be prompted to upload your files: Click on the “Browse” button and locate the file on your computer. Select the description of the file in the drop down next to the Browse button. When you have selected all files you wish to upload, click the “Upload” button. Review your submission before sending to the Editors. Click the “Submit” button when you are done reviewing. Authors are responsible for verifying all files have uploaded correctly.

You may stop a submission at any phase and save it to submit later. Acknowledgment of receipt of the manuscript by IJOCTA Online Submission System will be sent to the corresponding author, including an assigned manuscript number that should be included in all subsequent correspondence. You can also log-on to submission web page of IJOCTA any time to check the status of your manuscript. You will receive an e-mail once a decision has been made on your manuscript.

Each manuscript must be accompanied by a statement that it has not been published elsewhere and that it has not been submitted simultaneously for publication elsewhere.

Manuscripts can be prepared using LaTeX (.tex) or MSWord (.docx). However, manuscripts with heavy mathematical content will only be accepted as LaTeX files.

Preferred first submission format (for reviewing purpose only) is Portable Document File (.pdf). Please find below the templates for first submission.

Click here to download Word template for first submission (.docx)

Click here to download LaTeX template for first submission (.tex)

Revised Manuscripts

Revised manuscripts should be submitted via IJOCTA online system to ensure that they are linked to the original submission. It is also necessary to attach a separate file in which a point-by-point explanation is given to the specific points/questions raised by the referees and the corresponding changes made in the revised version.

To upload your revised manuscript, please go to your author page and click on the related manuscript title. Navigate to the "Review" link on the top left and scroll down the page. Click on the "Choose File" button under the "Editor Decision" title, choose the revised article (in pdf format) that you want to submit, and click on the "Upload" button to upload the author version. Repeat the same steps to upload the "Responses to Reviewers/Editor" file and make sure that you click the "Upload" button again.

To avoid any delay in making the article available freely online, the authors also need to upload the source files (Word or LaTex) when submitting revised manuscripts. Files can be compressed if necessary. The two-column final submission templates are as follows:

Click here to download Word template for final submission (.docx)

Click here to download LaTeX template for final submission (.tex)

Authors are responsible for obtaining permission to reproduce copyrighted material from other sources and are required to sign an agreement for the transfer of copyright to IJOCTA.

Article Processing Charges

There are **no charges** for submission and/or publication.

English Editing

Papers must be in English. Both British and American spelling is acceptable, provided usage is consistent within the manuscript. Manuscripts that are written in English that is ambiguous or incomprehensible, in the opinion of the Editor, will be returned to the authors with a request to resubmit once the language issues have been improved. This policy does not imply that all papers must be written in "perfect" English, whatever that may mean. Rather, the criteria require that the intended meaning of the authors must be clearly understandable, i.e., not obscured by language problems, by referees who have agreed to review the paper.

Presentation of Papers

Manuscript style

Use a standard font of the **11-point type: Times New Roman** is preferred. It is necessary to single line space your manuscript. Normally manuscripts are expected not to exceed 25 single-spaced pages including text, tables, figures and bibliography. All illustrations, figures, and tables are placed within the text at the appropriate points, rather than at the end.

During the submission process you must enter: (1) the full title, (2) names and affiliations of all authors and (3) the full address, including email, telephone and fax of the author who is to check the proofs. Supply a brief **biography** of each author at the end of the manuscript after references.

- Include the name(s) of any **sponsor(s)** of the research contained in the paper, along with **grant number(s).**
- Enter an **abstract** of no more than 250 words for all articles.

Keywords

Authors should prepare no more than 5 keywords for their manuscript.

Maximum five **AMS Classification number** (http://www.ams.org/mathscinet/msc/msc2010.html) of the study should be specified after keywords.

Writing Abstract

An abstract is a concise summary of the whole paper, not just the conclusions. The abstract should be no more than 250 words and convey the following:

1. An introduction to the work. This should be accessible by scientists in any field and express the necessity of the experiments executed.
2. Some scientific detail regarding the background to the problem.
3. A summary of the main result.
4. The implications of the result.
5. A broader perspective of the results, once again understandable across scientific disciplines.

It is crucial that the abstract conveys the importance of the work and be understandable without reference to the rest of the manuscript to a multidisciplinary audience. Abstracts should not contain any citation to other published works.

Reference Style

Reference citations in the text should be identified by numbers in square brackets "[ ]". All references must be complete and accurate. Please ensure that every reference cited in the text is also present in the reference list (and vice versa). Online citations should include date of access. References should be listed in the following style:

Journal article

Author, A.A., & Author, B. (Year). Title of article. Title of Journal, Vol(Issue), pages.

Castles, F.G., Curtin, J.C., & Vowles, J. (2006). Public policy in Australia and New Zealand: The new global context. Australian Journal of Political Science, 41(2), 131–143.

Book

Author, A. (Year). Title of book. Publisher, Place of Publication.

Mercer, P.A., & Smith, G. (1993). Private Viewdata in the UK. 2nd ed. Longman, London.

Chapter

Author, A. (Year). Title of chapter. In: A. Editor and B. Editor, eds. Title of book. Publisher, Place of publication, pages.

Bantz, C.R. (1995). Social dimensions of software development. In: J.A. Anderson, ed. Annual review of software management and development. CA: Sage, Newbury Park, 502–510.

Internet document

Author, A. (Year). Title of document [online]. Source. Available from: URL [Accessed (date)].

Holland, M. (2004). Guide to citing Internet sources [online]. Poole, Bournemouth University. Available from: http://www.bournemouth.ac.uk/library/using/guide_to_citing_internet_sourc.html [Accessed 4 November 2004].

Newspaper article

Author, A. (or Title of Newspaper) (Year). Title of article. Title of Newspaper, day Month, page, column.

Independent (1992). Picking up the bills. Independent, 4 June, p. 28a.

Thesis

Author, A. (Year). Title of thesis. Type of thesis (degree). Name of University.

Agutter, A.J. (1995). The linguistic significance of current British slang. PhD Thesis. Edinburgh University.

Illustrations

Illustrations submitted (line drawings, halftones, photos, photomicrographs, etc.) should be clean originals or digital files. Digital files are recommended for highest quality reproduction and should follow these guidelines:

- 300 dpi or higher
- Sized to fit on journal page
- TIFF or JPEG format only
- Embedded in text files and submitted as separate files (if required)

Tables and Figures

Tables and figures (illustrations) should be embedded in the text at the appropriate points, rather than at the end. A short descriptive title should appear above each table with a clear legend and any footnotes suitably identified below.

Proofs

Page proofs are sent to the designated author using IJOCTA EProof system. They must be carefully checked and returned within 48 hours of receipt.

Offprints/Reprints

Each corresponding author of an article will receive a PDF file of the article via email. This file is for personal use only and may not be copied and disseminated in any form without prior written permission from IJOCTA.

Submission Preparation Checklist

As part of the submission process, authors are required to check off their submission's compliance with all of the following items, and submissions may be returned to authors that do not adhere to these guidelines.

1. The submission has not been previously published, nor is it before another journal for consideration (or an explanation has been provided in Comments for the Editor).
2. The paper is in PDF format and prepared using the IJOCTA's two-column template.
3. All references cited in the manuscript have been listed in the References list (and vice-versa) following the referencing style of the journal.
4. There is no copyright material used in the manuscript (or all necessary permissions have been granted).
5. Details of all authors have been provided correctly.
6. ORCID profile numbers of "all" authors are mandatory, and they are provided at the end of the manuscript as in the template (visit https://orcid.org for more details on ORCID).
7. The text adheres to the stylistic and bibliographic requirements outlined in the Author Guidelines.
8. Maximum five AMS Classification number (http://www.ams.org/mathscinet/msc/msc2010.html) of the study have been provided after keywords.
9. The names and email addresses of at least FOUR (4) possible reviewers have been indicated in "Comments for the Editor" box in "Paper Submission Step 1-Start". Please note that at least two of the recommendations should be from different countries. Avoid suggesting reviewers you have a conflict of interest.

Peer Review Process

All contributions, prepared according to the author guidelines and submitted via IJOCTA online submission system are evaluated according to the criteria of originality and quality of their scientific content. The corresponding author will receive a confirmation e-mail with a reference number assigned to the paper, which he/she is asked to quote in all subsequent correspondence.

All manuscripts are first checked by the Technical Editor using plagiarism detection software (iThenticate) to verify originality and ensure the quality of the written work. If the result is not satisfactory (i.e. exceeding the limit of 30% of overlapping), the submission is rejected and the author is notified.

After the plagiarism check, the manuscripts are evaluated by the Editor-in-Chief and can be rejected without reviewing if considered not of sufficient interest or novelty, too preliminary or out of the scope of the journal. If the manuscript is considered suitable for further evaluation, it is first sent to the Area Editor. Based on his/her opinion the paper is then sent to at least two independent reviewers. Each reviewer is allowed up to four weeks to return his/her feedback but this duration may be extended based on his/her availability. IJOCTA has instituted a blind peer review process where the reviewers' identities are not known to authors. When the reviews are received, the Area Editor gives a decision and lets the author know it together with the reviewer comments and any supplementary files.

Should the reviews be positive, the authors are expected to submit the revised version usually within two months the editor decision is sent (this period can be extended when the authors contact to the editor and let him/her know that they need extra time for resubmission). If a revised paper is not resubmitted within the deadline, it is considered as a new submission after all the changes requested by reviewers have been made. Authors are required to submit a new cover letter, a response to reviewers letter and the revised manuscript (which ideally shows the revisions made in a different color or highlighted). If a change in authorship (addition or removal of author) has occurred during the revision, authors are requested to clarify the reason for change, and all authors (including the removed/added ones) need to submit a written consent for the change. The revised version is evaluated by the Area editor and/or reviewers and the Editor-in-Chief brings a decision about final acceptance based on their suggestions. If necessary, further revision can be asked for to fulfil all the requirements of the reviewers.

When a manuscript is accepted for publication, an acceptance letter is sent to the corresponding author and the authors are asked to submit the source file of the manuscript conforming to the IJOCTA two-column final submission template. After that stage, changes of authors of the manuscript are not possible. The manuscript is sent to the Copyeditor and a linguistic, metrological and technical revision is made, at which stage the authors are asked to make the final corrections in no more than a week. The layout editor prepares the galleys and the authors receive the galley proof for final check before printing. The authors are expected to correct only typographical errors on the proofs and return the proofs within 48 hours. After the final check by the layout editor and the proofreader, the manuscript is assigned a DOI number, made publicly available and listed in the forthcoming journal issue. After printing the issue, the corresponding metadata and files published in this issue are sent to the databases for indexing.

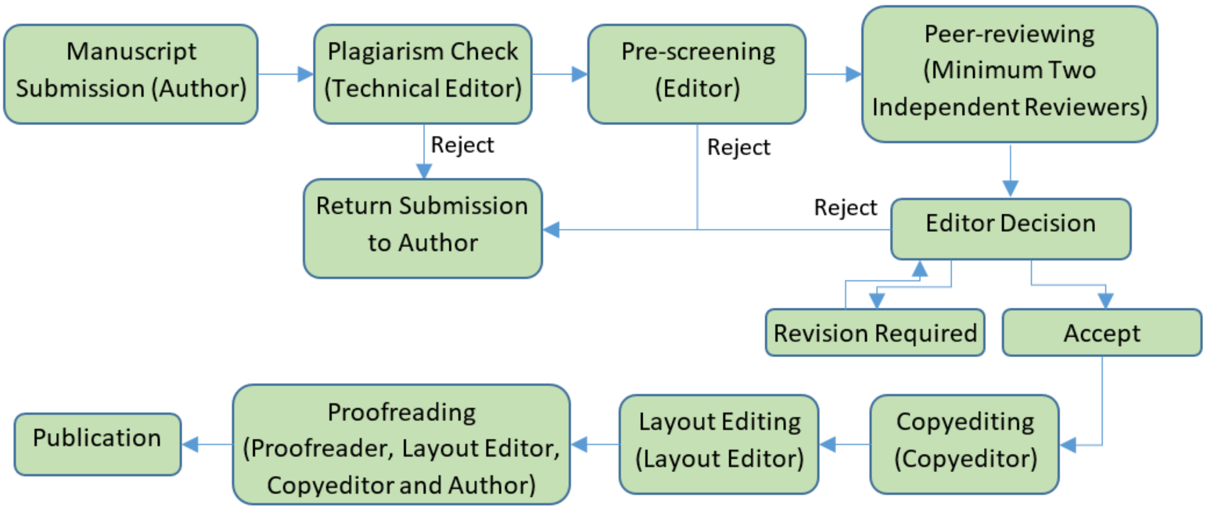

Publication Ethics and Malpractice Statement

IJOCTA is committed to ensuring ethics in publication and quality of articles. Conforming to standards of expected ethical behavior is therefore necessary for all parties (the author, the editor(s), the peer reviewer) involved in the act of publishing.

International Standards for Editors

The editors of the IJOCTA are responsible for deciding which of the articles submitted to the journal should be published considering their intellectual content without regard to race, gender, sexual orientation, religious belief, ethnic origin, citizenship, or political philosophy of the authors. The editors may be guided by the policies of the journal's editorial board and constrained by such legal requirements as shall then be in force regarding libel, copyright infringement and plagiarism. The editors may confer with other editors or reviewers in making this decision. As guardians and stewards of the research record, editors should encourage authors to strive for, and adhere themselves to, the highest standards of publication ethics. Furthermore, editors are in a unique position to indirectly foster responsible conduct of research through their policies and processes.

To achieve the maximum effect within the research community, ideally all editors should adhere to universal standards and good practices.

- Editors are accountable and should take responsibility for everything they publish.
- Editors should make fair and unbiased decisions independent from commercial consideration and ensure a fair and appropriate peer review process.
- Editors should adopt editorial policies that encourage maximum transparency and complete, honest reporting.
- Editors should guard the integrity of the published record by issuing corrections and retractions when needed and pursuing suspected or alleged research and publication misconduct.
- Editors should pursue reviewer and editorial misconduct.
- Editors should critically assess the ethical conduct of studies in humans and animals.
- Peer reviewers and authors should be told what is expected of them.
- Editors should have appropriate policies in place for handling editorial conflicts of interest.

Reference:

Kleinert S & Wager E (2011). Responsible research publication: international standards for editors. A position statement developed at the 2nd World Conference on Research Integrity, Singapore, July 22-24, 2010. Chapter 51 in: Mayer T & Steneck N (eds) Promoting Research Integrity in a Global Environment. Imperial College Press / World Scientific Publishing, Singapore (pp 317-28). (ISBN 978-981-4340-97-7) [Link].

International Standards for Authors

Publication is the final stage of research and therefore a responsibility for all researchers. Scholarly publications are expected to provide a detailed and permanent record of research. Because publications form the basis for both new research and the application of findings, they can affect not only the research community but also, indirectly, society at large. Researchers therefore have a responsibility to ensure that their publications are honest, clear, accurate, complete and balanced, and should avoid misleading, selective or ambiguous reporting. Journal editors also have responsibilities for ensuring the integrity of the research literature and these are set out in companion guidelines.

- The research being reported should have been conducted in an ethical and responsible manner and should comply with all relevant legislation.
- Researchers should present their results clearly, honestly, and without fabrication, falsification or inappropriate data manipulation.
- Researchers should strive to describe their methods clearly and unambiguously so that their findings can be confirmed by others.
- Researchers should adhere to publication requirements that submitted work is original, is not plagiarised, and has not been published elsewhere.
- Authors should take collective responsibility for submitted and published work.
- The authorship of research publications should accurately reflect individuals' contributions to the work and its reporting.
- Funding sources and relevant conflicts of interest should be disclosed.
- When an author discovers a significant error or inaccuracy in his/her own published work, it is the author's obligation to promptly notify the journal's Editor-in-Chief and cooperate with them to either retract the paper or to publish an appropriate erratum.

Reference:

Wager E & Kleinert S (2011) Responsible research publication: international standards for authors. A position statement developed at the 2nd World Conference on Research Integrity, Singapore, July 22-24, 2010. Chapter 50 in: Mayer T & Steneck N (eds) Promoting Research Integrity in a Global Environment.

Imperial College Press / World Scientific Publishing, Singapore (pp 309-16). (ISBN 978-981-4340-97-7) [Link].

Basic principles to which peer reviewers should adhere

Peer review in all its forms plays an important role in ensuring the integrity of the scholarly record. The process depends to a large extent on trust and requires that everyone involved behaves responsibly and ethically. Peer reviewers play a central and critical part in the peer-review process as the peer review assists the Editors in making editorial decisions and, through the editorial communication with the author, may also assist the author in improving the manuscript.

Peer reviewers should:

- respect the confidentiality of peer review and not reveal any details of a manuscript or its review, during or after the peer-review process, beyond those that are released by the journal;
- not use information obtained during the peer-review process for their own or any other person's or organization's advantage, or to disadvantage or discredit others;
- only agree to review manuscripts for which they have the subject expertise required to carry out a proper assessment and which they can assess within a reasonable time-frame;
- declare all potential conflicting interests, seeking advice from the journal if they are unsure whether something constitutes a relevant conflict;
- not allow their reviews to be influenced by the origins of a manuscript, by the nationality, religion, political beliefs, gender or other characteristics of the authors, or by commercial considerations;
- be objective and constructive in their reviews, refraining from being hostile or inflammatory and from making libellous or derogatory personal comments;
- acknowledge that peer review is largely a reciprocal endeavour and undertake to carry out their fair share of reviewing, in a timely manner;
- provide personal and professional information that is accurate and a true representation of their expertise when creating or updating journal accounts.

Reference:

Homes I (2013). COPE Ethical Guidelines for Peer Reviewers, March 2013, v1 [Link].

An International Journal of Optimization and Control: Theories & Applications

Volume: 14 Number: 1
January 2024

CONTENTS

ISSN 2146-0957

www.ijocta.org
editor@ijocta.org